THEORY OF NOVEL NONLINEAR OPTICS

Juan F. Lam

Hughes Research Laboratories
3011 Malibu Canyon Road
Malibu, California 90265

October 1990

F49620-88-C-0042
Final Report
1 February 1988 through 31 October 1990

Prepared for:
AIR FORCE OFFICE OF SCIENTIFIC RESEARCH
Physics Division
Bolling Air Force Base, DC 20332

UNCLASSIFIED

SECURITY CLASSIFICATION OF THIS PAGE

REPORT DOCUMENTATION PAGE

Form Approved OMB No. 0704-0188

1a. REPORT SECURITY CLASSIFICATION: UNCLASSIFIED

1b. RESTRICTIVE MARKINGS:

2a. SECURITY CLASSIFICATION AUTHORITY:

2b. DECLASSIFICATION / DOWNGRADING SCHEDULE:

3. DISTRIBUTION / AVAILABILITY OF REPORT: Approved for public release; distribution unlimited.

4. PERFORMING ORGANIZATION REPORT NUMBER(S):

5. MONITORING ORGANIZATION REPORT NUMBER(S):

6a. NAME OF PERFORMING ORGANIZATION: Hughes Research Laboratories

6b. OFFICE SYMBOL (If applicable):

7a. NAME OF MONITORING ORGANIZATION: AFOSR/Physics Division

6c. ADDRESS (City, State, and ZIP Code): 3011 Malibu Canyon Road, Malibu, CA 90245

7b. ADDRESS (City, State, and ZIP Code): BLDG 410 Bolling Air Force Base, Washington, DC 20332

8a. NAME OF FUNDING / SPONSORING ORGANIZATION: AFOSR

8b. OFFICE SYMBOL (If applicable): NP

9. PROCUREMENT INSTRUMENT IDENTIFICATION NUMBER: F49620-88-C-0042

8c. ADDRESS (City, State, and ZIP Code): BLDG 410 Bolling Air Force Base, Washington, DC 20332

10. SOURCE OF FUNDING NUMBERS

PROGRAM ELEMENT NO.	PROJECT NO.	TASK NO.	WORK UNIT ACCESSION NO.
61102F	2301	A1	

11. TITLE (Include Security Classification): Theory of Novel Nonlinear Optics

12. PERSONAL AUTHOR(S): Dr. Juan F. Lam

13a. TYPE OF REPORT	13b. TIME COVERED	14. DATE OF REPORT (Year, Month, Day)	15. PAGE COUNT
Final	FROM 1Feb88 TO 31Jul90	October 31, 1990	119

16. SUPPLEMENTARY NOTATION:

17. COSATI CODES		
FIELD	GROUP	SUB-GROUP

18. SUBJECT TERMS (Continue on reverse if necessary and identify by block number): Phase conjugation, rare earth doped solids, millimeter waves, superlattices, organic quantum wells, modulation techniques

19. ABSTRACT (Continue on reverse if necessary and identify by block number) A study of novel nonlinear optical processes is presented, along with comparison with available experimental data. Five key areas were investigated using novel theoretical approaches. Analysis of phase conjugate optics of rare earth doped solids predicts inhomogenous saturation behavior, pair quenching effects and concentration dependent filtering property, in agreement with experiments. Theory of millimeter wave phase conjugation and novel modulation techniques for communication purposes in semiconductor superlattices are described. The physics of self-pumped phase conjugation in resonant systems are quantified, and the demonstration of a self-pumped phase conjugate mirror at diode laser wavelengths is achieved. A theoretical model, based on the Davydov Hamiltonian, gives absorption lineshapes in agreement with experiments, and predicts the onset of bistability and energy transfer in two-beam coupling. An analysis of the role of multiple longitudinal phonon coupling to Wannier excitions yields Fano-like profiles in four-wave mixing spectroscopy.

20. DISTRIBUTION / AVAILABILITY OF ABSTRACT: ☒ UNCLASSIFIED / UNLIMITED ☒ SAME AS RPT. ☐ DTIC USERS

21. ABSTRACT SECURITY CLASSIFICATION: UNCLASSIFIED

22a. NAME OF RESPONSIBLE INDIVIDUAL: Dr. H. Schlossberg

22b. TELEPHONE (Include Area Code): (202) 767-4904

22c. OFFICE SYMBOL: NP

DD Form 1473, JUN 86 — Previous editions are obsolete

SECURITY CLASSIFICATION OF THIS PAGE: UNCLASSIFIED

TABLE OF CONTENTS

SECTION 1

INTRODUCTION

It has been recognized since the early 1960s that ion-doped solid state systems possess intrinsic optical properties that depend on the concentration of dopants.[1] One such property is the cooperative emission of radiation. The cooperative process relies on the simultaneous excitation of two ions, mediated by the static Coulomb interaction, in the presence of a radiation field. The understanding of cooperative processes in solids has been the subject of great interest in recent years due to the practical implementation of the upconversion laser.[2] These novel coherent sources are characterized by their high efficiencies, potential for high power operation, and demonstrated ability for emitting the red, green and blue colors when pumped by a diode laser system.[3] Recently, we extended the cooperative emission model to the regime of strong light-matter interaction, and discovered the phenomenon of quantum mechanical cancellation of the Van der Waals potential.[4] One of the objectives of this program is to explore the potential of ion-doped solid state system for applications in cooperative nonlinear optics.

The search for novel materials that are useful in the 94 GHz regime has led to the recent experimental demonstration of nonlinear phase shifts[5] and phase conjugation[6] in graphite suspensions. Along the same line, semiconductor superlattices have been found to be potential candidates as millimeter wave nonlinear materials.[7] The advantage of the superlattice materials as compared to bulk materials is that the frequency response of the superlattice can be tailored by use of molecular beam epitaxy. As part of the general thrust of this contract, the recent development of superlattice nonlinearities has been applied to an evaluation of their potential for applications in the 94 GHz regime.

Useful applications of phase conjugation in tactical lasers has been limited by the availability of optical materials which are fast responding, have a low intensity threshold, have a reasonable phase conjugate reflectivity, and can be operated in the passive mode of operation. The latest development that has the potential of solving all these issues is the demonstration of a resonantly enhanced self-pumped phase conjugate mirror.[8] The experiments indicated that this unique phase conjugate mirror has a response time of tens of nanoseconds, a threshold as low as 10 W/cm^2, a reflectivity of 2%, and operates only when an input aberrated laser beam is incident upon it. As part of our effort to understand the area of phase conjugate optics, a significant amount of research was devoted to the understanding of the physical mechanism that gives rise to self-pumped phase conjugate fields.

The recent successful fabrication of crystalline organic multiple quantum wells using molecular beam epitaxy techniques[9] has renewed interest on the physical origin of optical

responses in organic materials. Up to the present time, experimental studies have not been able to determine a single mechanism that conclusively explain the richness of the data.[10] Electronic structure studies of long chain polymers confirmed the existence of solitons.[11] However nonlinear optical experiments appeared to rule out the influence of solitons on the third order optical susceptibilities.[12] Along the same line, the theoretical model of third order susceptibilities due to electron delocalization was found to be inconsistent with recent experiments.[13] The objectives of the present contract is well suited for the solution of this important puzzle. The last 9 months of this contract was devoted to the understanding of the physical mechanism responsible for the sharp spectral features in these novel structures, as well as to explore its applications in nonlinear optics.

The understanding of many-body effects in the optical spectrum of GaAs/AlGaAs quantum wells has been the subject of active research in the past decade.[14] Gross features of the optical spectra appear to be accounted for by current theories,[15] provided that the experiments are performed in the picosecond regime. Simplified assumptions concerning the Coulomb interaction can be made to render the theories analytically tractable . An example is the prediction and observation of the dynamic Stark effect in bulk and quantum confined semiconductors.[16] The theoretical results agree with experiments provided that only virtual excitons are produced by the radiation fields. Recent cw four-wave mixing experiments[17] showed that the spectral lineshape is asymmetric, in contradiction with existing theoretical models. We believe that this anomaly is related to the problem of strong exciton-multiple longitudinal optic phonon coupling. The orientation of the problem is consistent with the objectives of this program. In the last few months, simultaneous with our study of the mechanism of crystalline organic quantum wells, we explored analytically the effects of the phonon spectrum on the lineshape of the Wannier exciton.

This theoretical effort has been enhanced by the constant inspiration that arose from the exchange of information and active participation in several concurrent experimental programs that have being funded by the Air Force Office of Scientific Research. In particular, the substance of this final report is made more relevant to the Air Force mission through the generosity and unselfish sharing of ideas and experimental data by Prof. Harold Fetterman of UCLA on millimeter wave nonlinearities, Prof. Steve Forrest of the University of Southern California on crystalline organic multiple quantum wells, Dr. Ross McFarlane of Hughes Research Laboratories and Prof. Stephen Rand of the University of Michigan on upconversion lasers, and Prof. Duncan Steel of the University of Michigan on novel spectroscopy of GaAs/AlGaAs quantum wells.

The understanding of resonant self-pumped phase conjugation would have not been complete without the experimental talent and perseverance of Dr. Celestino J. Gaeta, who implemented the first self-pumped phase conjugate mirror in sodium and cesium vapors. His contribution is gratefully acknowledged.

SECTION 2

BRIEF SUMMARY OF RESEARCH FINDINGS

2.1 SIGNIFICANT "FIRSTS"

- Solved the four-wave mixing problem in Nd doped beta alumina. The behavior of the theoretical phase conjugate reflectivity as a function of the laser intensity and dopant concentration is in agreement with experiments. Explained the quenching behavior of the linewidth and saturation intensity as a function of the concentration of dopants.

- Proposed the use of semiconductor superlattices as materials for millimeter wave phase conjugation, and explored novel modulation techniques for point-to-point communications at 94 GHz.

- Achieved an understanding of resonantly enhanced self-pumped phase conjugation, and demonstrated a cw self-pumped phase conjugate mirror in cesium vapor that operates at diode laser wavelengths.

- Identified the charge transfer exciton as the source of optical nonlinearities in crystalline organic quantum wells, and discovered the simultaneous occurance of intrinsic optical bistability and energy transfer in these materials.

- Calculated the effect of exciton-phonon coupling on the spectral lineshape of nearly degenerate four-wave mixing in GaAs/AlGaAs quantum wells, in qualitative agreement with experiments. The Fano or asymmetric profile arises from the configurational mixing due to the existence of a spectrum of longitudinal optical phonons.

The details of these theoretical accomplishments are discussed below.

2.2 FOUR-WAVE MIXING IN RARE EARTH DOPED SOLIDS

An analysis was made to study the effects of Coulomb interaction among a pair of ions on the spectral response of nearly degenerate four-wave mixing (NDFWM) in ion-doped systems. The spectrum of NDFWM provides a measure of the dynamic bandwidth of the phase conjugate mirror. The physical model used for the analysis is the interaction among two rare earth ions, each represented by a five-level system. In this model, the applied radiation field resonantly excites two of the energy levels (in the blue region of the spectrum), while the Coulomb interaction affects the probability of the population in the ground and metastable levels (in the red region of the spectrum). This simple model represents the important neodymium ion, which is the source of

coherent emission in the infrared and its optical spectrum is reasonably well understood. The effect of the Coulomb interaction among two identical ions is to introduce an effective energy exchange rate, which is calculated via the Fermi's golden rule.

The analysis involves the use of the density matrix equations, where the energy exchange rate is described in terms of an ion density dependent rate. The calculational steps taken are as follows: First, the five rate equations and the two optical coherence equations are solved exactly for the case of two strong counterpropagating pump fields. Second, these exact solutions are used to obtain the phase conjugate field in the degenerate four-wave mixing geometry. And last, the optical coherence is averaged over a Maxwellian profile, which approximates the effects of crystal field broadening. The calculations are valid for arbitrary values of the counterpropagating pump fields.

The results of the analysis can be described as follows: First, the spectral linewidth is equal to twice the infrared spontaneous emission decay rate, in the limit of low pump intensity and small ion concentration. For the case of neodymium ion, the spontaneous decay rate is of the order of a few kilocycles per second. This results points out a very important consequence of the calculation. That is, the nonlinear optical measurement of a rare earth ion using visible radiation gives direct information about the infrared behavior of the ion. Second, for fixed- and low-ion concentration, the linewidth is proportional to the square root of $1 + I/I_S$. I and I_S are the pump and ion saturation intensities, respectively. The squared root dependence on the pump intensity is a manifestation of the inhomogenous broadening due to the crystal fields. Hence, the theoretical model agrees quite well with the recent NDFWM experiments performed in Nd^{+3}-Na--beta Alumina.[18,19] And third, for fixed-pump intensity, the linewidth and saturation intensity decreases in magnitude as the ion density is increased. This behavior arises from the cooperative transfer of energy due to the Coulomb interaction, and is one of the fundamental pathways for population inversion in upconversion lasers. These results suggest that coupled ion pair interaction can play a significant role in tailoring the solid state materials for nonlinear optical applications. That is, the flexibility of changing the intensity and ion concentration may provide a means of selecting an appropriate filtering property of a phase conjugate mirror. As an example, an Nd-doped solid state system is a potential phase conjugate mirror operating at the double YAG frequency, with bandwidth capabilities in the few tens of kilocycles per second. It can be used for correcting atmospheric turbulence in nonlinear optical imaging applications of interest to the Air Force.

The details of our studies are given in Appendices A,B and C. The work contained in Appendix C was supported by a previous AFOSR contract F49620-85-C-0058 and has not been reported in the final report of that contract. Its inclusion in this final report is made for reporting purposes.

2.3 PHASE CONJUGATION AND MODULATION PROPERTIES OF SUPERLATTICES AT 94 GHZ

An analysis of the role of semiconductor superlattices in millimeter wave applications was performed using the effects of artificially induced band nonparabolicity. The application of molecular beam epitaxy technique for the growth of quantum confined structures leads to a modification of the band structure (along the growth direction) of the bulk material. Lam et al[7] have shown that the artificially induced band non-parabolicity gives rise to an effective mass that depends on the strength of the applied radiation field. Hence, the customized semiconductor material exhibits strong nonlinear response to applied radiation fields.

The application of the results found in Reference 7 to the case of operation at 94 GHz provides the following information. Using GaAs-AlGaAs as the test material and assuming a n-type doping density of 10^{16} cm^{-3}, one find that the third order susceptibility is equal to 4.6×10^{-1}esu. We assumed that the periodicity of the superlattice is 100 A, and the phonon-induced damping rate of 10 THz. The high dopant density brings about an important question: Can the millimeter wave radiation transmit through the material in the presence of free carrier scattering and absorption?. A simple calculation gives an effective plasma dielectric constant of approximately 0.7 (underdense) and a linear absorption coefficient of 3 mm^{-1}. Hence, the GaAs-AlGaAs superlattice promises to be an interesting material for operation at 94 GHz. Identical conclusions are reported Reference 7 for the case of operation at 250 GHz. However, the experimental feasibility of making a millimeter-wave nonlinear device using superlattices remains to be tested. Motivated by the theoretical conclusions and with the support of Hughes IRD, we made a 1 mm thick sample of GaAs-AlGaAs superlattice using the in-house MBE facilities. The sample is composed of ten 10-micron-thick 50 A (GaAs)/ 50 A (AlGaAs) superlattice stacks. Each stack was intentionally doped with 10^{14} cm^{-3} of silicon. The sample will be characterized for 94 GHz (at the millimeter wave laboratories of UCLA) and 250 GHz (at the facilities of Duke University) operation.

Furthermore, we carried out a detailed analysis of the possibility of obtaining time reversed waves via degenerate four-wave mixing in superlattices. Assuming the undepleted pump regime, we solved the nonlinear carrier velocity equation and derived an exact analytical expression for the nonlinear current density that produces time reversed waves. The nonlinear current density is valid for arbitrary values of the pump fields, and enters as a source in Maxwell's equations. The production of the time reversed field depends upon the validity of the slowly varying envelope approximation since the dimension of the sample can be large compared to the wavelength of the radiation field. In the case of 94 GHz radiation, the linear absorption coefficient for carrier density of 10^{14} cm^{-3} is small compared to $2\pi n/\lambda = 7.8$ mm^{-1}, which validates the use of the quasi-optical

picture. We also calculated the reflectivity of the time reversed field, and found that it achieves a maximum of 7% at a normalized superlattice Rabi frequency of approximately 2. This value corresponds to a saturation pump field of 780 V/cm.

And last, we applied our understanding of millimeter wave nonlinearities to the important case of millimeter wave communication. We solved two interesting cases. The first one involves the application of a static electric field along the superlattice growth direction, and a radiation field propagating along the plane of the superlattice. We found that the polarization density produces a radiation field which is modulated at the static electric field induced Rabi frequency. It exhibits a linear modulation behavior even though the solution is nonlinear in the carrier frequency. Hence detection of the FM modulated signal gives rise to two symmetric sidebands centered around the carrier frequency. The second case involves the application of an oscillating electric field along the superlattice growth direction, and a radiation field propagating along the plane of the superlattice. We found that the polarization density produces a radiation field which is amplitude modulated. The strength of the modulation is determined by the electric field induced Rabi frequency. Hence, these results imply that semiconductor superlattices have novel properties that render them useful in millimeter wave signal processing applications provided that the fabrication of a real superlattice device can be achieved in the future,

The details and implications of our studies are presented in Appendix D and E

2.4 RESONANTLY ENHANCED SELF-PUMPED PHASE CONJUGATION

An analysis of the mechanism that produces self-pumped phase conjugation in resonant materials was made using the coupled density matrix and Maxwell's equations. The results of our analysis identified the start-up conditions for the formation and coherent amplification of scattered noise. The starting mechanism is the production of resonance fluorescence, which is coherent with the input radiation field. The build up of the fluorescence or noise field is achieved through the formation of a traveling wave grating produced by the interference between the fluorescence and input fields, and followed by the coherent scattering of the pump field from the traveling wave grating. The generation of the phase conjugate field can be achieved in two distinct manners. The first one involves the stimulated backscattering of the input field from the traveling wave grating. This mechanism does not require the presence of an optical cavity. The second scheme uses a linear optical cavity to take advantage of the forward-going energy transfer process. The purpose of the optical cavity is to store the fluorescence radiation in a standing wave pattern. Coherent scattering of one of the standing wave component from the traveling wave grating produces a phase conjugate field. The latter is just the standard degenerate four-wave mixing configuration.

The solution of the density matrix equations provides the macroscopic polarization density, which is used in the wave equation to obtain a self-consistent, new radiation field. The density matrix equations are solved in two steps. First, we found the exact solution for the input field alone. Then these solutions are used to obtain the polarization density and gain condition in the presence of noise fields. We found that the coherent amplification of the noise field can only occur provided that the intensity of the input field is large compared with the medium saturation intensity. If the input field is tuned to resonance, the gain profile of the noise as a function of the difference frequency between the input field and noise has two symmetrical sidelobes, whose separation is equal to the Rabi flopping frequency. If the input field is detuned from resonance, the gain profile is asymmetrical such that amplification of the noise only occurs for either frequency upshift or downshift, but not both. The physical explanation of this result lies in the dynamical behavior of atomic states induced by strong radiation field. That is, the input field produces a dressed state of the system of atoms and radiation field, and gain occurs from a near degenerate four-wave mixing process taking place among each component of the dressed atom. Hence, amplification of noise can occur provided that the input field is above saturation. The gain profile determines the frequency shift acquired by the phase conjugate field.

In order to verify the physical mechanism responsible for the production of phase conjugate fields, we demonstrated the first self-pumped phase conjugate mirror in cesium vapor at 0.852 micron. We used a linear cavity configuration which consists of a cesium cell enclosed between two curved high reflecting mirrors. The incoming cw laser beam was directed into the cesium cell at an angle on the order of half a degree, leading to a large overlap between the input beam and resonator modes. A measured but un-optimized reflectivity of approximately 0.1% and a threshold intensity of 35 W/cm^2 were observed. This elegant experiment confirmed the key mechanism in resonantly-enhanced self-pumped phase conjugation. That is, energy transfer between the input beam and the induced resonance fluorescence provides a means of setting up the gratings from which coherent scattering of the radiation fields can take place. It just needs one single input aberrated beam to achieve such a nonlinear optical process.

Furthermore, we have extended our calculation beyond the two-level model in order to study the generation of self-pumped phase conjugate fields in rhodamine 6G. Experimental studies by Koptev et al [20] and Lam et al [21] indicated the presence of phase conjugate fields when the organic dye was illuminated by an intense laser pulse. The experimental studies was performed with a mode locked 10-nsec pulse emitted from a double YAG laser system, and a focused intensity at the dye cell of approximately 1 MW/cm^2. In order to understand the experimental data, we modeled the organic dye in terms of a 3-level system. Following the procedure stated above for the 2-level system, we calculated the nonlinear polarization density, and found that the gain

profile of the amplified signal is consistent with the wide bandwidth (300 A) obtained from the experiments.

The results of this work opens up the distinct practical application of self-pumped phase conjugation using semiconductor lasers. An scenario will be the implementation of satellite-to-satellite secure communication links using high power semiconductor lasers. This unique phase conjugate mirror can be modulated at gigahertz rate, has a low threshold intensity (tens of W/cm^2) for start-up operation, and possesses a negligigle frequency shift (within the laser linewidth).

The details of the analysis and experiments are compiled in Appendices F, G and H.

2.5 OPTICAL NONLINEARITIES IN CRYSTALLINE ORGANIC MULTIPLE QUANTUM WELLS

We investigated the physical mechanism that is responsible for the observed sharp spectral behavior in the linear absorption profile of PTCDA /NTCDA multiple quantum wells. PTCDA and NTCDA are the abbreviated notation for 3,4,9,10 perylenetetracarboxylic dianhydride and 3,4,7,8 naphthalene tetracarboxylic dianhydride; respectively. We found that charge transfer (CT) exciton is the dominant elementary excitation whose properties account for the measured spectra. A theoretical model was constructed to include the interaction of CT excitons with the external radiation fields and phonons. Using the Heisenberg equation of motion, we derived the set of coupled equations for the optical coherence of the CT exciton and the amplitude of the phonons. In the linear regime, we found an exact analytical solution for the absorption coefficient whose spectral behavior is in agreement with the experimental data of So et al[9].

We explored the nonlinear optical properties of these novel materials. An exact analytical solution of the coupled exciton-phonon system was obtained. The results can be described as follows. The exciton population exhibits an intrinsic bistable behavior as a function of the laser intensity. The origin of the bistability arises from the intensity dependent renormalization of the exciton energy. Bistability will occur provided that the size of the quantum wells is small enough such that the laser detuning from quantum confined exciton resonance is larger than the exciton linewidth, multiplied by the square root of 3. Second, we calculated the possibility of energy transfer from a strong optical beam to a weak optical beam by solving the coupled exciton-phonon and wave equations. We discovered that there exists a threshold for the transfer of energy to occur for all values of the well size. However, this threshold is bistable for a critical size of the quantum well. This behavior is consistent with the bistability criterion stated above. These unique results provide an interesting application in optical data processing. One can tailor the size of the quantum

well such that information from a strong optical beam is transferred to a set of weak optical beams provided that a certain threshold intensity is achieved.

The details of this section is described in Appendix I

2.6 FOUR-WAVE MIXING SPECTROSCOPY OF GaAs/AlGaAs QUANTUM WELLS

We explored the role of longitudinal optic phonon coupling to a Wannier exciton in GaAs/AlGaAs quantum wells. In spite of the magnitude of the LO phonon interaction energy of 36 meV, [22] current theoretical models do not include its effect in the dynamics of the excitonic transitions, except for a phenomenological decay rate in the exciton population. We used the Davydov Hamiltonian to study the four-wave mixing spectra in the weak optical signal regime. A perturbation calculation to third order in the radiation field was carried out from the coupled exciton-phonon-field equations. The results of our preliminary studies point to the following conclusions: If only one phonon mode is considered, then the nearly degenerate four-wave mixing spectrum shows a symmetric profile as a function of the frequency difference between the pump and the probe. However if a multiple phonon structure is inserted in the calculation, the four-wave mixing spectra shows an asymmetric profile similar to that found in the Fano effect of atomic spectra. A simple physical explanation can be given. In the presence of multiple phonons, there exists a configurational mixing leading to a competition of the different phonon modes. In a nutshell, the competition leads to an interference effect that cancels all contribution in certain portions of the spectral profile.

Furthermore, we were able to solve anaytically the strong pump/weak probe regime. The results indicate that intrinsic optical bistability is present, and has the same properties as those found in organic quantum wells. Hence, the phase conjugate reflectivity should exhibit cavity-free optical bistablity for a critical value of the pump intensity. Current four-wave mixing experiments are performed in the regimes where all input radiation fields are either below saturation or above saturation. However, there exists no observation of the intrinsic bistable behavior.

The physics and the analytical solutions have been communicated to the experimental group at the University of Michigan for further studies.

SECTION 3

CONFERENCE AND UNIVERSITY PRESENTATIONS

1. Nonlinear Optics of Semiconductor in zero- and one-dimensional systems
   Juan F. Lam
   Pennsylvania State University
   The IBM Seminar of the Center for Electronic Materials
   April 1988

2. Nonlinear Optics of Semiconductor in zero- and one-dimensional systems
   Juan F. Lam
   The University of Michigan
   Department of Physics and Electrical Engineering
   September 1988

3. Theory of optical phase conjugation in coupled ion pairs
   Juan F. Lam
   Annual Meeting of the Optical Society of America
   Santa Clara, California
   October 1988

4. Theory and applications of novel nonlinear optics
   Juan F. Lam
   Department of Electrical Engineering
   UCLA
   December 1988

5. Self-pumped phase conjugation in resonant systems
   Juan F. Lam
   Department of Electrical Engineering
   UCLA
   April 1989

6. Optical Nonlinearities in crystalline organic quantum wells
   Juan F. Lam, Steve R. Forrest and Gregory L. Tangonan
   IQEC (post-deadline paper)
   Anaheim, California
   April 1990

7. Self-pumped phase conjugation in cesium vapor
   Celestino J. Gaeta and Juan F. Lam
   IEEE Nonlinear Optics'90
   Hawaii
   July 1990

8. Optical Nonlinearities in crystalline organic quantum wells
   Juan F. Lam, Steve R. Forrest and Gregory L. Tangonan
   IEEE Nonlinear Optics'90
   Hawaii
   July 1990

REFERENCES

1. Spectroscopy of Solids Containing Rare Earth Ions, edited by A.A. Kaplyanskii and R.M. MacFarlane, Elsevier Science Publishers (1987). A.A. Kaminskii, Laser Crystals, Springer-Verlag (1981)

2. R.A. McFarlane, Appl. Phys. Lett. **54**, 2301 (1989).

3. T.,Hebert, R.Wannamacher, W.Lenth, and R.M. MacFarlane, Appl. Phys. Lett. **57**, 1727 (1990).

4. J.F. Lam, S.C. Rand, and R.A McFarlane, Laser Spectroscopy VII, edited by S. Svanberg, Springer-Verlag (1987). J.F. Lam, and S.C. Rand, Phys. Rev. **A 35**, 2164 (1987).

5. B.R. Bobbs, R. Shih, H.R. Fetterman, and W.W. Ho, Appl. Phys. Lett. **52**, 4 (1988).

6. Fetterman, et al, Phys. Rev. Lett. **65**, 579 (1990).

7. J.F. Lam, B.D. Guenther, and D.D. Skatrud, Appl. Phys. Lett. **56**, 773 (1990).

8. C.J. Gaeta, J.F. Lam and R.C. Lind, Opt. Lett. **14**, 245 (1989).

9. F.F. So, S.R. Forrest, Y.Q. Shi and W.H. Steier, Appl. Phys. Lett. **56**, 674 (1990).

10. Nonlinear Optics of Organics and Semiconductors, edited by T. Kobayashi, Springer-Verlag (1989).

11. W.P. Su, J.R. Schrieffer and A.J. Heeger, Phys. Rev. Lett. **42**, 1698 (1979). L. Rothberg, T.M. Jedju, S. Etemad and G.L. Baker, Phys. Rev. Lett. **57**, 3229 (1986).

12. C.G. Levey, D.V. Lang, S. Etemad, G.L. Baker and J. Orenstein, Synthetic Metals, **17**, 569 (1987).

13. See papers in Reference 10.

14. D.S. Chemla and D.A.B. Miller, JOSA **B 2**, 1155 (1987).

15. S. Schmitt-Rink, D.S. Chemla and D.A.B. Miller, Phys. Rev. **B 32**, (1987)

16. A. Mysyrowicz, D. Hulin, A. Antonetti, A. Migus, W.T. Masselink and H. Morkoc, Phys. Rev. Lett. **56**, 2748 (1986). S. Schmitt-Rink, D.S. Chemla and H. Haug, Phys. Rev. B 37, 941 (1988).

17. H. Wang, M. Jiang, D.G. Steel, Phys. Rev. Lett. **65**, 1255 (1990). J.T. Remilliard, et al, Phys. Rev. Lett. **62**, 2861 (1989).

18. R.W. Boyd, M.T. Gruneisen, P. Narum and D.J. Simkin, Opt. Lett. **11**, 162 (1986).

19. S.C. Rand, J.F. Lam, R.S. Turley and R.A. McFarlane, Phys. Rev. Lett. **59**, 597 (1987).

20. V.G. Koptev, et al, Sov. Phys. JETP Lett. **28**, 434 (1978).

21. J.F. Lam, S.C. Rand, R.C. Lind, R.A. McFarlane and A.L. Smirl, Proc. IQEC, San Francisco, 1986

APPENDIX A

THEORY OF DEGENERATE FOUR-WAVE MIXING IN RARE EARTH DOPED CRYSTALS

Juan F. Lam

Hughes Research Laboratories

Malibu. California 90265

I. INTRODUCTION

The proces of degenerate four-wave mixing (DFWM) has been used to produce phase conjugate fields in many optical materials. For example, DFWM was recently demonstrated in gaseous plasmas[1], semiconductor multiple quantum wells[2], nematic liquid crystals[3], and color centers[4]. The practical importance of phase conjugate optics lies in their potential applications for the correction of dynamic aberrations of laser beams[5], the implementation of associative memories[6], and the development of novel approaches in optical computers[7]. On the other hand, DFWM has also been utilized to sutdy the properties of atoms and molecules. Given a specific geometry, the spectral response of the phase conjugate field gives a direct and simultaneous measurement of both the longitudinal and transverse relaxation times of a resonant system[8]. Lately, DFWM was used in the measurement of subnatural linewidths (from few Hz to 1 MHz) in gases and solids using cw lasers. Furthermore, the effects of buffer gases on the behavior of the spectral lineshape of DFWM have increased our understanding of collisional processes in alkali vapors[9]. Both Dicke narrowing and multipole dephasing contributions were aluded to in order to explain the narrowing of the resonance line in the presence of few torrs of He and Argon buffer gases.[10]

The continous search for an optimum phase conjugate mirror that can operate in the solid phase has led to the demonstration of DFWM in Nd doped β alumina[11]. This material appears to possess nearly ideal operating characteristics. That is, it is a solid state material, its spectral response can be adjusted by using selective rare earth dopants, it has a high saturation intensity of the orders of kW/cm^2, and it has a reasonable linear absorption coefficient (approximately $100cm^{-1}$). Application of DFWM spectroscopy to the Nd doped β alumina has also yielded some very interesting and unexpected results.[12] The material is inhomogenously broadened, its linewidth increases as the $\sqrt{Intensity}$, and decreases for increasing dopant concentration. These observations are intriguing in itself, and raises important questions concerning the role of dopant-dopant interaction on the

DFWM signal. Furthermore, the competition between inhomogenously broadening and dopant-dopant interaction implies that these materials have unique filtering properties for phase conjugation applications. The purpose of this article is an attempt to quantify the DFWM process for the case of rare earth doped solids, with the purpose of providing new insight into its usefulness in phase conjugate optics. Some of the theoretical results were aluded in two previous publications without giving the details of the analysis. We hope to provide a simple physical picture as well as a roadmap required to extract the spectral response of DFWM in these materials. In particular, we would like to examine the consequence of dopant-dopant interaction by using a simple binary interaction model. This model appears to be valid even for pair excited solid state lasers[13]. Although the model chosen is specific in our discussions, the theoretical results are general and can be adapted to any dopant, provided that the spectroscopic features are known in advance.

In essence, the structure of this article can be described as follows. Section II describes the model to be used in the analysis, assuming that the Nd ion is taken to be the basis of our model. Section III provides a physical description of the DFWM process, in terms of density matrix equations including the role of dopant-dopant inetraction on the temporal evolution of each ion energy level. Section IV derives the spectral lineshape for the case of both weak and strong input radiation fields. The phase conjugate reflectivity is derived and plotted as a funciton of the counterpropagating pump intensities. We summarize the result of this article in Section V.

II. PHYSICAL MODEL

In order to arrive at an understanding of the DFWM process in rare earth doped crystals, it is important to delineate the specific model of the material as well as the nonlinear wave mixing process.

1. The model for the material

We shall take, as an example, the Nd ion as the rare earth dopant, whose energy level is described in Figure 1. The frequency of radiation excites the ground state $|1>$ to the excited state $|2>$. The latter relaxes to either level $|1>$ via spontaneous emission or to level $|3>$ via a nonradiative process. Relaxation back to the ground state from $|3>$ can take two distinct paths. The first one involves a radiative relaxation to state $|4>$,followed by a nonradiative decay to the ground state. The second path is activated by the presence of another Nd ion, which induces a pair coupling process in which an electron in the ground state interact with an electron in state $|3>$ to populate the intermediate state $|5>$. The second path will be significant for large Nd ion densities, such as those approaching $10^{21} cm^{-3}$.

The spectroscopic identification of the levels mentioned above is given by

$$|1> \equiv {}^4I_{9/2}$$

$$|2> \equiv {}^4G_{7/2}$$

$$|3> \equiv {}^4F_{3/2}$$

$$|4> \equiv {}^4I_{11/2}$$

$$|5> \equiv {}^4I_{15/2}$$

The Nd ion has a strong laser emission line at $1.06\mu m$ between states $|3>$ and $|4>$. To put it to perspective, let us consider the relative orders of magnitude of the decay rate (radiative and nonradiative) out of each state. The nonradiative transition from

$|2> \rightarrow |3>$ and from $|4> \rightarrow |1>$ occurs in a time scale of the order of subnanoseconds. This fast decay occurs by means of phonon emission and is intrinsically related to the small energy separation of the transitions. The radiative decay out of state $|3>$ into state $|4>$ occurs in a time scale of few hundreds of microseconds. This slow decay is connected to the metastability of the state $|3>$. The radiative decay time out of state $|2>$ back to the ground state is of the order of microseconds. These numerical parameters imply that the excitation of the electron in the ground state is rapidly transfer to the metastable state with negligible population in state $|2>$. This simple picture has a profound significance in nonlinear optics. That is, the formation of either spatial and/or traveling wave gratings in the first optical transition directly affects the evolution of the metastable state.

Recent optical experiments[14] performed on Nd^{-3} doped β" alumina indicated that the oscillator strength of the 5890$\AA$ absorption line in these material is approximately ten times larger than that found in Nd^{-3} doped YAG. The oscillator strength was measured to be 60.610^{-6} at an concentration of $4 \times 10^{20} cm^{-3}$. The strong absorption in the 5890$\AA$ region was also an indication of a very strong fluorescence at $1.06\mu m$ emission line. Detailed studies of doping characteristics of rare earth ions in sodium β" alumina indicates that both divalent and trivalent ions can be exchanged with the sodium ions. X-ray studies[15] also indicates that the ions are located in a planar structure between spinal blocks. The ion transport properties can be described quite accurately in terms of 2-dim motion. It is believed that the substitution of any rare earth ions is facilitated by the planar geometry of ionic transport.

Subsequent nonlinear optical studies have reached the conclusion that the Nd^{-3} doped β alumina has an intrinsic inhomogenously broadened saturation behavior. The saturation intensity was deduced to be in the range of few tens of kWs per cm^2. In spite of the experimental studies, there is a lack of understanding concerning the saturation behavior. Furthermore, Farrington and Dunn[16] have ion exchange procedure to doped Gd^{+3} and Eu^{+3} ions in β alumina. With the current effort in pair excited lasers, it will be important

to undergo a study of Er ion doped processes in these materials.

2. The model for the nonlinear wave mixing process

The four-wave mixing process is described by the interaction of two counterpropagating pump fields with an input probe field in a nonlinear medium. The geometry of the nonlinear wave mixing process is pictured in Figure 2.

We shall make the following assumptions:

* The radiation fields are assumed to be tuned near resonance to the optical transition $|1> \rightarrow |2>$. That is, the wavelength of radiation is near 575 nm. This assumption entails the use of the rotating wave approximation.

* The strength of the counterpropagating pump fields, E_f and E_b, is much larger than tha of the probe field, E_p. This assumption implies that the undepleted pump approximation is valid for our studies. Pump depletion effects in DFWM have been solved for the case of Kerr and photorefractive media.

* The frequency of oscillation of the probe field is assumed to vary with respect to that of the pump fields. This flexibility allows the DFWM process to probe the spectral bandwidth of the nonlinear optical process. To be more precise, a difference in the frequency between the pump and probe fields gives rise to an up-shift or downshift in the phase conjugate field because of the conservation law of energy. Furthermore, we shall assume that the length of the sample be small enough so that linear filtering due to phase mismatch do not play a role in the conclusion of our results.

III. FORMULATION OF THE PROBLEM

The nonlinear optical response function is obtained from the solution of the density matrix equations for the Nd^{3+} ion. The components of the density matrix satisfy the following evolution equations:

POPULATION

$$\frac{d\rho_{11}}{dt} = \gamma\rho_{22} + \gamma_{41}\rho_{44} + \gamma_{51}\rho_{55} - \Gamma\rho_{33}\rho_{11} - S \tag{1a}$$

$$\frac{d\rho_{22}}{dt} = -(\gamma + \gamma_{23})\rho_{22} + S \tag{1b}$$

$$\frac{d\rho_{33}}{dt} = \gamma_{34}\rho_{33} - \gamma_{41}\rho_{44} - \Gamma\rho_{33}\rho_{11} \tag{1c}$$

$$\frac{d\rho_{44}}{dt} = \gamma_{34}\rho_{33} - \gamma_{41}\rho_{44} \tag{1d}$$

$$\frac{d\rho_{55}}{dt} = -\gamma_{51}\rho_{55} + 2\Gamma\rho_{11}\rho_{33} \tag{1e}$$

OPTICAL COHERENCES

$$\{\frac{d}{dt} + \gamma_d - i\omega_o\}\rho_{12} = \frac{V_{12}}{i\hbar}(\rho_{22} - \rho_{11}) \tag{1f}$$

where $\rho_{\alpha\alpha}$ denotes the population of state $|\alpha>$, γ is the radiative decay rate of state $|2>$. $\gamma_{\alpha\beta}$ is the decay rate from level $|\alpha>$ to $|\beta>$, Γ is the dopant-dopant coupling with units of cm^3 per sec, ρ_{12} is the optical coherence of the excited transition, γ_d is the dephasing rate of the optical coherence, ω_o is the transition frequency. The quantity S is just the work done by the radiation field for excitation or de-excitation of the energy states. It is given as

$$S = \frac{1}{\hbar}(V_{21}\rho_{12} - \rho_{21}V_{12})$$

with $V_{12} = -\mu_{12}E(R,t)$ is the potential energy describing E1 coupling.

The set of equations (1) provides a description of the nonlinear optical processes in the Nd^{-3} doped material. The optical measurement of the four-wave mixing process is directly proportional to the total off diagonal elements of the density matrix. We shall approach the analytical solutions in several stages. with increasing complexity.

We shall delineate the prescription to be followed in order to obtain exact solutions

LOW INTENSITY REGIME

This regime is characterized by the intensities of the counterpropagating pump fields to be below the saturation intensity of the medium. In this regime the solution are found by the following scheme,

$$\rho_{11}^{(0)} \rightarrow \rho_{12}^{(1)} \rightarrow \rho_{\alpha\alpha}^{(2)}\{\alpha = 1 \rightarrow 5\} \rightarrow \rho_{12}^{(3)} \tag{2a}$$

where the superscript denotes the order of the radiation field enetering into each expression.

HIGH INTENSITY REGIME

This regime is characterized by the saturation effects imposed by the presence of strong counterpropagating fields. The intensities must be above the saturation intensity of the medium. In this regime, the solutions are found in the following manner

$$\rho\{E_f, E_b\} \rightarrow \rho_{12}^{(1)} \tag{2b}$$

where the superscript denotes the condition that the probe field E_p enters only as a first order quantity. The notation $\rho\{E_f, E_b\}$ has the meaning that the solution for the density matrix are exact to all orders in the counterpropagating pump fields.

We shall consider in our discussion both the case of homogenously and inhomogenously broadened material. For the latter, we shall use a analytically tractable distribution function that simulates the effects of crystal field broadening.

IV. SPECTRAL LINESHAPES

In this section we will derive an expression for the nearly degenerate four-wave mixing lineshape. We show that the bandwidth of the lineshape is determined by the effective deacy rate of the transition $|3> - |4>$ even though the radiation fields are tuned to the transition $|1> - |2>$. This result implies that nearly degenerate four-wave mixing is a powerful spectroscopic tool to probe IR transitions of rare earth ions using visible laser.

Using the prescription (2a), the solutions to Eq.(1) give the following spectral lineshape for the homogenously broadened regime.

$$I = \frac{1}{\delta^2 + [\gamma_{34} + \Gamma N(1 - 2I/I_s)]^2} \tag{3}$$

where N is the density of Nd^{+3} ions, and I_s is the saturation intensity of the medium. Several interesting feaures can be deduced from Eq.(3). First, the spectral linewidth is determiend by the decay rate of the metastable state $|3>$. This result indicates that the technique of DFWM can be used quite effectively for spectroscopic measurement of not easily accesible transitions. This technique is not affected by the laser jitter since one takes the difference between two oscillating fields to generate a traveling wave grating. Second, If $I/I_s \geq 2$, then the linewidth decreases for increasing dopant density. Figure 3 shows a plot of the spectral lineshape as a function of the pump-probe detuning parameter, δ for two different values of the dopant density. A decrease of the linewidth is observed as one increases the density from $1. \times 10^{20} cm^{-3}$ to $6. \times 10^{20} cm^{-3}$. And last, the saturation intensity is now defined by

$$I_s = \frac{\gamma_{54}}{2\Gamma N} I_o$$

where I_o is the intrinsic saturation intensity that takes into account only the fast nonradiative decay of state $|2>$. Hence the saturation is incersely proportional to the dopant density. This rather simple theory agrees quite well with recent experimental data.

It is possible to estimate the value of the third order optical susceptibilities given a knowledge of the oscillator strength of a specific transition. For the case of 575 nm, and an

oscillator strength of 10^{-5}, one estimates a $\chi^{(3)} \simeq 10^{-4}$ esu for dopant density of $10^{21} cm^{-3}$.

Consider now the inhomogenously broadened regime. The physical mechanism arises from crsytal field effects. In order to simulate such an effect, we shall invoke the Gaussian distribution function for the transition frequency ω_o. We shall consider the role of radiation field induced saturation. The calculation proceeds according to the prescription (2b), integrated over the Gaussian distribution yields the following results.

$$S = \frac{4\pi\omega\chi^{(3)}}{cn_o} \times \frac{\sqrt{I_f I_b I_p}}{\sqrt{1 + (I_f + I_b)/I_s + 2\sqrt{I_f I_b}/I_s}} \times \frac{2}{\pi} \times F(\frac{\pi}{2}, x)(4)$$

where $F(\pi/2, x)$ is the Elliptical Integral of the first kind with argument x. The argument x is defined by

$$x = \frac{2\sqrt{I_f I_b}/I_s}{\sqrt{1 + (I_f + I_b)/I_s}}$$

I_n denotes the intensity of radiation field n. Two interesting features can be deduced from Eq.(4). First, the intensity dependence of the spectral lineshape is inversely proportional to the square root of the counterpropagating pump intensity. Figure 4 plots the spectral lineshape as a function of the pump-probe detuning parameter, δ, for different values of the counterpropagating pump intensities. It shows the power broadening effects, which is characteristic of inhomogenously broadened materials. And second, the spectral linewidth is inversely proportional to the density of dopants, in agreement with the previous results. The physical understanding for the decrease in the linewidth as a function of dopant density is identical to the one stated above for the homogenously broadened case.

The DFWM phase conjugate reflectivity as a function of the counterpropagating pump intensity is plotted in Figure 6 for two different values of the ion dopant density. It is not surprising that the reflectivity is larger for large dopant density.

V. SUMMARY

We have carried out a detailed analysis of the spectral response of the nearly degenerate four-wave mixing process in rare earth doped crystals. We showed that the four-wave mixing spectroscopy is a powerful tool for the study of unaccessible optical lines using visible radiation. In specific, for the case of Nd^{-3} doped crystal, the nearly degenerate four-wave mixing spectral signal using 575 nm radiation gives a direct measurement of the effective decay rate of the 1.06 μm transition. The power of the four-wave mixing process rely on the measurement of ultranarrow linewidths using broad band lasers. This technique will be useful to study the dynamics of any rare earth doped materials. With the advent of pair excited tunable solid state laser sources, DFWM will provide the fundamental understanding of the role of competing decay mechanisms in these materials.

We have analyzed the spectral lineshape as a function of the counterpropagating pump intensities. We found that for inhomogenously broadened materials, the spectral linewidth is proportional to the intensity to the one half power. This behavior is intrinsically connected with a Gaussian distribution of transition frequencies. We have also found that the linewidth is quenched by an increase in the ion dopant density. This phenomenon is attributed to the interaction amongst adjacent neighbors via Coulomb or exchange forces. The decrease of the linewidth is a manifestation of the changes in the effective ground state lifetime. That is, population of the ground and metastable states are depleted by the pair interaction, leading to an increase of population in an intermediate state. The outflow of population implies that the lifetimes of the ground and metastable states are considerably longer. We have also studied the dependence of the saturation intensity as a function of the ion density. The pair process causes the saturation intensity to decrease for increasing dopant density. This is also a manifestation of the decrease of the lifetime of the metastable states.

The validity of the theoretical model must be tested against experiments. A crucial test is the evaluation of the phase conjugate reflectivity. We showed that the reflectiv-

ity increases with the ion dopant density, and is in qualitative agreement with recent experimental data of Boyd et al . Hence rare earth doped crystals are potentially useful materials for nonlinear optical phase conjugation . In specific, with the recent development of *3* alumina as the host, it is posssible to choose an ideal rare earth dopant for broadband applications.

ACKNOWLEDGEMENT

This work is supported by the Air Force Office of Scientific Research

REFERENCES

1. Kitagawa, Y., R.L. Savage and C. Joshi, Phys. Rev. Lett. 62, 151 (1989)
2. Hegarty, J., M.D. Sturge, A.C. Gossard, and W. Wiegmann, Appl. Phys. Lett. 40, 132 (1982)
3. Khoo, I.C., Prog. in Optics, 26, 107 (1988)
4. Rand, S.C. Opt. Lett. 13, 140 (1988)
5. Lind, R.C. and G.J. Dunning, in Proceedings of the CLEO, paper THC5, (1983)
6. Soffer, B.H., G.J. Dunning, Y. Owechko, and E. Marom, Opt. Lett., 11, 118 (1986)
7. See the Proceedings of the OSA Meeting on Optical Computers, Feb. 1989
8. Lam, J.F., D.G. Steel and R.A. McFarlane, Phys. Rev. Lett. 49, 1628 (1982)
9. Lam, J.F., D.G. Steel, and R.A. McFarlane, Phys. Rev. Lett. 56, 1679 (1986)
10. Liu J., and D.G. Steel, Phys. Rev. A 38, 4639 (1988)
11. Boyd, R.W., M.T. Gruneisen, P. Narum, and D.J. Simkin, Opt. Lett. 11, 162 (1986)
12. Rand, S.C., J.F. Lam, R.S. Turley, R.A. McFarlane, and O.M. Stafsudd, Phys. Rev. Lett. 59, 597 (1987)
13. Rand, S.C. and S. Pollack, in the Proc. of the OSA Meeting, Rochester (1987)
14. Jansen, M., A. Alfrey, O.M. Stafsudd, B.Dunn, D.L. Yang, and G.C. Farrington, Opt. Lett. 10, 119 (1984)
15. Boilot, J.P., G. Collin, Ph. Colomban and R. Comes, Phys. Rev. B 22, 5912 (1980)
16. Farrington, G.C. and B. Dunn, Solid State Ionics 7, 267 (1982); Dunn, B. and G.C. Farrington, Solid State IOnics 9/10, 223 (1983)

FIGURE CAPTIONS

Figure 1. Energy levels of the Nd ion

Figure 2. Geometry for the degenerate four-wave mixing process

Figure 3. Spectral lineshape for the case of homogenously broadened material

Figure 4. The normalized spectral lineshape as a function of the counterpropagating pump intensity

Figure 5. The inhomogenously broadened spectral lineshape for distinct values of the dopant density

Figure 6. The phase conjugatre reflectivity as a function of pump intensity

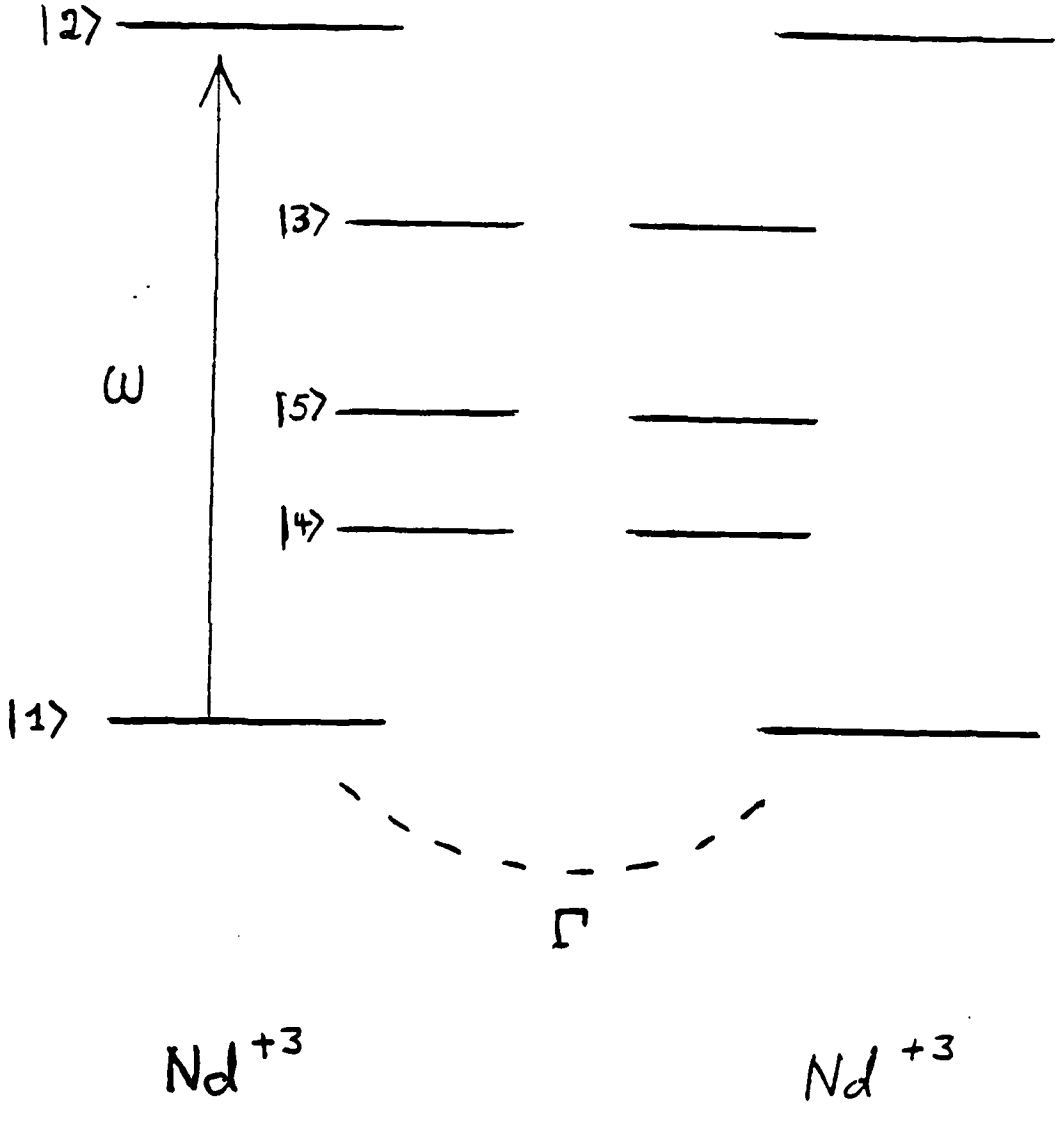

Figure A-1

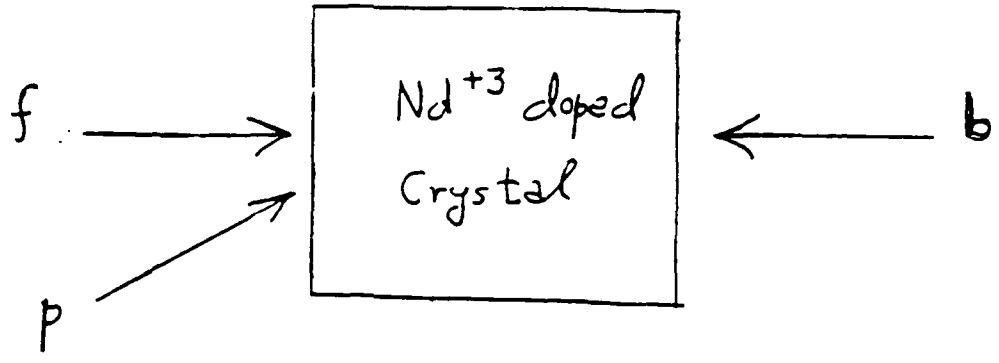

Figure A-2

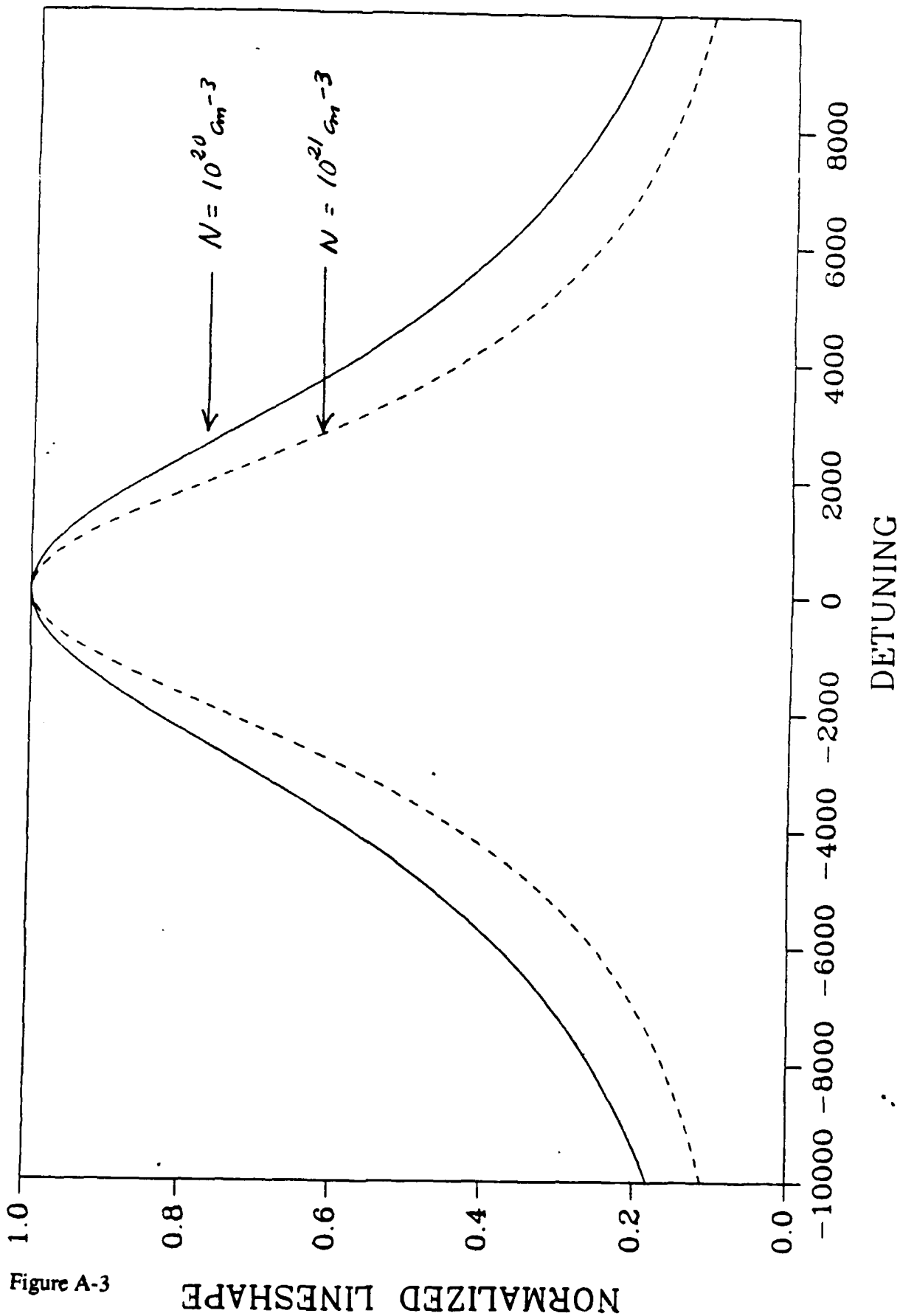
N = 10^20 cm^-3
N = 10^21 cm^-3
NORMALIZED LINESHAPE
1.0
0.8
0.6
0.4
0.2
0.0
-10000
-8000
-6000
-4000
-2000
0
2000
4000
6000
8000
DETUNING

Figure A-3

NORMALIZED LINESHAPE
1.0
0.8
0.6
0.4
0.2
0.0
-10000
-8000
-6000
-4000
-2000
0
2000
4000
6000
8000
DETUNING (HERTZ)
NATURAL
15 KW/cm²
30 KW/cm²

Figure A-4

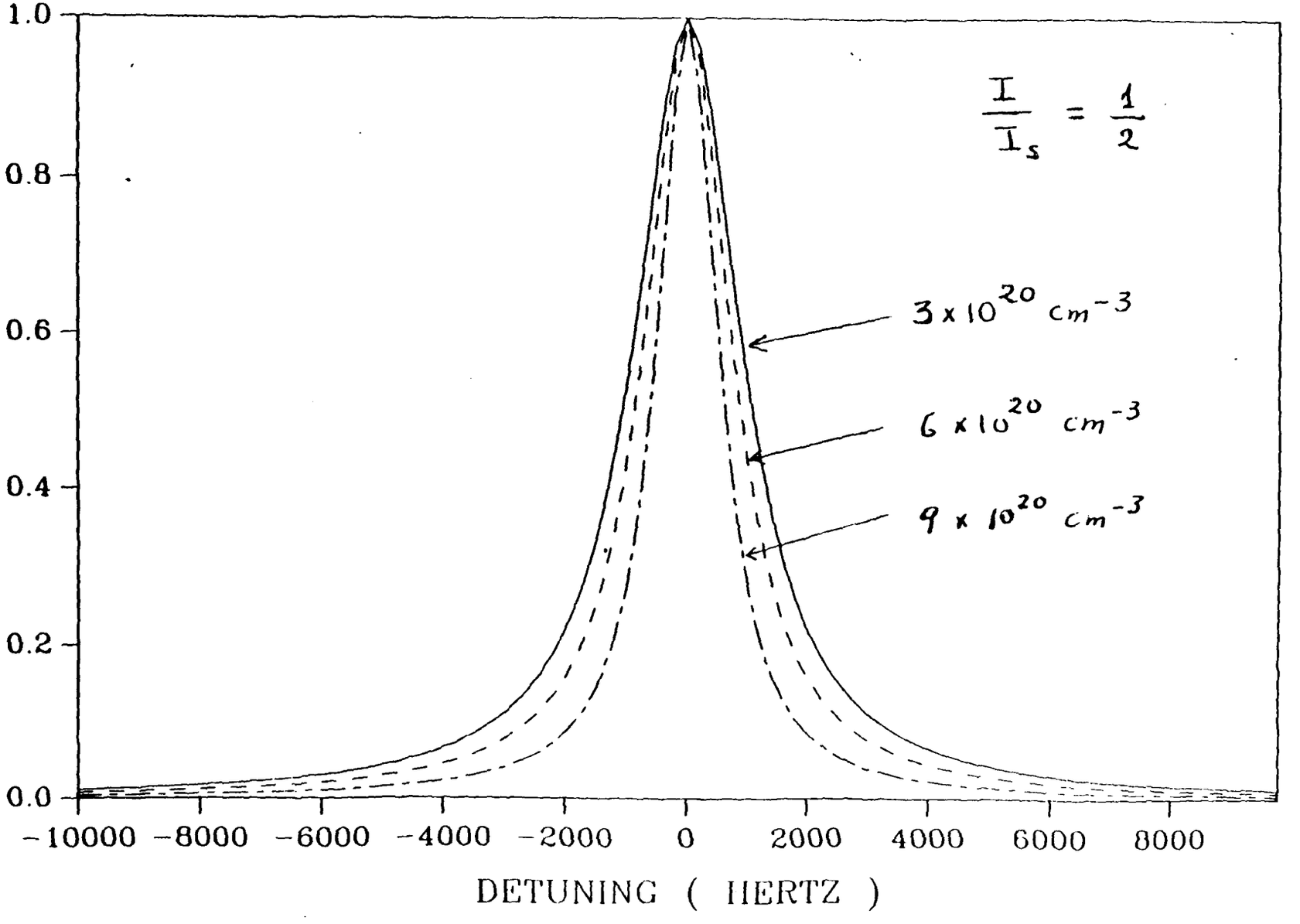
NORMALIZED LINESHAPE
1.0
0.8
0.6
0.4
0.2
0.0
$\frac{I}{I_s} = \frac{1}{2}$
3×10^{20} cm^{-3}
6×10^{20} cm^{-3}
9×10^{20} cm^{-3}
−10000 −8000 −6000 −4000 −2000 0 2000 4000 6000 8000
DETUNING (HERTZ)

Figure A-5

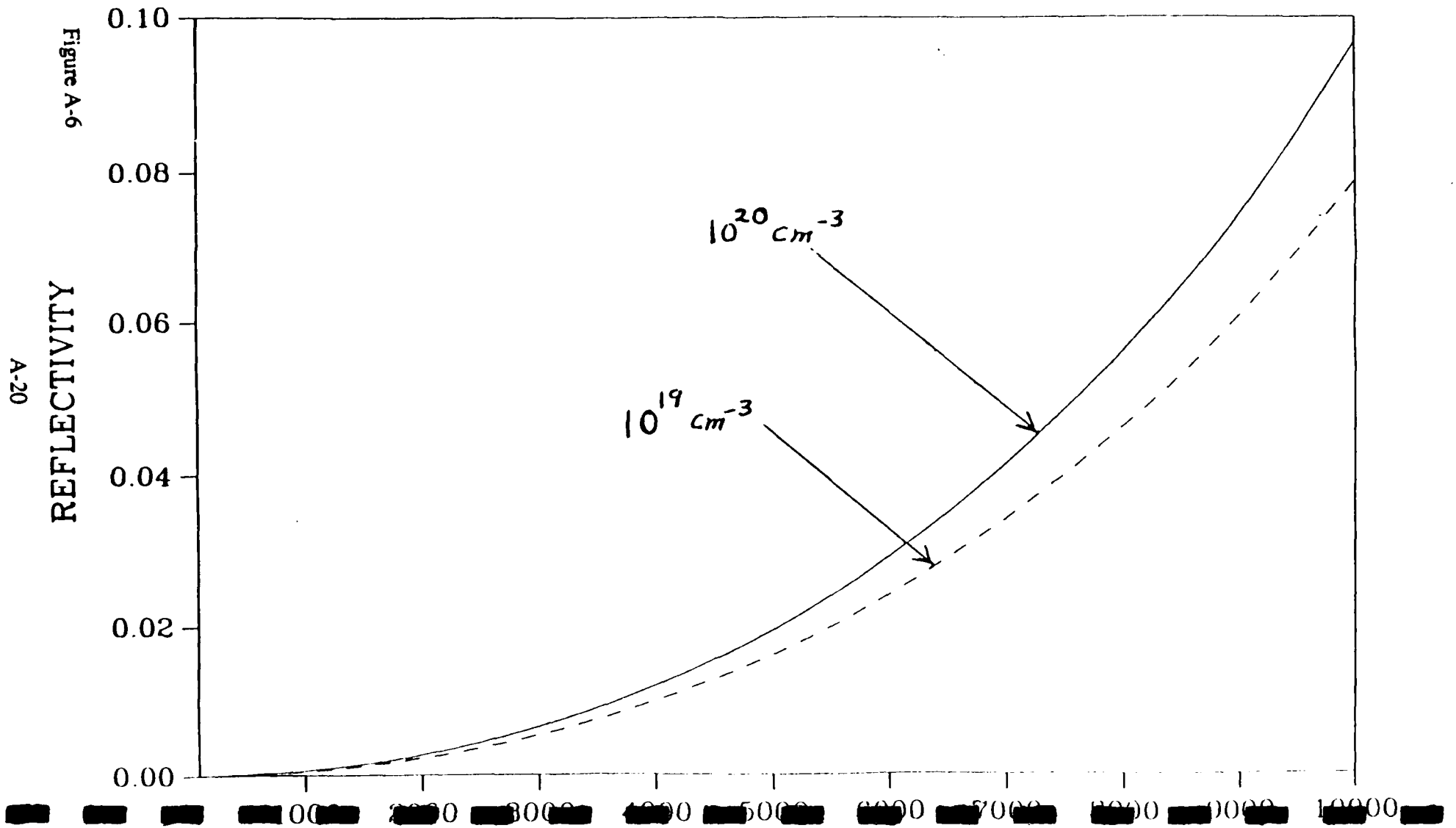

Figure A-6

Abstract of Paper

1988 Annual Meeting of the Optical Society of America

Santa Clara, California

Abstract Deadline: June 3, 1988

Each author of a paper submitted for presentation at the 1988 Annual Meeting is required to furnish a 25-word abstract of the paper as well as a summary of not more than 200 words. The abstracts will appear in the September issue of *Optics News*. The summaries will be printed in the technical digest and distributed at the meeting.

It is expected that contributed papers will represent original contributions to optical science and technology. Subjects treated in second and subsequent papers on the same or similar topics by an author or by a partially or completely overlapping group of authors should represent distinct contributions. Authors are encouraged to submit their full papers for publication in the journals of the Optical Society of America.

As an aid to the program committee in arranging the various sessions, please designate above your abstract, from the following list or from the list of symposia subjects that appears in the call for papers, the field that most closely reflects the subject of the paper:

acousto-optics
adaptive optics
astronomy
atmospheric optics
atomic spectroscopy
biology and medicine
bistability
coherence
color
computational vision
displays
electro-optics
fiber optics
geometrical optics
graded-index materials
gradient index materials
guided-wave optics
holography
image processing
image understanding
information processing
instrumentation
integrated optics
interferometry
laser chemistry
laser fusion
laser propagation
lasers
machine perception
machine vision
materials
medical optics
molecular spectroscopy
multiple excitation of atoms
nonlinear optics
optical communication
optical computing
optical data storage
optical design
optical detectors
optical devices
optical fabrication
optical inspection
optical metrology
optical physics
optical sensors
optical squeezing
optoelectronics
phase conjugation
photography
physical optics
photon counting
physiological optics
radiometry
radiation pressure
remote sensing
solar energy
space optics
speckle
statistical optics
surface physics
thin films
tomography
ultrafast phenomena
x-uv techniques
vision

Equipment will be available at the meeting for projecting 2-inch X 2-inch slides used with 35-mm transparencies and overhead transparencies. Any author requiring another type of projection equipment should so indicate in a letter accompanying this abstract. The finished 2-inch X 2-inch slide should bear a thumb mark, or operator's spot, placed at the lower-left-hand corner of the slide when it is viewed as it will appear on the screen. There will be provision at the meeting for authors to preview and load their 2-inch X 2-inch slides before the sessions in which their papers will be presented.

Please note the instructions that follow regarding preparation of the abstract and the summary. FAILURE TO COMPLY WITH THESE INSTRUCTIONS MAY MAKE IT NECESSARY TO OMIT THE PAPER FROM THE PROGRAM. NO PAPERS WILL BE ACCEPTED AFTER THE DEADLINE DATE.

Abstracts and summaries should be submitted, *as far as possible in advance of the announced deadline date,* to Optical Society of America, 1988 Annual Meeting, 1816 Jefferson Place, N.W., Washington, D.C. 20036.

DIRECTIONS FOR PREPARATION OF ABSTRACT AND SUMMARY

The purpose of the summary is to give (1) a more definite description of the *nature* and *scope* of the paper than can be conveyed in the title and (2) the essential results, insofar as it is possible in the limited space allowed. *Unusual symbols and complex mathematical formulas should not be used. Do not use any undefined acronyms. Do not use abbreviations in your address or elsewhere.* Footnotes should refer only to papers with which the listeners need to be acquainted to understand your paper, as you intend to present it. Do not include more than 5 references. Abstracts appear in the September issue of *Optics News;* summaries are printed in the Annual Meeting Technical Digest available to the registrants at the meeting.

Type DOUBLE SPACE in SINGLE PARAGRAPH, on this form. To ensure that references to this paper and your other publications are consistently entered in computerized indexing systems, please use the form of your given name (first name and initials) that you commonly use in published papers. Please exercise the same caution with the names of your coauthors. Please limit your abstract to 25 words and your summary to 200 words. Word the TITLE clearly so that the abstract may be properly placed in the subject index on the basis alone. The author block follows the title of the paper is to be that of the first-named author. *If you wish to cite another institution, or if the coauthors have different addresses, the condensed names (only) of these institutions may be given as footnotes.* Your full mailing address should be used only in the summary.

All communications concerning the paper will be sent to the first author unless otherwise indicated. The telephone number for the author who should receive all communications should be entered on the abstract in the space provided.

Please designate from the list on the front page of this form or from the list of symposia subjects that appear in the call for papers the one most closely reflect the subject of this paper.

Optical phase conjugation

Theory of optical phase conjugation in coupled ion pairs

Juan F. Lam

Hughes Research Laboratories

A theory of the spectral response and saturation behavior of four-wave mixing mediated by coupled ion pairs is presented.

Send all correspondence to: Juan F. Lam (213)317-5929
(Name) (Telephone number)

Contributed papers may be presented in regular sessions, poster sessions, or demonstration sessions. Full information on each of the sessions appears in the call for papers. Please review the material and check the applicable box.

Check one

This paper is ☐ to be scheduled for poster presentation.
☑ to be scheduled for oral presentation.
☐ to be scheduled for oral presentation only if poster presentation is not possible or desirable.
☐ to be scheduled for poster presentation only if oral presentation is not possible or desirable.
☐ to be scheduled for a demonstration session.

SPONSORSHIP PERMISSION
(For Nonmember Authors)

Contributed papers may be presented at the Annual Meeting by OSA members. A nonmember may present papers only with the sponsorship of an OSA member. I have read this abstract and recommend that it be presented. I agree to sponsor the paper.

MEMBER'S NAME: _____ (print)

MEMBER'S SIGNATURE: _____

Theory of optical phase conjugation in coupled ion pairs

Juan F. Lam

Optical Physics Hughes Research Laboratories

3011 Malibu Canyon Road Malibu California 90265

Coupled ion pairs in solids have played an important role in the development of new solid state lasers. The long range interaction among two or more ions provides a channel for the inversion of population, leading to the discovery of new emission lines. Because of the relatively large optical cross sections, coupled ion pairs may provide new media for the implementation of a solid state phase conjugate mirror. We present a theory of optical phase conjugation, via four-wave mixing, in such novel materials. For a model ion doped solid state system, the calculations give the following conclusions. First, the spectral linewidth is proportional to the square root of the intensity of the radiation field in a inhomogenously broadened material, for fixed ion density. Second, the linewidth decreases with increasing ion density, for fixed intensity level. And last, the saturation intensity also decreases with increasing ion density, for fixed optical intensity. The behavior of the linewidth and the saturation intensity is attributed to the strong interaction among two nearest neighbor ion pairs, which leads to the generation of additional energy dumping pathways.

Work supported by AFOSR under contract #F49620-88-C-0042

AMERICAN INSTITUTE OF PHYSICS
CONFERENCE PROCEEDINGS NO. 172

OPTICAL SCIENCE AND ENGINEERING SERIES 9

ADVANCES IN LASER SCIENCE–III

ATLANTIC CITY, NJ 1987

EDITORS: ANDREW C. TAM, JAMES L. GOLE
& WILLIAM C. STWALLEY

FOUR-WAVE MIXING SPECTROSCOPY OF STATE SELECTIVE COLLISIONS IN GASES AND SOLIDS*

Juan F. Lam
Hughes Research Laboratories
Malibu, California 90265

ABSTRACT

The quantum evolution from a closed to an open system, induced by collisional processes, is presented in the framework of nearly degenerate four-wave mixing (NDFWM) spectroscopy. We show that an open system manifests itself by the appearance of a subnatural linewidth in the spectrum of the phase conjugate signal. Examples are described for sodium vapor in the presence of buffer gases and in Nd^{+3} doped β''-Na-Alumina for high concentration of Nd^{+3} ions.

INTRODUCTION

The discovery of real time phase conjugate optics by Stepanov et al[1] and Woerdman[2] has provided the foundation for the use of four-wave mixing processes as novel spectroscopic tools. The inherent advantages of backward degenerate four-wave mixing over saturated absorption techniques are the existence of Doppler-free spectrum combined with their nearly background-free signals, and the simultaneous measurement of the longitudinal and transverse relaxation times in a single spectral scan. The Doppler free feature was first pointed out by Liao and Bloom[3] in their investigation of resonantly enhanced phase conjugate mirrors. While the simultaneous presence of the longitudinal and tranverse relaxation times in the spectrum were described by Lam et al[4].

Recent studies of collisional processes using four-wave mixing techniques have shed new insights on how collisional processes affect the spectral lineshape[5]. A point in question was the measurement of ground state behavior in spite that the laser was resonant to an optical transition. This fact illustrates the complexity involved in our understanding of collision-induced lineshapes. The objective of this review is to provide an up-to-date account of how the technique of nearly degenerate four-wave mixing probes the evolution of a quantum system in the presence of perturbers[6].

THE TECHNIQUE OF NDFWM SPECTROSCOPY

The technique of NDFWM spectroscopy[4] involves the generation of a travelling wave excitation in the medium (with an atomic resonance ω_o) by the interference of two nearly co-propagating radiation fields oscillating at frequency ω and $\omega+\delta$; respectively. The nearly phase conjugate field is produced by the scattering of a counter-propagating read-out beam off the travelling wave excitation. The nearly conjugate field oscillates at frequency $\omega-\delta$ and travels in opposite direction to the input beam oscillating at $\omega+\delta$.

The small signal spectrum of the phase conjugate fields takes on distinct behavior depending on whether the resonant medium is homogenously or inhomogenously broadened. For the case of a two-level homogenously broadened system, the theoretical spectral lineshape[7] for $\omega=\omega_o$ exhibits a resonance at $\delta=0$ with linewidth given by $.41\gamma$, where γ is the spontaneous decay rate, in the absence of a buffer gas. In the presence of a buffer gas, the NDFWM lineshape shows an effective narrowing in the linewidth. This phenomenon arises from the formation of a long-lived ground-state population excitation formed by the interference of two input radiation fields. The limiting factor is ultimately determined by the transit time of an atom traveling across a laser beam.

The spectral lineshape takes on a similar behavior for the case of an inhomogenously broadened system when $\omega=\omega_o$. It describes the evolution of the spectral lineshape as buffer gas is added to the quantum system. For $\omega=\omega_o$, the lineshape contains two resonances located at $\delta=-2\Delta$ and $\delta=0$. However the linewidths have different behavior in the presence of buffer gases[4]. The resonance line located at $\delta=-2\Delta$ experiences phase interrupting collision, which tends to broaden the linewidth. The resonance line at $\delta=0$ experiences a decoupling of the ground state from the excited state and the width of the line is determined by the lifetime of the ground state (in this case it is the transit time). Δ is the detuning of the pump from resonance.

The spectral behavior of the nearly phase conjugate field illustrates two important points. First, the spectrum contains simultaneous information on the energy and dipole relaxation times, when $\omega=\omega_o$. And second, the spectrum provides a direct measurement of the ground state lifetime in the presence of a buffer gas.

COLLISION-INDUCED RESONANCES IN SODIUM VAPOR

Sodium vapor provides a testing ground for the concept outlined above. We consider the excitation of the D_2 line of sodium using two correlated cw lasers having a bandwidth of approximately 1 Mhz. Since the spectral lineshape depends on the difference of frequency between the two correlated lasers, phase fluctuations are automatically eliminated and the fundamental limitation to the sensitivity of our measurement technique is the time of flight of the atom across the optical beam or the laser linewidth, whichever is larger. Figure 1a shows the spectral behavior of the nearly phase conjugate field for equally polarized input fields and for ω tuned to the $3\ S_{1/2}$ (F=2) to $3\ P_{3/2}$ (F=3) transition[4]. It depicts a

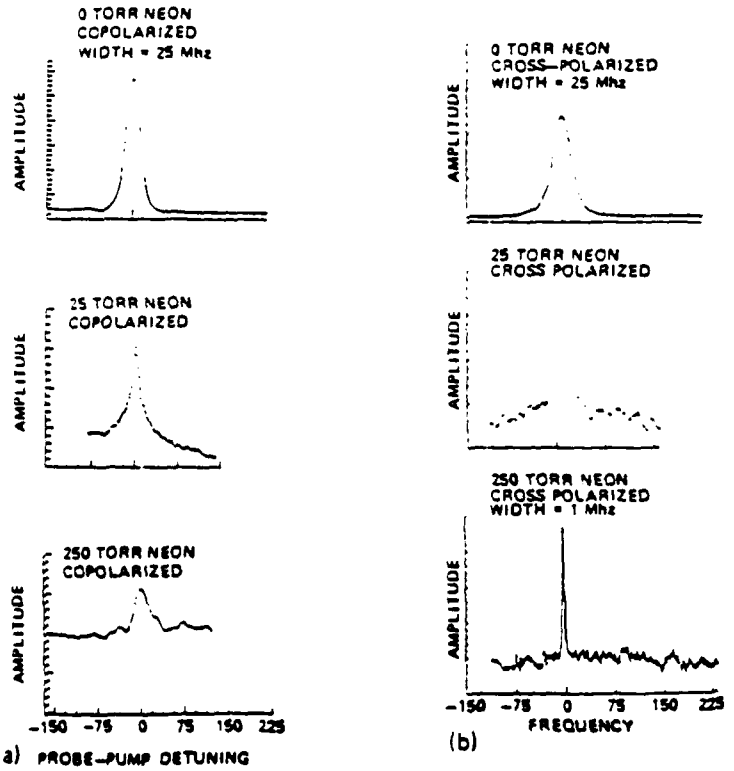

Figure 1. Spectral lineshape of the NDFWM of sodium for (a) co-polarized radiation fields, (b) cross-polarized radiation fields.

narrowing of the linewidth, from 20 Mhz to 1 Mhz, as argon buffer gas is added to the sodium cell. It can also be interpreted as the appearance of a new resonance with a much narrower linewidth. Hence it provides a direct measurement of the effective lifetime of the $3\ S_{1/2}$ state. As the buffer gas pressure increases to 250 torr, the linewidth broadens up due to the excited state.

Figure 1b shows the spectral lineshape for the case where the counterpropagating fields, oscillating at ω, is orthogonally polarized with respect to the field oscillating at $\omega + \delta$. Again as the buffer gas pressure increases, the linewidth decreases from 20 Mhz to 1 Mhz, even beyond the 250 torr regime. The use of cross polarized radiation fields induces a Zeeman coherence grating rather than a population grating[8]. The collision cross section for Zeeman coherences is relatively small, which accounts for the 1 Mhz linewidth even at a pressure of 250 torr. These data provides a glimpse of the simplicity of collisional processes on the NDFWM spectrum. However, Khitrova and Berman[9] has predicted that additional ultranarrow features are also present even in the absence of buffer gases. These features are the result of optical pumping processes that exist when the atomic multipoles are produced by the interference of two orthogonally polarized light beam. A detail account of the theory and experiment related to these novel features are presented by Steel et al.[10].

OPTICAL PAIR INTERACTION IN Nd^{+3}-β"-Na-Alumina

The study of cooperative processes in solids has been a subject of great interest since they determine the practical limitations of solid state optical devices. The technique of NDFWM spectroscopy has provided an initial step toward understanding the role of ion-ion interaction in the spectral lineshape[11]. An interesting candidate material is Nd^{+3} doped β-Na-Alumina[12,13]. For this material, the four-wave mixing process takes place at 575 nm between the $^4I_{9/2}$ and $^4G_{7/2}$ states. However due to the fast nonradiative relaxation rate of the excited state $^4G_{7/2}$, the NDFWM spectrum shows a ultranarrow resonance whose width is determined by radiative decay rate at 1.06 μm (which is of the order of few hundreds μsec). The transition at 1.06 μm is between the $^4F_{3/2}$ and $^4I_{11/2}$ states of Nd^{+3}.

Figure 2a depicts the spectral lineshape of the nearly phase conjugate field for three different pump

intensities. The curve labeled by 25 mW provides a direct measurement of the spontaneous decay rate at 1.06 μm even though the laser used in the experiments has a wavelength of 575 nm. At higher value of the laser intensity, the linewidth broadens up due to pump-induced saturation. Rand et al[11] showed that the intensity behavior of the NDFWM linewidth is consistent with the system being inhomogenously broadened. Figure 2b describes the dependence of the saturation intensity and the linewidth as a function of Nd^{+3} concentration. For densities larger than $.5 \times 10^{21}$ cm^{-3}, both physical parameters experience a decrease. Lam and Rand[14] has shown that this behavior arises from the increase in the pair interaction which creates an additional channel for the electron located in $^4F_{3/2}$ to escape, leading to such a behavior.

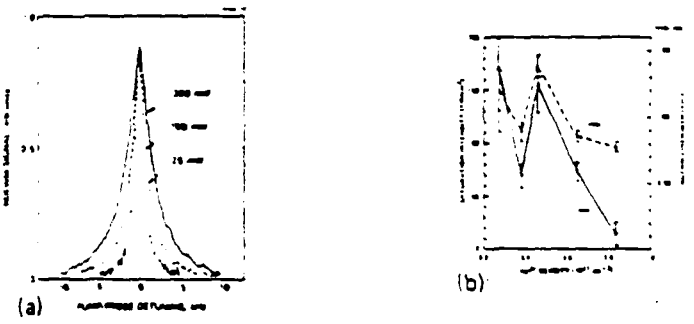

Figure 2. (a)Spectral lineshape for different intensities. (b) Behavior of the saturation intensity and linewidth as a function of dopant density.

SUMMARY

We have described some of the subtle issues associated with spectral lineshape of NDFWM in the presence of collisional processes. The results have demonstrated that collisions do indeed provide a means of separating the ground state from the excited state. The ultranarrow linewidth of the NDFWM spectrum is a manifestation of the ground state effective lifetime.

Work supported by the United States Army Research Office under contract #DAAL03-87-C-0001 and by the Air Force Office of Scientific Research under contract #F49620-85-C-0058

ACKNOWLEDGEMENT

The author gratefully acknowledge the important contributions made by Drs. Duncan Steel, Steve Rand, Ross McFarlane, Steve Turley and Oscar Stafsudd.

REFERENCES

1. Stepanov, B.I., E.V. Ivakin and A.S. Rubanov,, Sov. Phys. Dokl. Tech. Phys. 15, 46 (1971)
2. Woerdman, J.P., Opt. Commun. 2, 212 (1971)
3. Liao, P.F., and D.M. Bloom, Opt. Lett. 3, 4 (1978)
4. Lam, J.F., D.G. Steel and R.A. McFarlane, Phys. Rev. Lett. 49, 1628 (1982)
5. Rothberg, L., in PROGRESS IN OPTICS, ed. by E. Wolf, North Holland, Amsterdam (1987)
6. Berman, P.R., in NEW TRENDS IN ATOMIC PHYSICS, Les Houches, ed. by G. Grynberg and R. Stora, North Holland, Amsterdam (1984)
7. Lam, J.F., D.G. Steel and R.A. McFarlane, in LASER SPECTROSCOPY VII, ed. by T.W. Hansch and Y.R. Shen, Springer Verlag, Berlin (1985)
8. Lam, J.F., D.G. Steel and R.A. McFarlane, Phys. Rev. Lett. 56, 1679 (1986)
9. Khitrova, G. and P.R. Berman, to be published (1988)
10. Steel, D.G., J. Liu, G. Khitrova and P.R. Berman, unpublished (1988).
11. Steel, D.G. and S.C. Rand, Phys. Rev. Lett. 55, 2285 (1985)
12. Boyd, R.W., M.T. Gruneisen, P. Narum, D.J. Simkin, B. Dunn and D.L. Yang, Opt. Lett. 11, 162 (1986)
13. Rand, S.C., J.F. Lam, R.S. Turley, R.A. McFarlane and O.M. Stafsudd, Phys. Rev. Lett. 59, 597 (1987)
14. Lam, J.F. and S.C. Rand, (unpublished 1988)

APPENDIX D

TIME REVERSAL OF MILLIMETER WAVES IN SUPERLATTICES

Juan F. Lam

Hughes Research Laboratories

Malibu, California 90265

The study of quantum confined semiconductor structures has led to the development of electronic and opto-electronic devices with significant improvement in their operating characteristics as compared to those that work on the basis of bulk effects. For example, quantum well lasers that have threshold current density of few hundreds of $\mu W/cm^2$ and can be tuned over few hundreds of nanometers have been demonstrated.[1] On the other hand, novel millimeter sources, such as the High Electron Mobility Transistor, have been implemented by taking advantage of the enhanced electronic properties of these 2-Dim structures.[2]

Nonlinear optical properties of semiconductor superlattices were explored by Tsu and Esaki,[3] who concluded that the optical nonlinearities inherent in these structures were larger by orders of magnitude as compared to those found in bulk GaAs. However little is understood concerning their nonlinear responses to millimeter wave radiation. It was not until recently that experiments[4] have shown the possibility of enhanced nonlinear mixing of two distinct coherent millimeter sources, thus producing a radiation at the difference frequency. Work along a complementary line of exploring the nonlinear index of refraction in graphite suspensions at 94 GHz has shown encouraging results for applications in signal processing.[5]

The objective of this work is to explore the possibility of millimeter wave four-wave mixing in superlattices. This work applies the concept of radiation induced non-parabolicity, through the superlattice effective mass, to the the standard four-wave mixing phase conjugate process. We also delineates the criterion for the observation of phase conjugate waves since the wavelength of the radiation field can be as large as the size of the interaction region.

Before proceeding to the formulation and solution of the problem of nonlinear wave mixing in superlattices, it is important to quantify the boundaries imposed by the wavelength of the radiation field and the size of the sample. Unlike the case in the optical regime, where the wavelength of light is much smaller than that of the sample, there exists

a limitation concerning the validity of the slowly varying envelope approximation in thin samples. This approximation ensures the description of the nonlinear processes in terms of well defined (angular) input and scattered fields. First, consider the linear absorption coefficient, which is determined by free carrier absorption. In the regime of 94 GHz radiation and a collisional damping time of .1 psec, the absorption coefficient is $2.24mm^{-1}$. Second, the SVEA implies that the envelope of the field varies slowly compared to a wavelength of radiation inside the medium. In the case of 94 GHz radiation propagating inside, say, a GaAs-AlGaAs superlattices, the SVEA is valid provided that the nonlinear interaction length is larger than 7.8 mm. These estimates aasume that the transverse dimension of the sample is large compared to the wavelength corresponding to 94 GHz.

The starting point of our analysis is the equation of motion for the charge carriers in the superlattice structure of periodicity d. Assuming that the one-band Kronig-Penney model is valid, the velocity of the charge carriers moving along the direction of the superlattice growth axis is described by

$$\frac{dv}{dt} + \frac{v}{\tau} = \frac{qE(t)}{m_z} \times cos\frac{qd}{\hbar}\int E(t')dt' \tag{1}$$

where m_z is the superlattice effective mass at the Γ point. The radiation field consists of strong counterpropagating pump fields, E_f and E_b; and a weak incident probe and backscattered fields, E_p and E_s. We shall assume that all radiation fields oscillate at frequency ω. Equation (1) can be solved in the following manner. Let us write the total radiation field as $E = E_0 + \lambda E_1$, where $E_0 = E_f + E_b$, $E_1 = E_p + E_s$, and λ is a dummy variable that keeps track of the strength of each quantity. That is, E_0 is much larger than E_1. In the same manner, one assumes that the carrier velocity is given by $v = v_0 + \lambda v_1$. Inserting this prescription into Eq.(1), one obtains the following equations

$$\frac{dv_0}{dt} + \frac{v_0}{\tau} = \frac{qE_0(t)}{m_z} \times cos\frac{qd}{\hbar}\int E_0(t')dt' \tag{2a}$$

$$\frac{dv_1}{dt} + \frac{v_1}{\tau} = \frac{qE_1(t)}{m_z} \times cos\frac{qd}{\hbar}\int E_0(t')dt'$$

$$-\frac{qE_0(t)}{m_z}\times\frac{qd}{\hbar}\int E_1(t')dt'\times sin\{\frac{qd}{\hbar}\int E_0(t')dt'\} \tag{2b}$$

where Eq.(2a) describes the evolution of the strong radiation fields, and Eq.(2b) describes the process of the interference between the strong and weak radiation fields. The first term on the right hand side of Eq.(2*b*) results in changes in both the linear index of refraction and the absorption coefficient of E_1 due to the presence of E_0. While the second term describes the spatial interference between E_1 and E_0, resulting in the formation of spatial gratings. This term is the mechanism responsible for the coherent generation of backscattered field due to Bragg scattering. Furthermore, Eqs.(2) assumes the undepleted pump approximation. The nonlinear current density is given by

$$J = qnv \tag{3}$$

which enters into the Maxwell's equations as a source term.

The evolution of a new radiation field is determined by the solution of Eq.(2b). The solutions to Eq.(2a) were determined by Lam et al.[5] and predicts the effect of induced transparency, within the one-band Kronig-Penney model for the superlattice. Equation (2b) has the following solution for the case of degenerate four-wave mixing

$$\begin{aligned} v =& \frac{q}{2m_z}\times\frac{E_s exp(i\phi_s)}{\frac{1}{\tau}-i\omega}\times\{A-iB\} \\ &+\frac{q}{2m_z}\times\frac{E_p^* exp[i(\phi_f+\phi_b-\phi_p)}{\frac{1}{\tau}-i\omega}\times C \end{aligned} \tag{4}$$

where

$$\begin{aligned} A =& J_0(\Omega_f)J_0(\Omega_b) \\ &+2\sum_{n=1}^{\infty}J_{2n}(\Omega_f)J_{2n}(\Omega_b)cos(2n\Delta\varphi) \\ &-2\sum_{n=0}^{\infty}J_{2n+1}(\Omega_f)J_{2n+1}(\Omega_b)cos[(2n+1)\Delta\varphi] \end{aligned}$$

$$B = -\Omega_f\{J_0(\Omega_f)J_1(\Omega_b)sin\Delta\varphi$$

$$+\sum_{n=1}^{\infty}[J_{2n-1}(\Omega_f)+J_{2n+1}(\Omega_f)]J_{2n}(\Omega_b)sin2n\Delta\varphi$$
$$+\sum_{n=1}^{\infty}J_{2n-1}(\Omega_b)J_{2n}(\Omega_f)sin(2n-1)\Delta\varphi$$
$$+\sum_{n=1}^{\infty}J_{2n-1}(\Omega_b)J_{2n}(\Omega_f)sin(2n+1)\Delta\varphi\}$$
$$-(b,f)\rightarrow(f,b)$$

$$C=-\{\Omega_f J_1(\Omega_b)[J_0(\Omega_f)+J_2(\Omega_f)]+\Omega_b J_1(\Omega_f)[J_0(\Omega_b)+J_2(\Omega_b)]$$

with $\varphi=(k_b-k_f)z$. $J_n(x)$ is the Bessel function of order n

The carrier velocity has two components. The first one, proportional to E_s is just the modification due to the presence of the strong field E_0. The second component, proportional to E_p^*, results from the nonlinear mixing of E_p and E_0. The latter is responsible for the generation of time reversed or phase conjugate radiation field. The terms on the right hand side of A and B have very simple physical interpretation. The terms which are independent of $\Delta\varphi$ correspond to intensity changes. While the terms that depends on $\Delta\varphi$ are due to the interference between E_f and E_b, resulting in the formation of a spatial grating with periodicity $\lambda/2n$. n being the index of refraction of the material. The quantity C describes the coupling strength of the nonlinear mixing process.

The current density that is obtained from the carrier velocity is now used to obtain the equation describing the spatial evolution of the radiation field amplitudes. Assuming that the size of the sample validates the use of the SVEA, one derives the following coupled wave equations

$$i\frac{dE_s}{dz}=\alpha E_s+\beta E_p^* \qquad (5a)$$
$$i\frac{dE_p^*}{dz}=-i\alpha^* E_p*-i\beta^* E_s \qquad (5b)$$

where

$$\alpha=-\frac{\omega}{c}\frac{\omega_p^2}{i\omega(\frac{1}{\tau}-\omega)}\frac{\langle(A-iB)\rangle}{2}$$
$$\beta=-\frac{\omega}{c}\frac{\omega_p^2}{i\omega(\frac{1}{\tau}-\omega)}\frac{\langle C\rangle}{4}$$

where $\omega_p = \sqrt{4\pi nq^2/\epsilon m_z}$ is the plasma frequency. ϵ is the dielectric constant of the material. The notation $\langle -- \rangle$ denotes the spatial averaging over $\lambda/2n$, which is the minimum requirement for macroscopic nonlinear optical phenomena to occur. That is, if the sample dimension is as large or larger than $\lambda/2n$, the generated radiation field is described in terms of spherical waves emanating from a point source.

The solution of Eqs.(5) is

$$E_s(0) = -\beta E_p^*(0) \frac{1 - exp(-2ibL}{a - b + \alpha - (a + b + \alpha)exp(-2ibL)} \tag{6}$$

where $a = Real(\alpha)$ and $b = \sqrt{(Real(\alpha))^2 + |\beta|^2 - |\alpha|^2}$. L is the nonlinear interaction length. Figure 1 shows the reflectivity $R = |E_s(0)/E_p(0)|^2$ as a function of the Ω_f, assuming that $E_f = E_b$. The oscillatory behavior of the reflectivity is a consequence of the functional dependence of the Bessel functions. A saturation behavior is obtained at $\Omega_f = 2$.

A feature of degenerate four-wave mixing process is the existence of self-oscillation or mirrorless oscillation. In our case the condition for such a phenomenon to occur is given by

$$tanbL = \frac{b}{\alpha} \tag{7}$$

The result of Eq.(7) indicates that large phase conjugate reflectivity is possible provided that certain stringent conditions are satisfied for the lengthe of the nonlinear medium and and intensity of the pump fields.

In conclusion, we have studied the possibility of producing a degenerate four-wave mixing process in a superlattice. We showed that it is possible to achieve reasonable reflectivity of few percents. Furthermore, under certain conditions, a weak probe field can generate large values of the reflected field. What remains to be considered is the practical limitation in producing a superlattice structure which is large enough for macroscopic nonlinear phenomena to take place. This will remain a challenge for the epitaxial growth techniques.

* This work is supported by the Air Force Office of Scientific Research

ACKNOWLEGEMENT

The author thanks Prof. Harold Fettermann for many valuable discussions concerning the physics of millimeter waves.

REFERENCES

1. D. Mehuys, M. Mittelstein, A. Yariv, R. Safarty and J.E. Ungar, Electron. Leet. **25** 145, (1989)
2. U.K. Mishra, A.S. Brown, S.E. Rosenbaum, C.E. Hooper, M.W. Pierce, M.J. Delaney, S. Vaughn, and K. White, IEEE Electron. Device Lett. **9**, 647 (1988)
3. R. Tsu and L. Esaki, Appl. Phys. Lett. **19**, 246 (1971)
4. M.M. Kechiev; A.A. Kostenko, V.D. Durek, O.A. Kuznetsov, V.A. Tolomasov, O.N. Filatov, G.I. Khlopov, and V.P. Shestopalov, Sov. Phys. Semicond. **17**, 1024 (1983)
5. B. Bobbs, R. Shih, H.R. Fetterman, and W.W. Ho, Appl. Phys. Lett. **52**, 4 (1988)
6. J.F. Lam, B.D. Guenther, and D. Skatrud, Appl. Phys. Lett. 1989

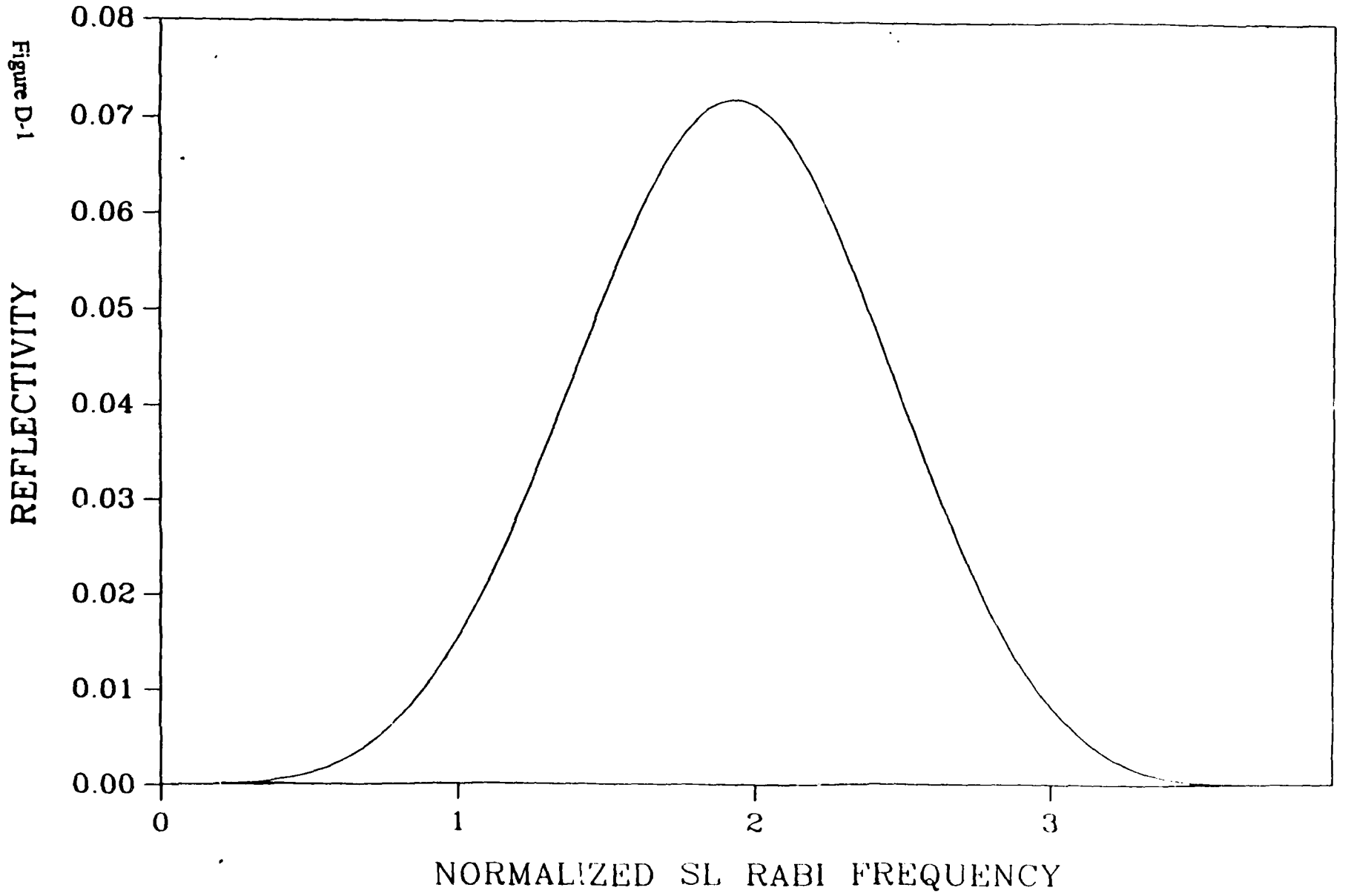
0.08
0.07
0.06
0.05
0.04
0.03
0.02
0.01
0.00
REFLECTIVITY
0
1
2
3
NORMALIZED SL RABI FREQUENCY

Figure D-1

APPENDIX E

MODULATION PROPERTIES OF MILLIMETER WAVES IN SEMICONDUCTOR SUPERLATTICES

Juan F. Lam

Hughes Research Laboratories

Malibu, California 90265

ABSTRACT

We report new results on the modulation characteristics of semiconductor superlattices in the millimeter wave regime. FM modulation is achieved if a static electric field is applied along the superlattice growth direction. AM modulation is predicted for an applied AC electric field.

Recently, several experiments[1-4] have been performed that probe the material requirements and their suitability for use in the far infrared regime. The demonstration of difference frequency generation in Si/Ge superlattices, the measurement of the nonlinear index of refraction and phase conjugation at 94 GHz in graphite suspensions indicated that nonlinearities in the millimeter range could be quite large, in comparison to those found in the optical regime. We reported a detailed study of millimeter wave nonlinearities in semiconductor superlattices, and predicted giant third order susceptibilities [5]. We carried out an analysis that describes the generation of phase conjugate waves in these customized materials.[6] In view of the importance of millimeter wave for signal processing purposes, we extend our previous studies to the case of modulation properties of these materials.

The starting point in our analysis is the coupled charge transport and crystal momentum equations for the motion of the Bloch carriers directed along the direction of the superlattice growth (labelled by the subscript z).

$$\frac{dv_z}{dt} + \frac{v_z}{\tau} = \frac{d}{dt}\left\{\frac{1}{\hbar} \times \frac{\partial U}{\partial k_z}\right\} \tag{1}$$

$$\hbar \times \frac{dk_z}{dt} = q(E_o + E(t)) \tag{2}$$

where v_z is the carrier velocity, τ is the carrier momentum relaxation time[7] along z, k_z is the crystal momentum, E_o is the applied electric field, $E(t)$ is the radiation field with polarization state oriented along z, q is the charge of the carrier and U is the superlattice band structure.

In the one-band or Kronig-Penney model, U takes a simple form

$$U = U_0\{1 - \cos k_z d\} \tag{3}$$

where d is the superlattice period. Equations (1), (2) and (3) can be combined together to yield the following expression

$$\frac{dv}{dt} + \frac{v}{\tau} = \frac{q(E_o + E(t))}{m_z} \tag{1a}$$

where the superlattice effective mass m_z is given by

$$\frac{1}{m_z} = \frac{U_0 d^2}{\hbar^2} \times \cos\frac{qd}{\hbar}\int (E_o + E(t'))\,dt' \tag{4b}$$

Equations (4) describes the physical origin of the nonlinearity and modulation properties in semiconductor superlattices. That is, both phenomena arise from the artificially induced nonparabolicity, through the superlattice effective mass. In the absence of E_o and $E(r,t)$, m_z becomes the superlattice mass, m_o, at the high symmetry point. The nonlinear current density is given by

$$J = nqv_z \tag{5}$$

where n is the carrier concentration.

Equation (1) is solved exactly for arbitrary values of E_o and $E(t)$. Simple expressions are physically transparent for the case where E_o is small compared to the magnitude of $E(t) = Acos(kx - \omega t)$. We shall restrict to this important but realistic regime. Consider first the case of a static electric field. Using the relation between the trigonometric and Bessel functions, the nonlinear current density is given by

$$J = (\frac{\omega_p}{\omega})A[J_0(R) + J_1(R)]cos(kx - \omega t)cos(\Omega t) \tag{6}$$

where $\omega_p = 4\pi nq^2/m\omega$ is the plasma frequency, $J_0(R)$ and $J_1(R)$ are the zeroth and first order Bessel functions with argument $R = qdA/\hbar\omega$, and $\Omega = qdE_o/\hbar$ is the static field induced Rabi frequency.

Equation (6) has a very simple physical interpretation. The use of a static electric field and an applied radiation field gives rise to a frequency modulation (FM) of the radiation field. In arriving the above stated results, we assume that $\omega\tau$ is much greater than unity.

Next, we consider the case of an applied oscillating field, $E_o = Bcos\beta t$ and an input radiation field $E(t) = Acos(kx - \omega t)$. The solution of Eq.(4) is given by

$$J = (\frac{\omega_p}{\omega})A[J_0(R) + J_2(R)]sin(kx - \omega t)cos(ssin(\beta t)) \tag{7}$$

where $s = \Omega/\beta$ is the normalized applied electric field induced Rabi frequency.

Equation (7) implies that the application of an oscillating electric field gives rise to an amplitude modulated (AM) radiation field.

In conclusion, we explored the distinct possibility of modulation techniques in semiconductor superlattices, and found that these materials possess unique properties. We predict the existence of FM and AM modulation under the condition of a static and an oscillating electric field oriented along the superlattice growth axis. Interestingly enough, these results could be applied to current signal porcessing operation in the millimeter wave regime.

ACKNOWLEDGEMENT

This work is supported by the Air Force Office of Scientific Research.

REFERENCES

1. A.A. Kostenko, O.A. Kuznetsov, V.A. Tolomasov, O.N. Filatov, G.I. Khlopov, and V.P. Shestopalov, Sov. Phys. Dokl. **28**, 670 (1983)
2. M.M. Kechiev, A.A. Kostenko, V.D. Kurek, O.A. Kuznetsov, V.A. Tolomasov, O.N. Filatov, G.I. Khlopov, and V.P. Shestopalov, Sov. Phys. Semicond. **17**, 1021 (1983)
3. B. Bobbs, R. Shih, H.R. Fetterman and W.H. Ho, Appl. Phys. Lett. **52**, 1 (1988)
4. H.R. Fetterman, et al, Phys. Rev. Lett. **65**, 579 (1990)
5. J.F. Lam, B.D. Guenther and D.D. Skatrud, Appl. Phys. Lett. **56** , 773 (1990)
6. J.F. Lam, "Time reversal of millimeter waves in superlattices" (1990)

APPENDIX F

THEORY OF STIMULATED SCATTERING PHASE CONJUGATION IN RESONANT SYSTEMS

Juan F. Lam

Hughes Research Laboratories

Malibu , California 90265

ABSTRACT

A theory of self-pumped phase conjugation in resonant systems is presented. We postulate that stimulated backward two-wave mixing is the mechanism leading to the production of phase conjugate waves. We show that the conjugation process has a threshold behavior and the phase conjugate wave has an intrinsic frequency shift as a function of the pump intensity.

I. INTRODUCTION

Self-pumped phase conjugation (SPPC) has been a subject of great interest due to its application in the area of optical signal processing[1]. The phenomenon of SPPC was first discovered when Stimulated Brillouin scattering was generated in a nonlinear medium [2]. They found surprisingly that the backscattered radiation had the property for correcting any artificial aberration imposed on the input pump field. This observation led to the development of phase conjugate optics as an integral part of quantum electronics. The success of SPPC lies in its simplicity for the implementation of phase conjugate mirrors. That is, a single input pump field can generate a backward propagating radiation field, whose optical phase is the negative of that of the input pump field provided specific energy and momentum conservation laws are satisfied. This general remark needs to be quantified dependent upon the circumstances of the experimental set-up. For example, experiments performed in a geometry where an optical cavity is present might also involve the process of four-wave mixing which will produce phase conjugate fields. However even in this case, given a single input pump field, stimulated scattering appears to play the dominant role in producing the additional two other coherent beams which are required for the four-wave mixing process to take place.

Subsequently , the same phenomenon has been replicated in photorefractive materials[3], in Kerr media[4], saturable absorbers[5] and lately in atomic vapor[6]. Self-pumped phase conjugation in photorefractive materials arises from the amplification of noise by means of coherent energy transfer between the incident pump field and the scattered field.[7] The mechanism responsible for net gain is the formation of a nonlocal traveling wave grating, arising from the diffusion and drift of charge carriers. An internal space charge field is produced by the spatial separation of the photo-ionized carriers from the defects present in the electro-optic crystals. The change of the index of refraction, which is proportional to the intrinsic space charge field, is 90 degree out of phase with respect to the intensity interference pattern. The scattering of the pump field from the refractive index generates

a coherent amplification of the scattered noise. Although this simple physical picture is acknowledged to be correct, there are complex behaviors such as intrinsic frequency shifts and instabilities that obscure the interpretation of the experimental data. The production of phase conjugate fields in a Kerr medium was observed in the presence of an optical cavity. In this case, the physics became clear. The pulsed laser induced stimulated Brillouin scattering which is allowed to bounce back and forth inside the resonator. Hence the counterpropagating beams in the resonator constitute the pump beams in the standard four-wave mixing configuration. Phase conjugate fields arise from the scattering of one of the counterpropagating beam from the interference pattern generated by the input pump and the other one of the intracavity beams. Intrinsic to the stimulated Brillouin scattering, there exists a large frequency shift of the order of one Ghz. In a similar manner, SPPC in sodium vapor was also observed in an intracavity configuration. Identical argument can be given to ascertain the origin of phase conjugate fields in the latter case.

In spite of these studies, little is understood concerning the role of stimulated scattering processes in the generation of phase conjugate fields in resonant materials. The experimental discovery of nearly phase conjugate wave in rhodamine 6 G by Koptev et al [4] led to the understanding that saturable absorbers impose a large frequency shift (few hundreds angstroms) between the input light and the scattered light. A preliminary theoretical model by Lam et al [8] appears to confirm the experimental findings. Furthermore, this theory predicted that even two-level systems do indeed generate gain in the absence of population inversion, leading to the appearance of phase conjugate fields. In addition, careful experiments[8] performed on rhodamine 6G indicated that the spectrum of the spontaneous emission noise was much wider than the spectrum arising from lasing action. And the phase conjugate spectrum mimcs that of the spontaneous emission. These observations raise the question whether or not SPPC is a universal phenomenon; i.e. can this effect be generated in any nonlinear optical material ?. The objective of this work is to show that the fundamental physical mechanism giving rise to SPPC is stimulated two-wave

mixing. This is the same mechanism proposed to explain the origin of phase conjugate waves in photorefractive materials[7]. Furthermore, we shall show that the mechanism can be operative in any resonant systems. Hence, the objective of this work is to extend the results [8] and put into a coherent form a physical description of the fundamental physics of phase conjugate field generation arising from resonant systems.

Section II provides an intuitive physical description of the scattering mechanisms responsible for the generation of phase conjugate fields. This section discusses, in terms of simple physical arguments, criteria that are necessary for the stimulated two-wave mixing to occur. Utilization of the basic concepts such as conservation laws lead to a clear understanding of the scattering processes. The discussion set the stages for the detail calculation of the nonlinear response function, which is the objective of Section III. We assume that the resonant medium can be described in terms of a set of homogenously broadened two-level systems. We calculate the medium response using the density operator formalism, and couple the results with the wave equations in a self-consistent manner. Section III is included for sake of completeness. The results for the case of pump-probe interactions have been extensively analyzed previously[9-15]. Section IV provides a physical model for the generation of phase conjugate fields in resonant systems. This model gives additional insight into the nonlinear processes responsible for the origin of the phase conjugate field in stimulated scattering. A description of the nonlinear gain and dispersion functions for both the backward and forward scattered lights is presented. We will show that the optimum gain condition determines the frequency of the scattered field. A summary of our results is presented in section V.

II. PHYSICAL PICTURE

The dynamics of backward stimulated two-wave mixing relies on the Rayleigh scattering to provide the noise source required in the formation of an interference pattern. Consider a pump field E_p incident upon an absorbing medium. The simultaneous absorption of the pump field and the generation of a fluorescence emission field produces an isotropic distribution of scattered fields. However only the component of the scattered field that is counterpropagating to that of the pump can generate, in general, a traveling wave grating (assuming that they do not coincide in frequency) . Subsequent scattering of the pump field reinforces and produces additional backscattered field E_s. Backward scattering possesses the advantage of achieving maximum spatial overlap between the incident and generated radiation fields. In analogy to the Zeldovich's argument of phase conjugation via stimulated Brilloiun scattering, the component of the backscattered field that achieves maximum transverse spatial overlap with the input pump field is the phase conjugate field.[2]

The qualitative description given above can be quantified in the following manner. Consider the work done by the radiation field $E(r,t)$ which is defined by $W = < J.E >$, where J is the nonlinear current density induced by the radiation field, and $< -- >$ stands for the spatial average over one wavelength of light. The spatial averaging is required since macroscopic optical phenomena can only take place for interaction volume larger than one wavelength of light. Energy transfer between the incident pump field and the scattered field can only take place provided that $W \neq 0$. This fact can only be satisfied if there exists certain phase relationship between J and E. Figure 1 illustrates the essence of this discussion. At the top center of the figure is a picture of the intensity distribution for a period of one wavelength. On the left hand and right hand columns of the figure, the medium response, the current density and the work done by the field are illustrated from top to bottom. Now, the work done is just the total area under the curve. If the area is nonzero, then the work is finite. In this case energy transfer occur. As one can see nonzero

work is possible provided that the medium response is 90 degree out of phase with respect to intensity interference pattern, as seen from the figures in the left column. If the medium response is in phase with the intensity pattern, then the work done is identically equal to zero, as shown in the figures on the right column.

The important question to ask is how this simple picture relates with the problem encountered in resonant systems. These systems are known to possess two components in their optical responses to radiation fields. They are the absorption coefficient and the index of refraction. Gain does not occur except under conditions of population inversion or nonlinear wave mixing. The fundamental of energy transfer process can be understood in the framework of the dressed atom. The effect of a strong pump field is to induce changes in the eigenstates of the atom. Effectively the radiation field breaks the degeneracy of the eigenfunction in the following manner. The electric dipole interaction with the radiation field mixes the atomic eigenstates into a coherent superposition. Each atomic energy level acquires both a symmetric and an anti-symmetric wavefunctions, whose separation is the Rabi flopping frequency. Hence for an initial two-level system, the application of a strong radiation field gives rise to a 4-level system. The process of energy transfer can then be described in terms of a Raman-type interaction in which the absorption and reemission of the pump field gives rise to an amplification of the scattered field.

III. FORMULATION OF THE PROBLEM

To quantify these ideas we carried out a calculation of the spectral lineshape gain for an ensemble of homogenously broadened two-level atoms in the presence of an input pump field E_p, oscillating at a frequency ω, and a backscattered field E_s, with a spectrum of oscillating frequencies $\omega + \delta$. The latter is due to the noise properties of scattered radiation, as remarked in the previous section. We shall allow δ to vary in order to find out the condition under which the backscattered signal achieves an optimum gain, hence taking away energy from the pump. Furthermore it is assumed the magnitude of E_p is much stronger than that of E_s;i.e. pump depletion is not taken into account. Starting from the density matrix equations, the strategy we shall follow is to solve exactly the response of the medium to E_p and then use the solutions to find the response of the medium to the wave mixing process due to E_p and E_s. The nonlinear wave mixing problem is then reduced to a self-consistent coupling between the density matrix equations and the Maxwell's equations.

The density operator ρ obeys the quantum transport equation

$$i\hbar\frac{d\rho}{dt} = [H_o, \rho] + [V, \rho] + i\hbar(\frac{d\rho}{dt})_{rel} \tag{1}$$

where H_o is the unperturbed Hamiltonian, $V = -\mu E$ is the electric dipole coupling to the radiation field, and the last term on the right hand side is the relaxation due to reservoir coupling. In a closed two-level system (no state selective collisions present), the last term takes on a very simple form for the case of a two-level system. If $| 1 > and | 2 >$ are the ground and excited states of H_o; then

$$(\frac{d\rho_{11}}{dt})_{rel} = \gamma\rho_{22} \tag{2a}$$

$$(\frac{d\rho_{22}}{dt})_{rel} = -\gamma\rho_{22} \tag{2b}$$

$$(\frac{d\rho_{12}}{dt})_{rel} = -\frac{\gamma}{2}\rho_{12} \tag{2c}$$

where γ is the radiative decay rate of the excited state. Using the assumption that the incident pump field is much stronger than the scattered field, one can write the electric dipole coupling in the following manner

$$V = -\mu E_p(r,t) - \mu E_s(r,t) \tag{3}$$

We shall first solve the density operator equation for E_p exactly, and then use the solution to solve the density operator equation for E_s.

The components of the density operator equation for the pump field E_p are given by

$$\frac{d\rho_{11}^{(0)}}{dt} = \gamma\rho_{22}^{(0)} + \frac{1}{i\hbar}\{V_{12}^{(0)}\rho_{21}^{(0)} - \rho_{12}^{(0)}V_{21}^{(0)}\} \tag{4a}$$

$$\frac{d\rho_{22}^{(0)}}{dt} = -\gamma\rho_{22}^{(0)} - \frac{1}{i\hbar}\{V_{12}^{(0)}\rho_{21}^{(0)} - \rho_{12}^{(0)}V_{21}^{(0)}\} \tag{4b}$$

$$\{\frac{d}{dt} + \frac{\gamma}{2} - i\omega_o\}\rho_{12}^{(0)} = \frac{1}{i\hbar}V_{12}^{(0)}(\rho_{22}^{(0)} - \rho_{11}^{(0)}) \tag{4c}$$

where ω_o is the two-level transition frequency and the superscript , (0), stands for the equations and solutions pertinent to E_p. That is, $V_{12}^{(0)} = -\mu_{12}E_p(r,t)$ is the potential energy due to the electric dipole moment μ_{12} coupled to E_p.

In a similar manner, the components of the density operator equation for the scattered field E_s are given as

$$\frac{d\rho_{11}^{(1)}}{dt} = \gamma\rho_{22}^{(1)} + \frac{1}{i\hbar}\{V_{12}^{(0)}\rho_{21}^{(1)} - \rho_{12}^{(1)}V_{21}^{(0)}\} + \frac{1}{i\hbar}\{V_{12}^{(1)}\rho_{21}^{(0)} - \rho_{12}^{(0)}V_{21}^{(1)}\} \tag{5a}$$

$$\frac{d\rho_{22}^{(1)}}{dt} = -\gamma\rho_{22}^{(1)} - \frac{1}{i\hbar}\{V_{12}^{(0)}\rho_{21}^{(1)} - \rho_{12}^{(1)}V_{21}^{(0)}\} - \frac{1}{i\hbar}\{V_{12}^{(1)}\rho_{21}^{(0)} - \rho_{12}^{(0)}V_{21}^{(1)}\} \tag{5b}$$

$$\{\frac{d}{dt} + \frac{\gamma}{2} - i\omega_o\}\rho_{12}^{(1)} = \frac{1}{i\hbar}V_{12}^{(0)}[\rho_{22}^{(1)} - \rho_{11}^{(1)}] + \frac{1}{i\hbar}V_{12}^{(1)}[\rho_{22}^{(0)} - \rho_{11}^{(0)}] \tag{5c}$$

where $V_{12}^{(1)} = -\mu E_s(r,t)$ is the potential energy of the electric dipole moment μ_{12} coupled to E_s.

The density operator equations have very simple physical interpretation. The right hand side of the equations for the population of the ground and excited states describe the work done by the field on the atoms. The right hand side of the equations for the optical coherence describe the coherent scattering of light from induced gratings in the population difference.

The polarization density that contributes to the evolution of $E_s(r,t)$ is defined by

$$P(r,t) = Trace(\rho^{(1)}\mu) = \rho_{12}^{(1)}\mu_{21} + h.c. \tag{6}$$

where h. c. stands for the hermitean conjugate of the first term. The polarization density enters into the Maxwell's equations as a source term. The wave equation can be reduced into a simple form if one assumes that the envelope of the radiation field varies slowly on a spatial scale as compared to the wavelength of light. This is just the slowly varying envelope approximation. That is, if $E(r,t) = (1/2)\int d\omega A(r,\omega)expi(kr - \omega t) + c.c.$, then one can neglect the second order spatial derivative, along the direction of k, of A in the wave equation. Using this assumption , one obtains the following expression for the Fourier envelope

$$\frac{dA}{dr} = i\epsilon(\frac{\omega}{c}) < P(r,t)exp(-i(kr - \omega t)) > \tag{7}$$

where $\epsilon = 1$ for forward scattered light and $\epsilon = -1$ for backward scattered light. The boundary conditions for the problem is the following. For the forward scattered light, a finite amplitude of the radiation field is given at the entrance to the material. For the case of backward scattered light, the amplitude of the scattered light is set to a constant at the back of the material. This constant is determined by the amount of resonance fluorescence present in the material.

IV. ANALYTICAL SOLUTIONS AND PHYSICAL INTERPRETATION

We shall assume that all physical quantities are the Fourier components , unless otherwise stated. Using the slowly varying envelope and rotating wave approximations, the steady state solutions are given as

$$\rho_{22}^{(0)} - \rho_{11}^{(0)} = -\frac{N_o}{1 + Re\{L(\Delta)\} \times (\frac{I}{I_s})} \tag{8}$$

is the population difference between the excited and ground state of the two-level systems. Re stands for the real part of a complex quantity. The factor $L(\Delta) = 1/(\gamma/2 + i\Delta)$ is the complex spectral lineshape. $\Delta = \omega - \omega_o$ is the pump detuning from resonance.

$$\rho_{12}^{(0)} = iR_o^* L(\Delta)[\rho_{22}^{(0)} - \rho_{11}^{(0)}] \tag{9}$$

is the optical coherence induced by E_p. $R_o = \mu E/2\hbar$ is the Rabi flopping frequency. These solutions are well known in the context of saturated absorption and dispersion of coherent light.

Equations () are used to find the nonlinear optical coherence which is obtained from an exact solution of Eqs. (), and is given as

$$\rho_{12}^{(1)} = (\frac{1}{D})\{iR_1^*[\rho_{22}^{(0)} - \rho_{11}^{(0)}] + \frac{2R_1^* R_0^* \rho_{21}^{(0)}}{\gamma - i\delta}\} \tag{10}$$

with

$$D = \frac{\gamma}{2} + i(-\delta + \Delta) + (I/I_s) \times \frac{\gamma^2}{\gamma + i\delta}$$

where δ is the frequency detuning of the scattered field with respect to the pump field. Equation (10) has the following physical interpretation. The first term is just the absorption coefficient of E_s, modified by the presence of E_p. That is, the population difference is altered by the action of the pump field. The second term gives rise to stimulated two-wave mixing processes, and its strength is attributed to the formation of a traveling wave grating. The grating contribution is reflected in the nonzero value of δ.

The equation for the scattered field is derived with the help of Eq.(), and the results is

$$\frac{1}{A_s}\frac{dA_s}{dt} = -\epsilon F(\Delta, \delta, I/I_s) \tag{11}$$

where the complex function F determines the condition for net gain or loss, as well as the nonlinear dispersion coefficient of the material. In specific, F is given as

$$F(\Delta, \delta, I/I_s) = \frac{\alpha}{2} \frac{1}{1 + \frac{I/I_s}{1+(2\Delta/\gamma)^2}} \frac{1}{1 - i(\Delta - \delta) + \frac{(I/2I_s)}{(1-i\delta/\gamma)}} \{1 - \frac{(I/2I_s)}{1 + i\delta/\gamma} \times L(\Delta)\}$$

where α is the linear on-resonance absorption coefficient of A_s. The second factor on the right hand side is the saturation parameter due to the strong pump field. The third factor is the pump modified spectral response of A_s. And the last factor consists of two terms. The first one, which is proportional to 1, is just the linear loss and dispersion contribution. The second term describes the two-wave mixing interaction. Equation (12) has the following physical interpretation. Given a specific Δ and I/I_s, there exists a range of δ such that coherent energy transfer takes place from the input pump field to the scattered field. For example, if the real part of F is negative for certain range of δ, then the backscattered field is coherently amplified. On equal footing, if the real part of F is positive for certain values of δ, then the forward scattered field is amplified.

In order to appreciate the results obtained, we proceed to provide a pictorial description of the real and imaginary part of F. The real part describes the effect of absorption or amplification. The imaginary part is just the effective dispersion coefficient. Figure 2 represent the real part of F when the input pum field is tuned to resonance ($\Delta = 0$). The results indicate that for low input pump field, no net two-wave mixing gain is ever achieved. Amplification of the scattered light occurs for $I/I_s = 10$ as shown in Figure (2c). A double sideband amplification is achieved for the scattered field detuned from the

input pump field by about 2.5 times the linewidth. For higher values of I/I_s, one noticed a ring like structure for the scattered light. This phenomenon has been observed in high intensity experiments performed in Na vapor, and will occur provided that the spectrum of the scattered light has enough bandwidth in order to accomodate the gain spectrum.

Figure 3 describes the effect of detuning of the pump field from resonance. Again, for low intensity of the input pump field, gain does not take place. Gain is achieved as shown in Figure 3c, where $I/I_s = 10$. The spectrum acquires a skew symmetry, remminescence of dispersionlike lineshape. Gain is possible only for the low frequency component of the scattered light. The dispersionlike character is accentuated in Figure 3*d* where the input intensity is far above saturation. The origin of the dispersive character is easily understood as arising from the response of the material to the applied radiation field. When the input field is detuned, the two-level system has a tendency to follow the radiation field, and the lineshape is determined by the detuning parameter, and not by the linewidth , as is true in resonant situations.

Figure 4 describes an extreme case where the incident pump field is far detuned from resonance. Again, no gain is present for low intensity. Small amount of gain start to appear for $I/I_s = 10$. The gain feature becomes more pronounced when the intensity of the pump is far above saturation.

These spectral line features becomes more complicated when one factors in the flouresence spectrum of the atom. That is, if one takes into account the spectral width of the scattered radiation. An intuitive deduction can be obtained in the following manner. Suppose that the spectrum of the scattered light mimics that of the input pump field, assumed to have a bandwidth $\Delta\Omega$. Then the scattered radiation will be amplified provided that the spectral gain falls within the bandwidth of the pump field.

The nonlinear dispersion coefficient is displayed in Figure 5 and 6 for the case of on-resonance and far detuned from resonance. The dispersion line shapes are just the

derivatives of the nonlinear lineshape, as should be from the Kramers-Kronig relation. The dispersion lineshape determines the nonlinear index of refraction of the material.

A brief summary is in order. The Fourier component of F contains two terms. The first one in the numerator describes the effect of linear absorption and dispersion, modified by the wave mixing effects. The second term arises from the intrinsic two-wave mixing process. The sign of F determines the condition for the amplification of the scattered light. However, a condition must be satisfied. The spectrum of the input incident field must fall within the gain bandwidth in order for the scattered radiation to acquire energy without population inversion. This picture is consistent with the fundamental physics of resonance fluorescence. If the radiation field spectral bandwidth is narrower compared to the natural linewidth, then the scattered light spectral bandwidth is identical to that of the pump field.

Equation (11) has a simple exponential solution within the regime of our approximation. The occurance of gain for the backscattered field depends entirely on the behavior of F. Several interesting features can be derived from Eq. (11). First, F has two contributions. The real part of F describes the gain or loss characteristics of the self-pumped wave mixing process. For a specific set of Δ and δ, the real part of F goes through a null as a function of I/I_s. It implies that the self-pumped process has a threshold behavior. This conclusion is shown in Figure 8 where the net absorption coefficient is plotted for the case of a model atomic vapor with density of 10^{11} cm^{-3} and the input pump field is tuned on resonance. It is assumed that there exists no frequency mismatch. For this case, threshold for gain is obtained at 10 W/cm^2. For input intensities higher than 10 W/cm^2, the backscattered field E_s is coherently amplified from the spontaneous noise. The second contribution is the imaginary part of F which gives rise to the nonlinear dispersive behavior of the backscattered wave.

V. GENERATION OF PHASE CONJUGATE FIELDS: A SIMPLE MODEL

And last, although the analysis above shows the possibility of backward gain under the condition of achieving threshold, it is important to point out that the backscattered field is the phase conjugate of the pump field. This can be accomplished by applying the rudiments of scattering theory to wave mixing processes. The pump field can be written as

$$E_p = E_o exp(iKz) + \lambda \int d\kappa E_1(\kappa, z) exp(i\kappa r_\perp + ikz) \tag{12}$$

where the first term is a plane wave propagating along the z axis and the second term contains all the distorted components of the pump field, after passing through an aberrator. The dummy parameter λ describes the relative magnitude of the second term with respect to the first term. In a similar manner, one can write the scattered field as

$$E_s = E_1 exp(-iK'z) + \lambda \int d\kappa E_m(\kappa, z) exp(i\kappa r_\perp - ik'z) \tag{13}$$

where the first term is again a plane wave propagating in the opposite direction to the pump field and the second term arises from the scattered component due to wave mixing processes. We shall assume in our analysis that $\lambda < 1$;i.e. the magnitude of the scattered component in Eq.(13) is small compared to the plane wave component. Using Eq.(12) in Eq.(13), one obtains the following spatial evolution equation for the scattered field envelope E_m

$$\frac{dE_m}{dz} = AE_m + B\{E_1 E_0 E_1^* + E_1 E_0^* E_1 exp(i\Delta kz)\} \tag{14}$$

Where A= a F(I), B= -2 A G(I)/E_{sat}^2, F(I)=(1-I)/(1+I)(1+2I), G=1/(1+2I)+1/(1-I2), $I = I_0/I_s$ and $\Delta k = 2(k-K)$. The on-resonance saturating field E_{sat} is equal to $2I_s/c\epsilon_o{}^{1/2}$. Equation (14) has a very simple physical interpretation. The first term on the right hand side is just the DC response of the medium. The second term has all the important information concerning the degree of phase conjugation. The first term inside the bracket represents the degenerate four-wave mixing process giving rise to phase conjugate fields.

i.e. proportional to E_1^*. The second term inside the bracket describes the existence of the non-conjugate field,i.e. proportional to E_1. However these two terms differ by a phase factor Wkz, which is a measure of the degree of distortion of the input pump field. The second term can be made negligible provided that the combination of distortion and/or the length of the medium is long enough to make $\Delta kz > 2\pi$. The appearance of the non-conjugate component in self-pumped phase conjugation is a consequence of the collinear geometry inherent in the problem. The same effect appears in collinear degenerate four-wave mixing. Hence for sufficiently long interaction length, the phase conjugate component of the backscattered field dominates. This result points out that if the pump intensity exceeds threshold for backscattering to take place and for long interaction length, the backscattered field is the phase conjugate of the input pump field.

CONCLUSIONS

In summary, a theory of self-pumped phase conjugation in resonant media has been presented. We predict the existence of a threshold behavior for backward gain, we attribute the origin of frequency sidebands to the dynamic Stark effect and we found that the nonconjugate component of the backscattered field can be eliminated by using a long interaction length.

* Work supported by the Army Research Office under contract $No.DAAL03-87-C-0001$ and by the Air Force Office of Scientific Research under contract $F49620-88-C-0042$

REFERENCES

1. R.A. Fisher, OPTICAL PHASE CONJUGATION, Academic Press (1983)
2. B.Y. Zeldovich, V.J. Popovichev, V.V. Ragulskii and F.S. Faisullov, JETP Lett. 15 , 109 (1972)
3. J. Feinberg, Opt. Lett. 7 , 486 (1982);
4. V.G. Koptev, et al , Sov. Phys. JETP Lett. 28 , 434 (1978); E.V. Ivakin et al, Sov. Phys. JETP Lett. 30 , 613 (1978); Lazaruk, Sov. J. Quantum Electron. 9 , 1041 (1979).
5. J.F. Lam, S.C. Rand, R.C. Lind, R.A. McFarlane and A.L. Smirl, Proc. International Quantum Electronics Conference, San Francisco (1986).
6. J.F. Lam, Appl. Phys. Lett. 46 , 911 (1985). T.Y. Chang and R.W. Hellwarth, Opt. Lett. 10 , 408 (1985).
7. S.H. Autler and C.H. Townes, Phys. Rev. 100 , 703 (1955).
8. J.H. Marburger, in OPTICAL PHASE CONJUGATION, edited by R.A. Fisher , Academic Press (1983).
9. S.G. Rautian and I.I. Sobel'man, Sov. Phys. JETP 14, 328 (1961), Sov. Phys. JETP 17, 636 (1963)
10. E.V. Baklanov and V.P. Chebotaev, Sov. Phys. JETP 34, 490 (1972)
11. S. Haroche and F. Hartman, Phys. Rev. A6, 1280 (1972)
12. B.R. Mollow, Phys. Rev. A5, 2217 (1972)
13. M. Sargent III, and P.E. Toschek, Appl. Phys. 11, 107 (1976)
14. G. Khitrova, P.R. Berman, and M. Sargent III, JOSA B 5, 160 (1988)
15. M.T. Grüneisen, K.R. McDonald and R.W. Boyd, JOSA B 5, 123 (1988)

FIGURE CAPTIONS

Figure 1. The intensity modulation, medium response, current density, and the work done by the field, from top to bottom.

Figure 2. The nonlinear lineshape or the real part of F as a function of pump-probe detuning, for distinct values of the input intensity. The case of resonant excitation is considered

Figure 3. The nonlinear lineshape or the real part of F as a function of pump-probe detuning, for distinct values of the input intensity. The case of the pump detuned one linewidth away from resonance

Figure 4. The nonlinear lienshape or the real part of F as a function of pump-probe detuning, for distinct value of the input intensity. The pump is detuned by 10 times the linewidth away from resonance

Figure 5. The nonlinear dispersion coefficient for the on-resonance case, for distinct values of the input intensity

Figure 6. The nonlinear dispersion coefficient for the case when the incident pump field is detuned by 10 times the linewidth away from resonance

Figure 7. The net absorption coefficient as a function of the input pump intensity. Positive values of the net absorption coefficients represent losses while negative values represent gain.

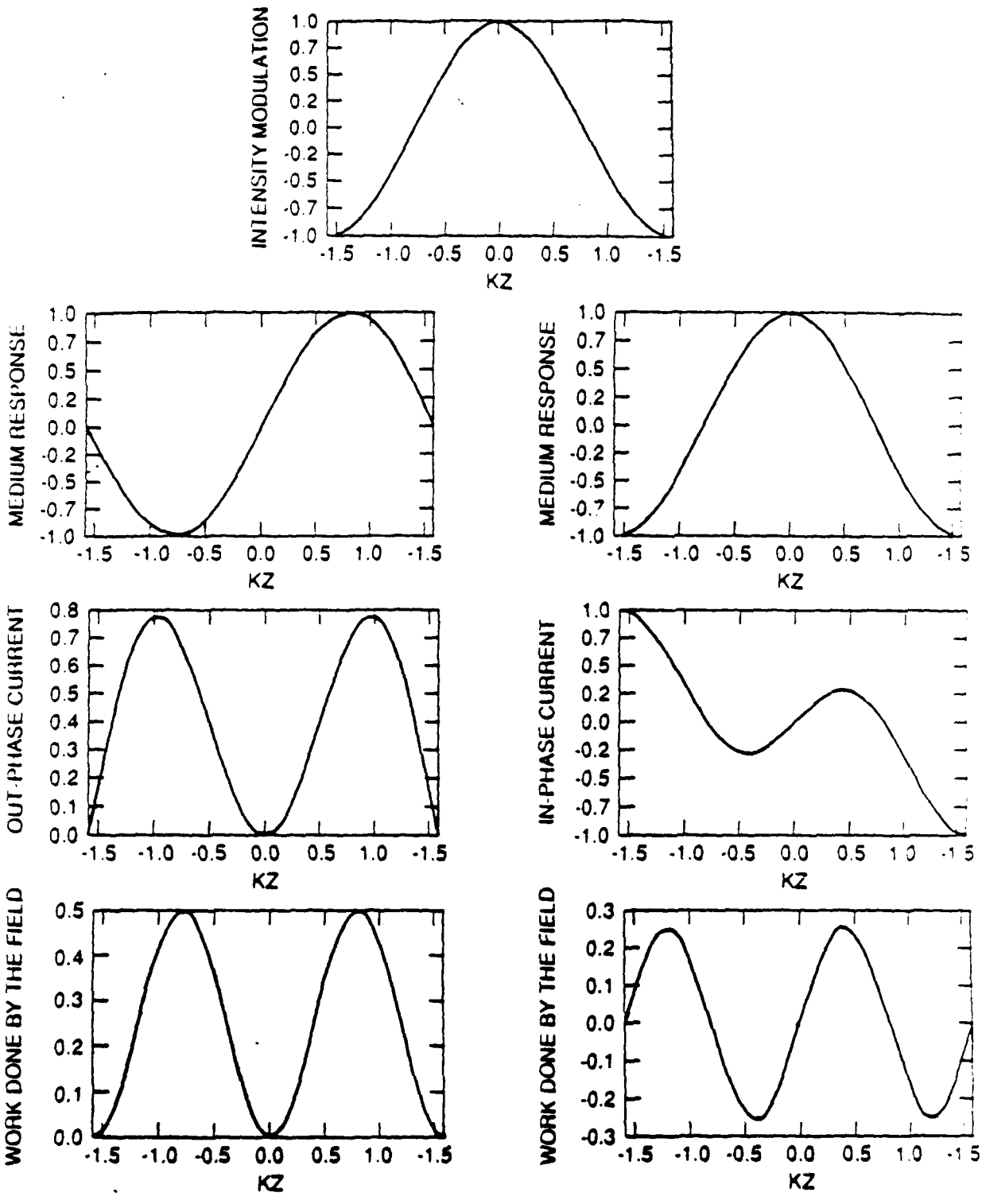
INTENSITY MODULATION
MEDIUM RESPONSE
MEDIUM RESPONSE
OUT-PHASE CURRENT
IN-PHASE CURRENT
WORK DONE BY THE FIELD
WORK DONE BY THE FIELD
KZ

Figure F-1

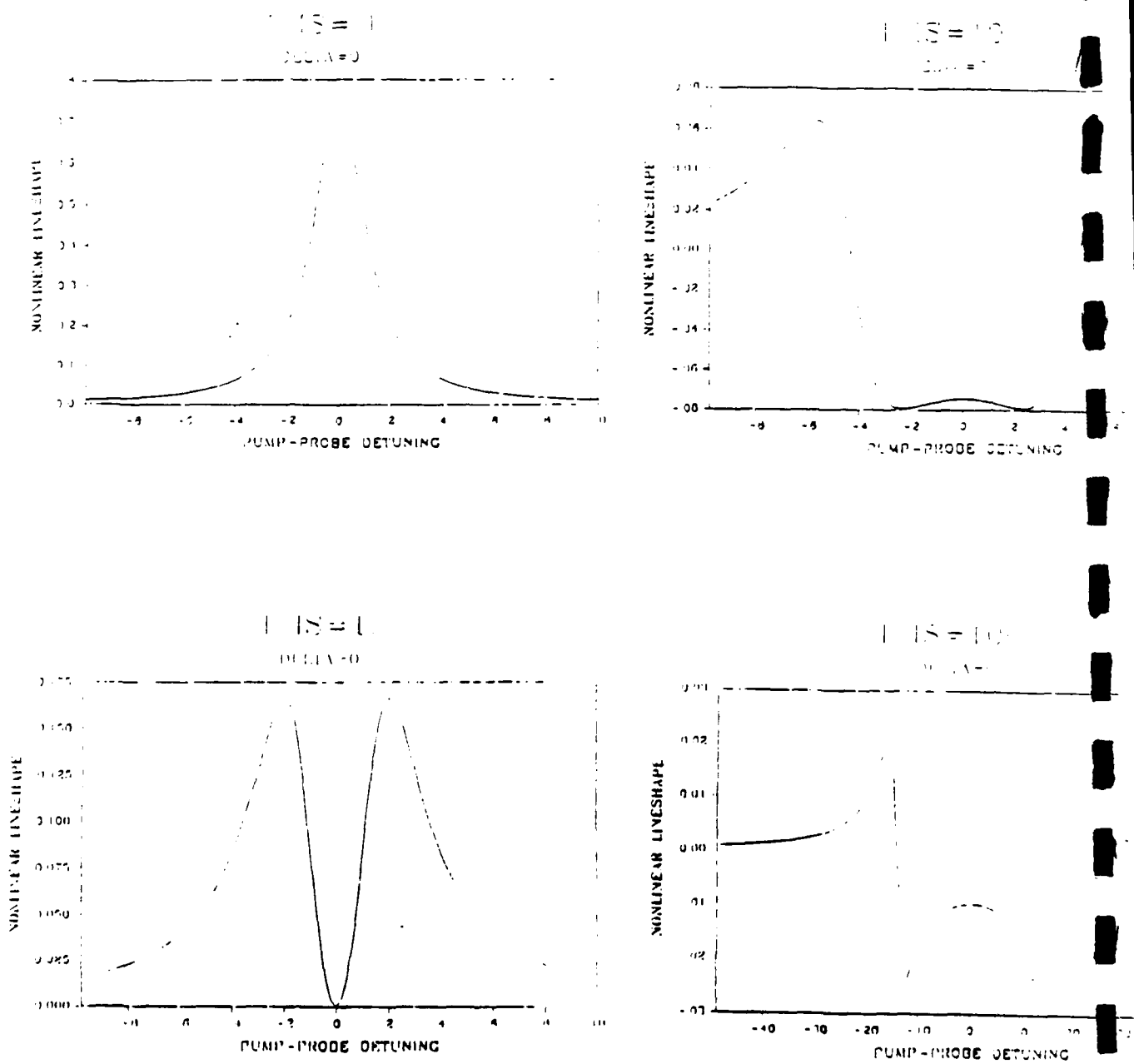
NONLINEAR LINESHAPE
PUMP-PROBE DETUNING
NONLINEAR LINESHAPE
PUMP-PROBE DETUNING
NONLINEAR LINESHAPE
PUMP-PROBE DETUNING
NONLINEAR LINESHAPE
PUMP-PROBE DETUNING

Figure F-2

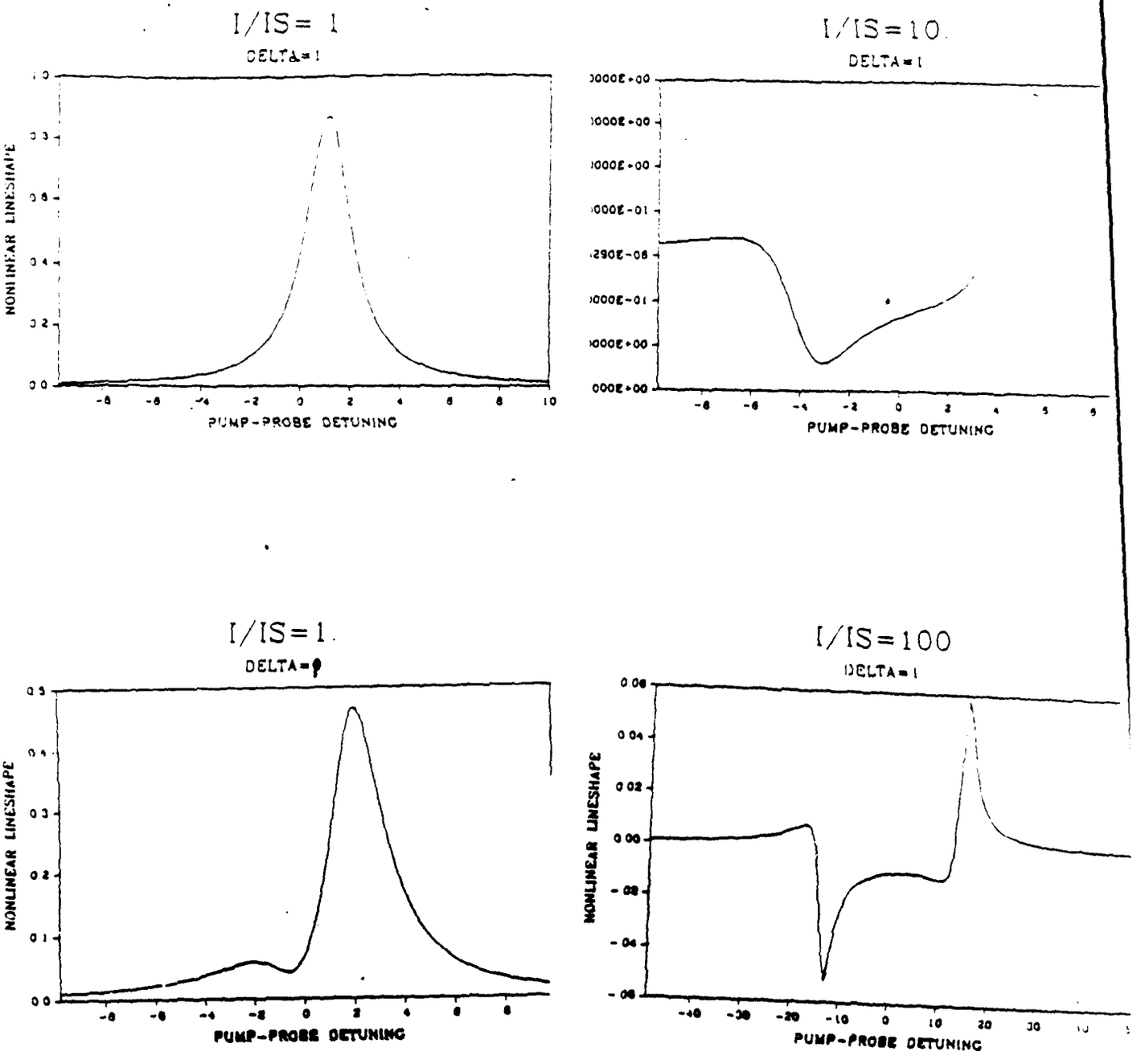
I/IS= 1
DELTA=1
NONLINEAR LINESHAPE
PUMP-PROBE DETUNING
I/IS=10
DELTA=1
PUMP-PROBE DETUNING
I/IS=1
DELTA=1
NONLINEAR LINESHAPE
PUMP-PROBE DETUNING
I/IS=100
DELTA=1
NONLINEAR LINESHAPE
PUMP-PROBE DETUNING

Figure F-3

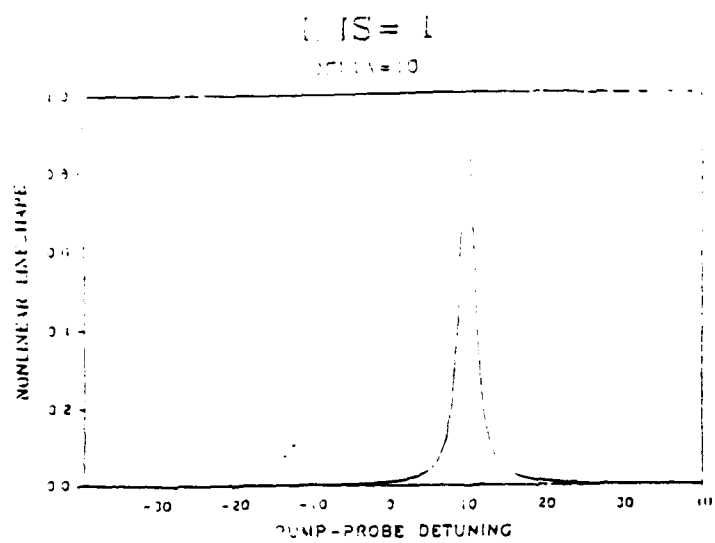
I/IS = 1
NONLINEAR LINE SHAPE
PUMP-PROBE DETUNING

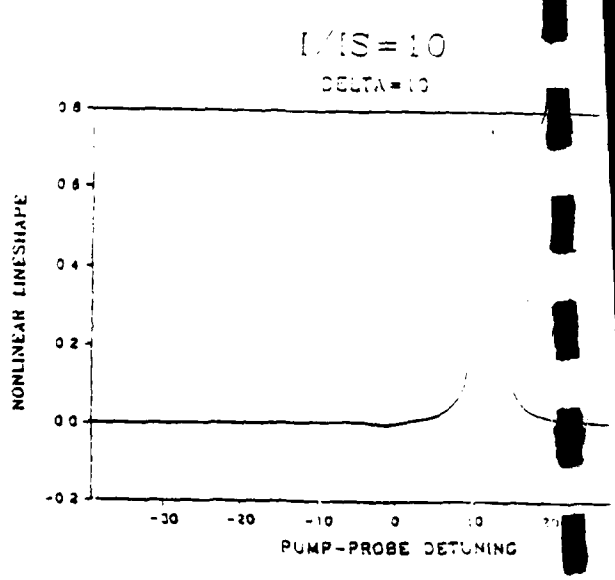
I/IS = 10
DELTA = 10
NONLINEAR LINESHAPE
PUMP-PROBE DETUNING

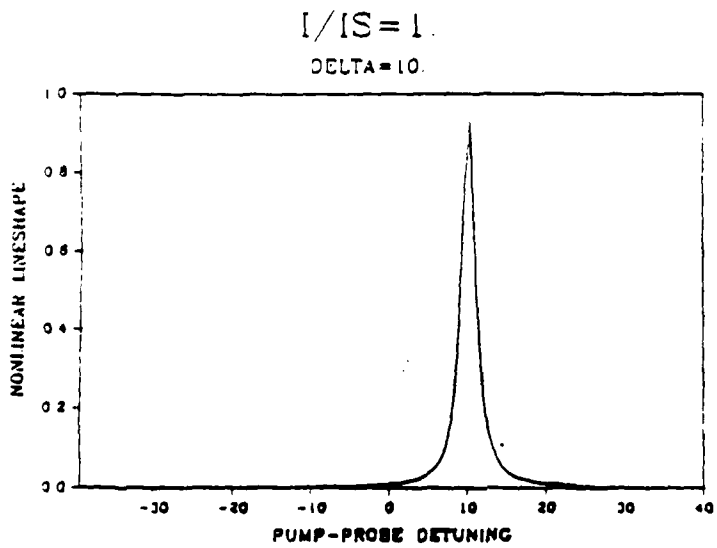
I/IS = 1
DELTA = 10
NONLINEAR LINESHAPE
PUMP-PROBE DETUNING

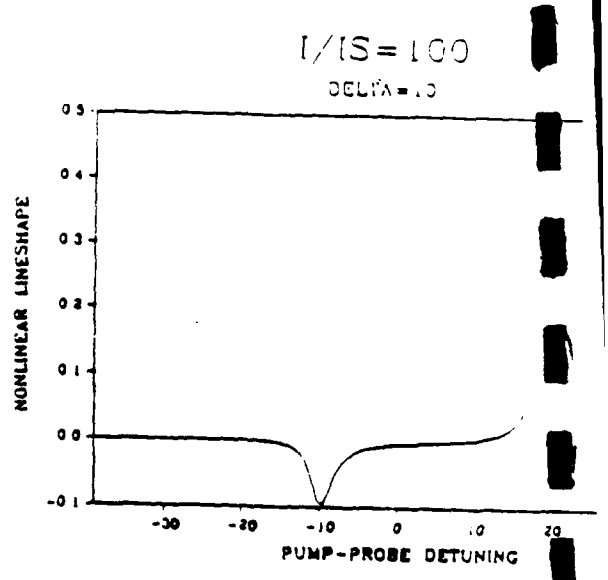
I/IS = 100
NONLINEAR LINESHAPE
PUMP-PROBE DETUNING

Figure F-4

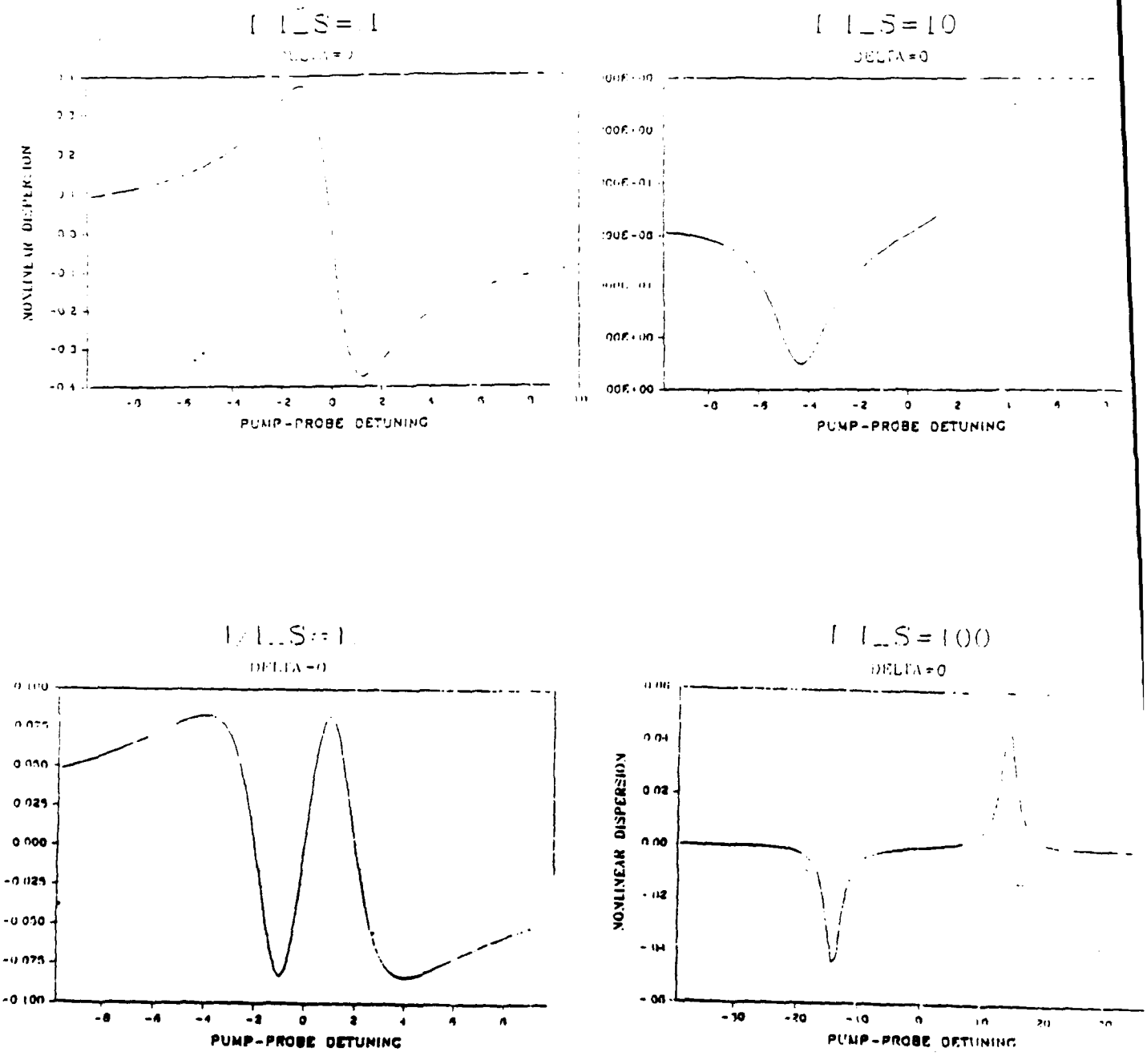
I_I_S=1
DELTA=0
NONLINEAR DISPERSION
PUMP-PROBE DETUNING
I_I_S=10
DELTA=0
PUMP-PROBE DETUNING
I_I_S=1
DELTA=0
PUMP-PROBE DETUNING
I_I_S=100
DELTA=0
NONLINEAR DISPERSION
PUMP-PROBE DETUNING

Figure F-5

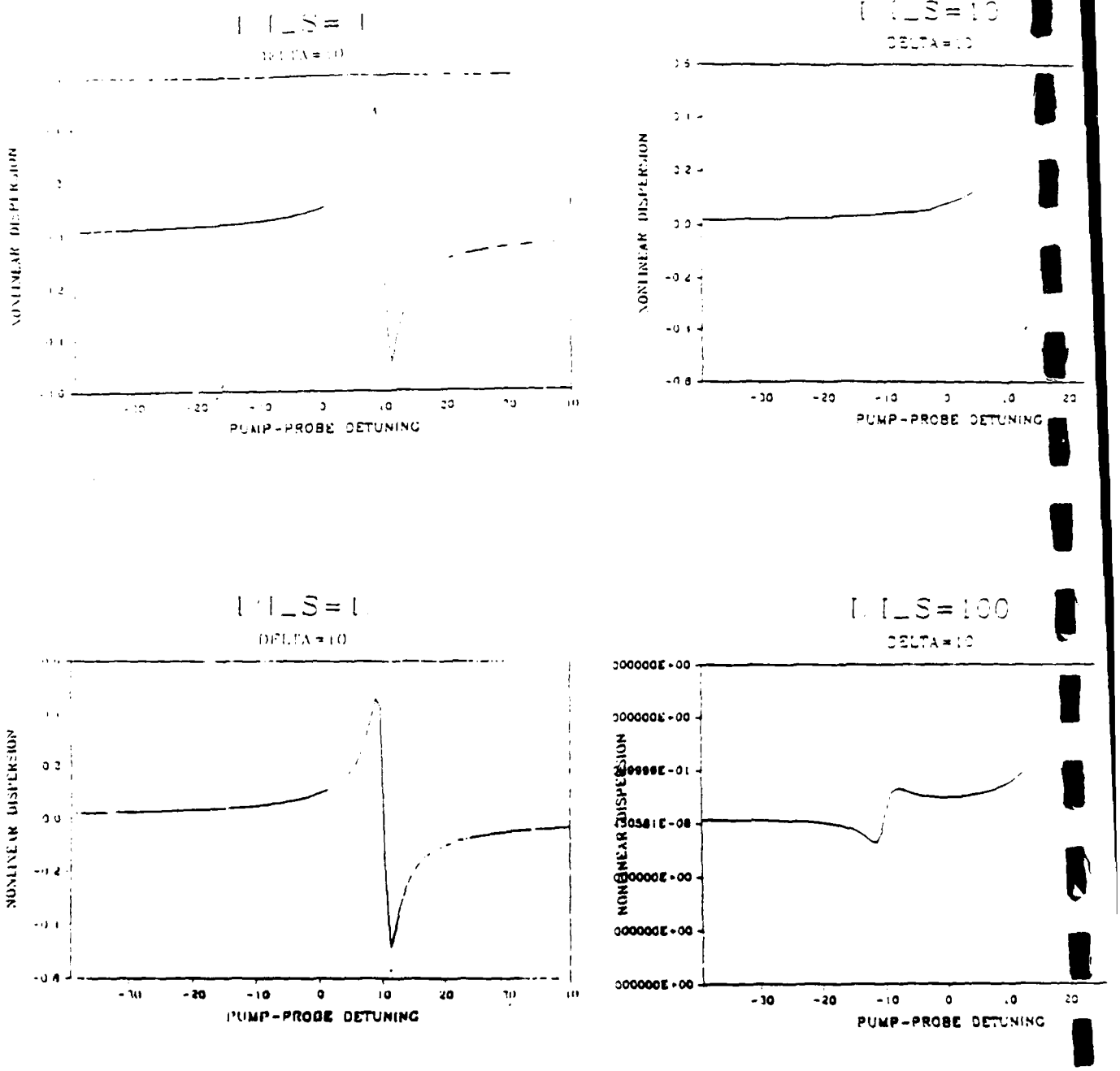
PUMP-PROBE DETUNING
PUMP-PROBE DETUNING
NONLINEAR DISPERSION
PUMP-PROBE DETUNING
NONLINEAR DISPERSION
PUMP-PROBE DETUNING

Figure F-6

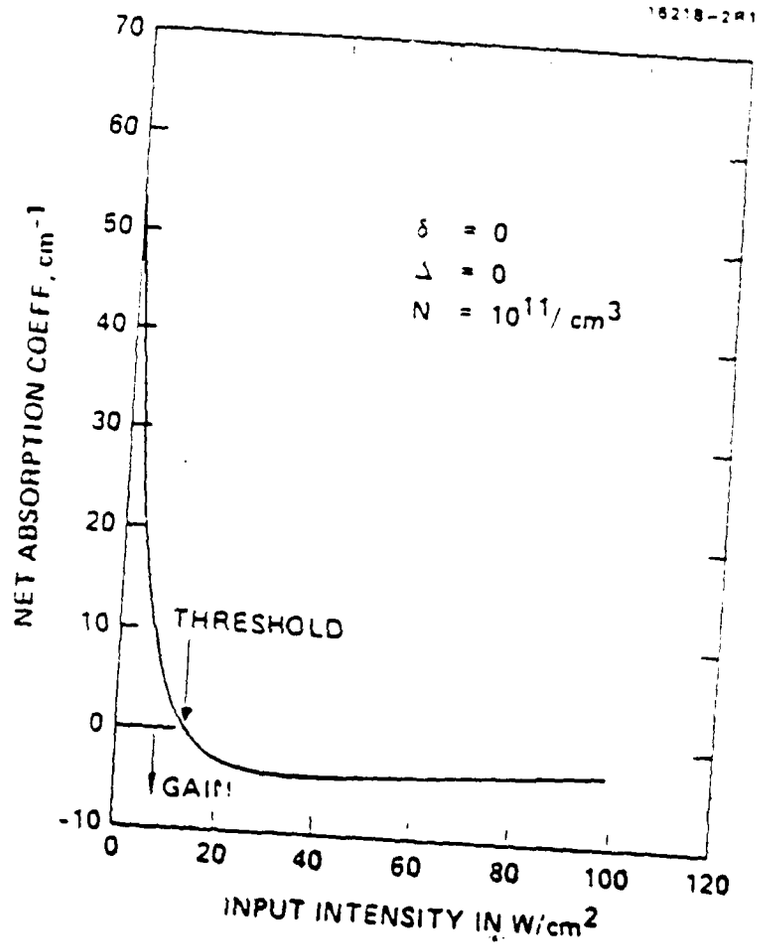
16218-2R1
70
60
50
40
30
20
10
0
-10
0
20
40
60
80
100
120
NET ABSORPTION COEFF, cm⁻¹
INPUT INTENSITY IN W/cm²
δ = 0
Δ = 0
N = 10¹¹/ cm³
THRESHOLD
GAIN

Figure F-7

APPENDIX G

Resonant self-pumped phase conjugation in cesium vapor at .85 micron

Celestino J. Gaeta and Juan F. Lam

Hughes Research Laboratories, Malibu, California 90265

We report the first observation of resonant self-pumped phase conjugation at diode laser wavelengths. A phase conjugate reflectivity of 0.1%, and a cw threshold intensity of 35 W/cm^2 were measured.

The search for an ideal self-pumped phase conjugate mirror has been an objective of active research in optics recently. This special mirror must have the following desirable properties: fast response and build-up times, a large phase conjugate reflectivity and a small frequency mismatch between the input and phase conjugate waves. Stimulated scattering processes[1] via acoustic and molecular vibrations have the disadvantage of high threshold intensity ($>$ MW/cm^2) and large frequency mismatch ($>$ 1 GHz). Photorefractive materials[2,3] are restricted by their slow build-up time ($>$ minutes) and an intensity dependent response time ($>$ seconds for typical cw laser input power). However both share the unique advantage of possesing large phase conjugate reflectivity. For example, reflectivity as large as 60% in barium titanate and $>$ 90% for stimulated Brillioun scattering have been measured.

Recently, we reported the demonstration of self-pumped phase conjugation in sodium vapor at visible wavelengths.[4] A measured reflectivity of 2% , response times of tens of nsecs , small frequency mismatch (within 500 kHz which is on the same order as the frequency jitter of the laser) and a threshold intensity of 10 W/cm^2 indicated the potential of alkali vapors as a reasonable self-pumped phase conjugate mirror. This letter reports the observation of self-pumped phase conjugation in cesium vapor,[5] whose $6S_{1/2} \rightarrow 6P_{3/2}$ electric dipole allowed transition is accesible by 852 nm sources. This demonstration opens the door for

the potential role of resonant materials in self-generated nonlinear optical applications that employ compact semiconductor laser diodes.

The physical mechanism responsible for self-pumped phase conjugation in resonant materials is self-generated intracavity four-wave mixing through two-wave mixing gain.[4,6] In a nutshell, the input optical beam induces resonance fluorescence radiation, a small portion of which propagates along the optical axis of the cavity. Energy transfer from the input beam to the nearly co-propagating fluorescence radiation takes place by means of coherent scattering of the input beam from the traveling wave grating produced by the interference of the input and nearly co-propagating fluorescence radiations. Hence it leads to an enhancement of the intracavity radiation. Phase conjugation occurs via a four-wave mixing process,[7] where the counterpropagating pumps are the standing waves in the cavity and the probe is the input beam. The intracavity four-wave mixing process can take place provided that the fluorescence radiation is coherent with the input beam. This is the case for resonant medium whose linewidth is larger than the laser linewidth. Such a condition is satisfied in our experiments.

A 3 cm long glass cell fitted with Brewster-angled windows placed at the center of an linear optical cavity comprised the self-pumped conjugator. Curved high reflector mirrors ($r = 30\ cm$) placed 56 cm apart produced a beam waist at the center of the resonator with a radius of approximately 120 μm. The incoming laser beam was directed into the cesium cell at an angle on the order of half a degree with respect to the resonator axis so that its 115 μm radius waist was spatially coincident with that of the resonator mode.[4]

Experiments were conducted with the cw laser source set near the D_2 line in cesium ($\lambda = 852\ nm$) at detunings on the order of 1 GHz on the low frequency side of the resonance. A typical scan of the reflectivity as a function of laser frequency is shown in Fig. 1 for a pump intensity of 290 W/cm^2 in the cell and a cesium temperature of 109 $^{\circ}C$. The phase conjugate return signal is obtained over a frequency span just under 1 GHz, although a relatively small amount of return energy is obtained at larger detunings. At the larger detunings the cesium

resonator was still oscillating at a power level that was about the same at that obtained for the range of detunings that produced a strong return signal. This behavior is similar to results obtained previously in sodium vapor.[4] It is attributed to the different gain mechanisms associated with the two–wave mixing process. In general, the resonator will oscillate due to both a nearly–degenerate (Raleigh) gain process and a three photon gain process that provides gain over a range of frequency that is shifted from that of the original laser beam by approximately the generalized Rabi frequency.[6] However, the return signal is obtained at frequencies close to that of the pump beam that experience net gain in the resonator due to the Raleigh feature. At the larger detunings mentioned previously the net gain is due mainly to the three photon process and thus does not yield a strong return signal.

The effects of varying the pump beam intensity within the cesium vapor are shown in Fig. 2. A threshold intensity of about 35 W/cm^2 was measured for the phase conjugation process. This measurement was performed at a detuning of about -0.8 GHz from line center which maximized the reflectivity at the highest pumping level shown in the figure. This threshold is not, in general, the same as that for oscillation in the resonator since the three photon process will typically yield a different oscillation threshold. However, the oscillation threshold for frequencies at which gain is provided by the Raleigh feature does appear to be the same as that for the phase conjugation process, as expected.

Varying the temperature of the cesium reservoir (number density) showed that phase conjugation is obtained for a finite range of temperture with a maximum reflectivity obtained at about 110 $^{\circ}C$ for the conditions of our experiment. This effect (shown in Fig. 3) is consistent with the variation of the Raleigh gain with temperature that we have determined from two–wave mixing experiments in sodium vapor.

We have demonstrated and characterized a self–pumped optical phase conjugation process in cesium vapor at typical laser diode wavelengths. This work has shown that the threshold for this process is low enough that it is feasible to attempt to employ this type of conjugator in applications which utilize laser diode sources.

The authors wish to thank Dr. Monica Minden for stimulating technical discussion concerning the spectroscopy of cesium. The work is supported by DARPA/ONR (contract #N00014-87-C-0090), Army Research Office (contract #DAAL03-87-C-0001), and Air Force Office of Scientific Research (contract #F49620-88-C-0042).

REFERENCES

1. B. Ya. Zel'dovich, V.I. Popovichev, V.V. Ragul'skii and F.S. Faizullov, J.E.T.P. Lett. **15**, 109 (1972).

2. J. Feinberg, Opt. Lett. **7**, 486 (1982).

3. J.O. White, M. Cronin-Golomb, B. Fischer and A. Yariv, Appl. Phys. Lett. **40**, 450 (1982); M. Cronin-Golomb, B. Fischer, J.O. White and A. Yariv, Appl. Phys. Lett. **41**, 689 (1982).

4. C.J. Gaeta, J.F. Lam and R.C. Lind, Opt. Lett. **14**, 245 (1989).

5. C.J. Gaeta and J.F. Lam, "Self-pumped optical phase conjugation in cesium vapor," I.E.E.E. NLO Talk #*THP*22 (Kauai, Hawaii, 1990).

6. S. Haroche and F. Hartmann, Phys. Rev. A **6**, 1280 (1972); M.T. Gruneisen, K.R. MacDonald and R.W. Boyd, JOSA B **5**, 123 (1988);G. Khitrova, P.R. Berman and M. Sargent III, JOSA B **5**, 160 (1988); C. Cohen-Tannoudji and S. Reynaud, J. Phys. B: Atom. Molec. Phys. **10**, 345 (1977); B.R. Mollow, Phys. Rev. A **5**, 2217 (1972).

7. D.M. Bloom and G.C. Bjorklund, Appl. Phys. Lett. **31**, 592 (1977); R.L. Abrams and R.C. Lind, Opt. Lett. **2**, 94 (1978); D.M. Bloom, P.F. Liao and N.P. Economou, Opt. Lett. **2**, 58 (1978).

LIST OF FIGURES

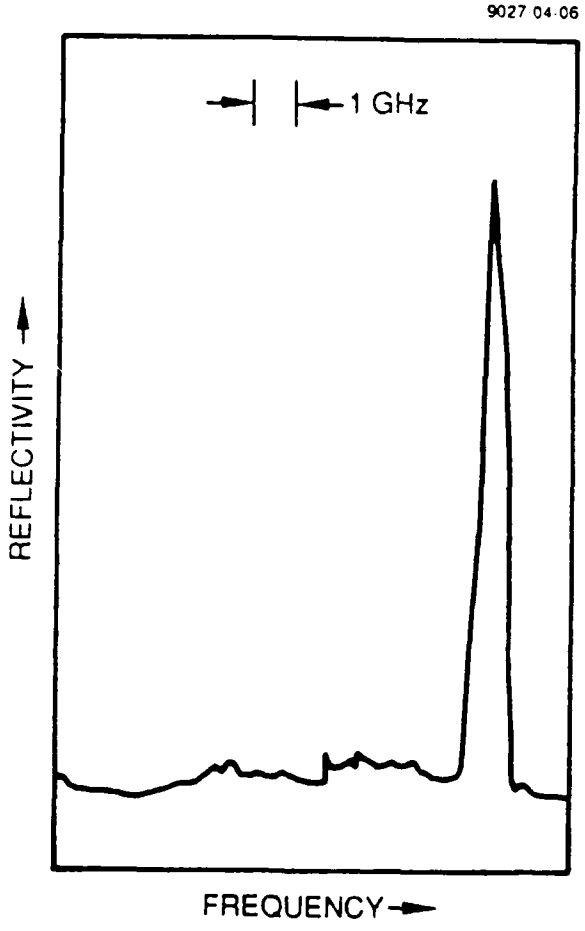

Figure G-1

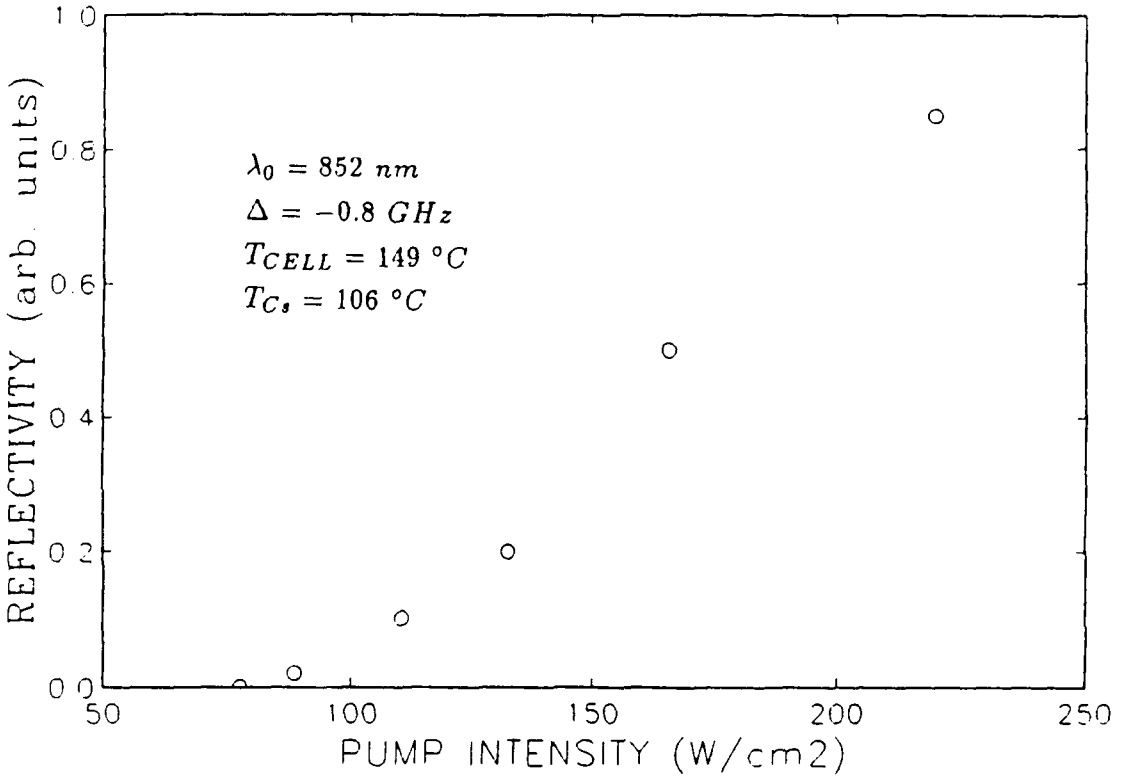
1.0
0.8
0.6
0.4
0.2
0.0
REFLECTIVITY (arb. units)
$\lambda_0 = 852\ nm$
$\Delta = -0.8\ GHz$
$T_{CELL} = 149\ °C$
$T_{Cs} = 106\ °C$
50
100
150
200
250
PUMP INTENSITY (W/cm2)

Figure G-2

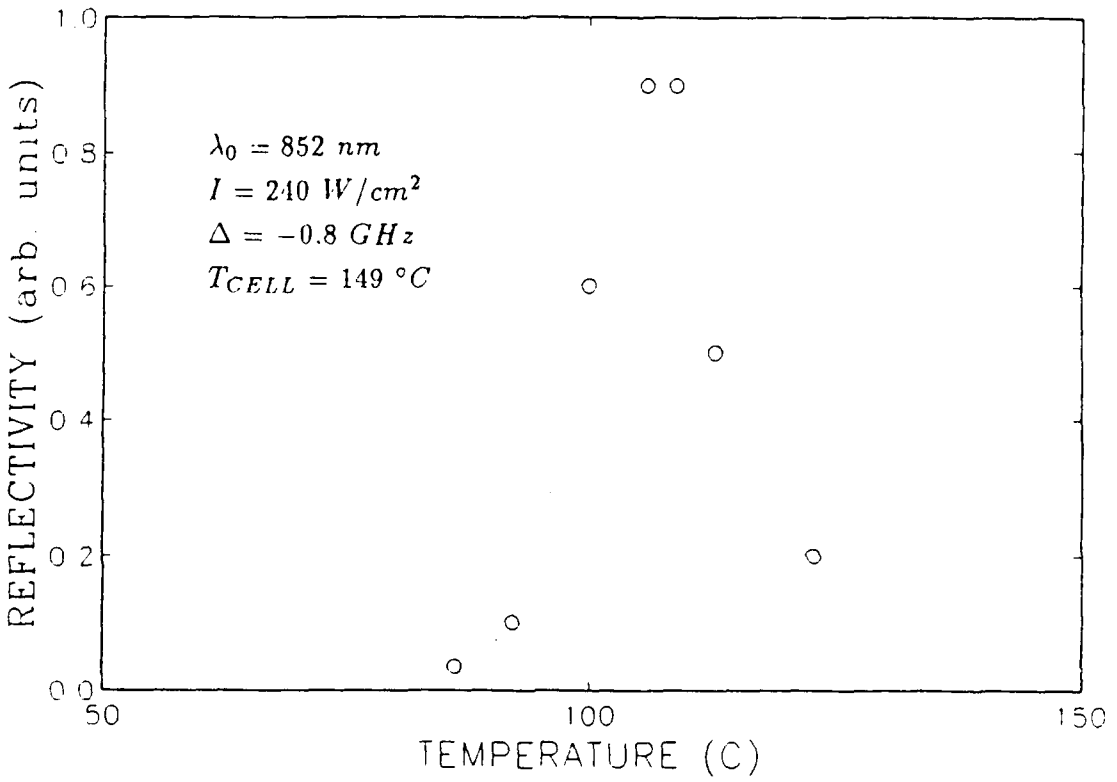
1.0
0.8
0.6
0.4
0.2
0.0
REFLECTIVITY (arb. units)
$\lambda_0 = 852\ nm$
$I = 240\ W/cm^2$
$\Delta = -0.8\ GHz$
$T_{CELL} = 149\ °C$
50
100
150
TEMPERATURE (C)

Figure G-3

Pressure–induced coherent energy transfer and temporal oscillations of two–wave mixing in sodium vapor

Celestino J. Gaeta and Juan F. Lam

Hughes Research Laboratories, Malibu, California 90265

An experimental investigation of collision–assisted energy transfer from a strong pump beam to a weak probe in pressure–broadened sodium vapor is discussed. A peak gain coefficient of 0.7 cm^{-1} was measured for a cw pump intensity of 25 W/cm^2. At higher intensities temporal oscillations of both two–wave mixing gain and the transmission of an isolated cw laser beam were observed and characterised. An explanation for this latter effect in terms of light–induced drift and diffusion is also presented.

The study of collision–aided processes in atom–laser interactions has led to the understanding of novel nonlinear optical phenomena. Pressure–induced extra resonances[1], collisional narrowing of the population[2]– and Zeeman[3]–mediated spectral lineshapes and pressure–induced cavity oscillation[4] are just recent examples in the context of four–wave mixing. A physical interpretation of the changes in the four–wave mixing signal is the non–cancellation of the quantum mechanical amplitudes due to the presence of a state–selective collisional process.

We report the observation of collision–aided energy transfer between two optical beams oscillating at different frequencies. The theory of such a process was put forward by Berman, Khitrova and Lam[5]. Using a density matrix approach, the two–beam coupling coefficient exhibits a pressure dependent term that provides an intensity gain for the weak optical beam at the expense of the strong optical beam. Collisions play a significant role. It induces a phase shift ($> 0°$) between the interference pattern of the two beams and the population

difference. This phase shift allows a transfer of energy from the strong optical beam to the weak optical beam. At higher intensities we observed and characterized temporal oscillations in both the pump beam transmission through sodium vapor and the associated two-wave mixing gain in the presence of a buffer gas.

Nonlinear wave mixing processes involving the interaction of two optical fields in a resonant medium which allow the transfer of energy from one beam to the other have been used to demonstrate low-power techniques for producing phase conjugate waves that do not require separate pump beams.[6] Such a self-pumped phase conjugator is in the form of a laser resonator which uses two-wave mixing as the gain mechanism. The counterpropagating fields within this resonator would then interact with the pump laser beam to produce a fourth optical field (phase conjugate to the pump beam) via an internal four-wave mixing process.

Two-wave mixing gain due to both the ac-Stark effect[7] and stimulated Raman scattering[8] has been observed in sodium vapor. These gain processes typically require cw pump intensities in the range of hundreds of watts per square centimeter. We report here the observation of gain using a collision-assisted process which may be implemented using a pump intensity that is an order of magnitude lower. In this type of interaction a strong pump beam and a relatively weak probe beam are overlapped with each other at a small angle ($< 0.5°$) inside of a nonlinear resonant medium. The two beams produce an interference pattern which results in an index of refraction grating through the nonlinear response of the medium. Energy transfer from the pump to the probe beam can occur when the population grating is temporally delayed with respect to the interference pattern. Normally the interference pattern and the grating are in phase. However, in the presence of collisions and when the pump and probe laser frequencies do not coincide, the population grating can be delayed. The pump beam can then reflect from this grating into the probe path (in phase with the probe beam) resulting in gain for the optical field of the probe laser.

A diagram of the experimental arrangement is presented in Figure 1. The mixing process

occurred in a 1 cm long metal cell with sodium densities on the order of 10^{11} cm^{-3}. Since the theory of the two wave optical process to be studied here assumes a pressure-broadened transition in the sodium vapor, argon gas was introduced into the cell at pressures up to 100 $Torr$. A Coherent model 590 passively stabilized single frequency dye laser served as the pump beam. This laser is capable of providing power densities in the range of tens of watts per square centimeter in a single longitudinal mode, which is close to the theoretically determined levels needed to drive the nonlinear susceptibility. Part of the output from the 590 was directed into a reference sodium cell equipped with an orthogonal viewport to allow the fluorescence to be monitored. Observation of both the fluorescence level and the 590 spectrum on a scanning Fabry Perot was used to set the 590 laser frequency to the desired detuning from the center of the sodium resonance.

A relatively weak probe beam from a Coherent 699 autoscan single frequency ring dye laser was introduced into the metal cell so that it overlapped with the pump beam at a small angle ($\leq 0.5°$). The probe beam was amplitude modulated using a chopper at a rate of approximately 1 kHz allowing lock-in amplifiers to be used in the detection system to provide a better signal/noise ratio. Part of the probe beam was diverted into a detector so that probe beam power could also be monitored. Both the reference and transmitted probe beam power levels were recorded as the probe frequency was scanned through the sodium D_2 resonance. The 699 autoscan laser system is computer controlled and includes an integral wavemeter and interface electronics which record data as a function of laser frequency.

Gain was observed for the forward probe beam within the resonance with the pump laser frequency detuned by about 1.5 GHz on either side of the center of the sodium transition. The transmission of the probe beam through the sodium cell as a function of probe laser frequency is shown in Figure 2 for three cases. These curves actually represent the ratio of transmitted probe beam power to a reference probe power level, measured before the cell (see Figure 1), so that the effects of output power variations in the probe laser could be reduced. One scan (Figure 2a) is a reference in which the pump laser was blocked and no

buffer gas was present. Under these conditions the probe beam is strongly absorbed within the resonance. When argon buffer gas was introduced into the sodium system at pressures in the range of 10–80 *Torr* the transmission characteristic for the probe beam was modified in the presence of the pump beam and exhibited gain, as shown in Figures 2b and 2c. A peak gain coefficient of 0.7 cm^{-1} was obtained for an argon buffer gas pressure of 60 *Torr* (Figure 2c). Higher buffer gas pressures appeared to have a quenching effect on the gain. We believe that this is due to collisional depopulation of the upper level of the sodium transition. This is a competing process which reduces the gain at sufficiently high pressure. Pump beam intensity is estimated to have been approximately 25 W/cm^2 while the probe intensity was about a factor of 50 below the pump level. The dip in the center of the curve in Figure 2b is believed to be due to the fact that the absorption is strongest in the center of the resonance and may dominate over the gain under certain conditions. In the wings of the resonance the absorption is reduced so that the two-wave mixing gain dominates.

Later the experimental set-up was upgraded by replacing the pump source with a Coherent 699-21 actively stabilized ring dye laser. A 3 *cm* long quartz cell fitted with Brewster-angled windows was also substituted for the metal cell as a prelude to work with sodium oscillators. Laser beam waist radii in the cell were 125 μm and 260 μm for the probe and pump beams, respectively.

When the two-wave mixing experiments were resumed much higher pump powers were employed in order to evaluate two-wave mixing gain resulting from the ac-Stark effect. Under the appropriate conditions, and only in the presence of a buffer gas (argon), oscillations were observed in the transmission of both the cw pump and probe optical fields. The probe field was still amplitude modulated at 1 kHz prior to injection into the cell to allow for phase-sensitive detection. However, the oscillations were observed to have much longer periods (on the order of seconds to tens of seconds) and were present on the pump beam even with the probe beam blocked. Such oscillations have previously been observed in sodium vapor for a cw laser beam but the phenomenon was not fully characterized as a function of experimental

parameters. We have extended the previous work to include such a characterization, as well as the effects upon two-wave mixing gain.

A typical temporal sequence is shown in Fig. 3 for the case of both the pump and probe beams present. The plots represent the transmission of the laser beams through the sodium cell as a function of time. At the start of the sequence both laser beams are blocked before the cell in order to mark the zero transmission levels. After a time, the probe beam is unblocked to indicate its transmission level without a two-wave mixing assist. Next, the pump beam is unblocked causing the probe beam transmission to approximately double. After a few seconds argon buffer gas is added to the cell at a pressure of 1 $Torr$. At this time the transmission of the pump beam through the cell decreases rapidly to zero while the probe beam transmission increases by about 50% (a factor of 2.5 increase due to two-wave mixing overall). The pump and probe beam power levels at the output of the cell then begin to oscillate with a period of about 10 seconds and a phase difference of approximately 270° (transmitted probe oscillation delayed about 7.5 seconds with respect to that of the pump. During the oscillations the transmitted pump beam power alternated between zero and a level about 30% lower than the level obtained prior to the introduction of the buffer gas. It is interesting to note that during the *on* state for the pump its transmitted power level decreases approximately linearly until it is reduced by a factor of about two and then switches very quickly to zero. During this decrease the transmitted probe beam power level is increasing relatively slowly as shown in Fig. 3 until the pump beam transmission switches to the *off* state resulting in the probe transmission suddenly switching to its maximum level. In contrast, the transition from *off* state to *on* state for the pump, or the converse for the probe, is very rapid. When the buffer gas is removed the pump and probe beam power levels at the output of the cell are once again constant in time.

These results were obtained for temperatures of 261 $^{\circ}C$ and 227 $^{\circ}C$ for the cell body and reservoir regions, respectively, and a pump beam intensity of 280 W/cm^2 in the cell region. The pump beam frequency was about 0.5 GHz below the center of the sodium D_2 resonance

while that of the probe beam was about 5.7 GHz below linecenter.

The oscillations were also observed at other values of probe detuning with that of the pump beam set at approximately the same value as in the previous case. For example, when the probe detuning was set at $\Delta = 2.9\ GHz$ (above linecenter) and the pump beam was unblocked the probe transmission was reduced to 1/3 of its original level. In the presence of argon buffer gas (1 $Torr$) the pump and probe power levels at the output of the cell dropped to zero and after an interval of about 25 seconds began to oscillate with a period of about 6 seconds. The oscillation of the probe transmission was delayed from that of the pump by approximately 5 seconds (300°). When the buffer gas was removed the pump and probe power levels after the cell returned to their respective values before the buffer gas was added after a buildup on the order of 50 seconds. The pump beam was then blocked and the probe transmission returned to its initial level. The experiment was repeated for a probe detuning equal to that of the pump. In this case the same oscillations were present for the pump beam transmission but that of the probe was essentially zero at all times. This is because the probe frequency was set closer to linecenter and the probe was highly absorbed. Since its frequency was nearly identical to that of the pump beam the population and interference gratings were not properly delayed with respect to each other and two–wave mixing gain did not occur for the probe beam.

Oscillations were observed for the pump beam even with the probe beam absent. A plot of the variation of the oscillation period with buffer gas pressure is presented in Fig. 4a for a pump beam intensity of 280 W/cm^2 and pump beam detuning of $-0.5\ GHz$ from linecenter. The period increases from just under 10 seconds at a pressure of 1 $Torr$ to almost 200 seconds at 40 $Torr$. The functional relationship appears to be nonlinear. Fig. 4b shows the effect of varying the pump beam intensity for a buffer gas pressure of 1 $Torr$. The oscillation period appears to vary nonlinearly with intensity. A threshold for the oscillations was also observed and measured to be about 165 W/cm^2. Below this threshold the pump beam transmission went to zero when the buffer gas was added and did not recover. It is

interesting to note that although the period increases as the intensity is increased the buildup time for the oscillations to occur after the introduction of the buffer gas was observed to decrease dramatically from ten's of seconds for intensities close to the threshold level to a few seconds at higher intensities. The period obtained for an intensity of 280 W/cm^2 is slightly higher in Fig. 4b than that discussed earlier in the temporal sequences and is probably due to the fact that the data in Fig. 4b was taken on a different day and the detuning may have been slightly different.

A plausible explanation of the temporal oscillation can be given in terms of the phenomenon of light induced drift. In a nutshell, the different collisional cross sections for the excited and ground states of the D_2 line of sodium atoms produce a net macroscopic velocity of the atoms along the axis of the optical beam. This atomic drift produces a cluster of atoms towards the end of the cell, leading to a light-assisted temporal increase of the sodium vapor density in that location. The higher density gives rise to a decrease of optical transmission because of increase absorption. However, the effects of diffusion eventually lead to a decrease of the density of the cluster, leading to increase optical transmission. This process repeats itself provided that the buffer gas pressure is mantained in the cell.

We carried a detailed calculation of the effect of light-induced drift on the temporal behavior of two-wave mixing processes. Starting from the density matrix equations, we derived the microscopic equations for the population difference and the optical coherence, and the macroscopic equations for the average density and velocity of the atoms. A nonlinear diffusion equation for the atomic density was derived, and whose qualitative solution exhibits oscillatory behavior as a function of time. Furthermore, the theoretical model predicts that the rise time of the oscillation is inversely proportional to the laser intensity and the buffer gas density, in qualitative agreement with experiments.

The measurements described above show that a relatively low power cw-pumped two-wave mixing process is possible in resonant systems. In fact, this type of gain has been used to demonstrate a unidirectional ring laser. This process may also be useful in reducing the

operating intensity levels of self-pumped phase conjugate mirrors in resonant media such as sodium and cesium vapors from hundreds to tens of watts per square centimeter. The oscillations observed in the presence of buffer gas have a definite impact upon devices based upon two-wave mixing gain and our characterization is an important step in understanding and possibly controlling this phenomenon and its implications.

The authors would like to thank Rick Harold for his assistance in performing the experiments, as well as Tony Pepitone for his help with the vacuum system used to evacuate the sodium cell. This work was supported by DARPA/ONR under contract #N00014-87-C-0090, Army Research Office under contract #DAAL03-87-C-0001, and Air Force Office of Scientific Research under contract #F49620-88-C-0042. The results of this work were first presented at CLEO'88 and IQEC'90.

REFERENCES

1. J. Ducuing, **Nonlinear Optics**, Academic Press 1977. N. Bloembergen, **Laser Spectroscopy IV**, Springer-Verlag, 1979

2. J.F. Lam, D.G. Steel and R.A. McFarlane, Phys. Rev. Lett. **49**, 1628 (1982)

3. J.F. Lam, D.G. Steel and R.A. McFarlane, Phys. Rev. Lett. **56**, 1679 (1986)

4. D. Grandclement, G. Grynberg and M. Pinard, Phys. Rev. Lett. **59**, 44 (1987)

5. P.R. Berman, G. Khitrova and J.F. Lam, in **Spectral Line Shapes**, edited by F. Rostas, W. de Gruyter, Berlin 1985

6. C.J. Gaeta, J.F. Lam and R.C. Lind, Opt. Lett. **14**, 245 (1989)

7. G. Grynberg, E. Le Bihan and M. Pinard, J. Physique **47**, 1321 (1986)

8. M.T. Gruneisen, K.R. McDonald and R.W. Boyd, JOSA B **5**, 123 (1988)

LIST OF FIGURES

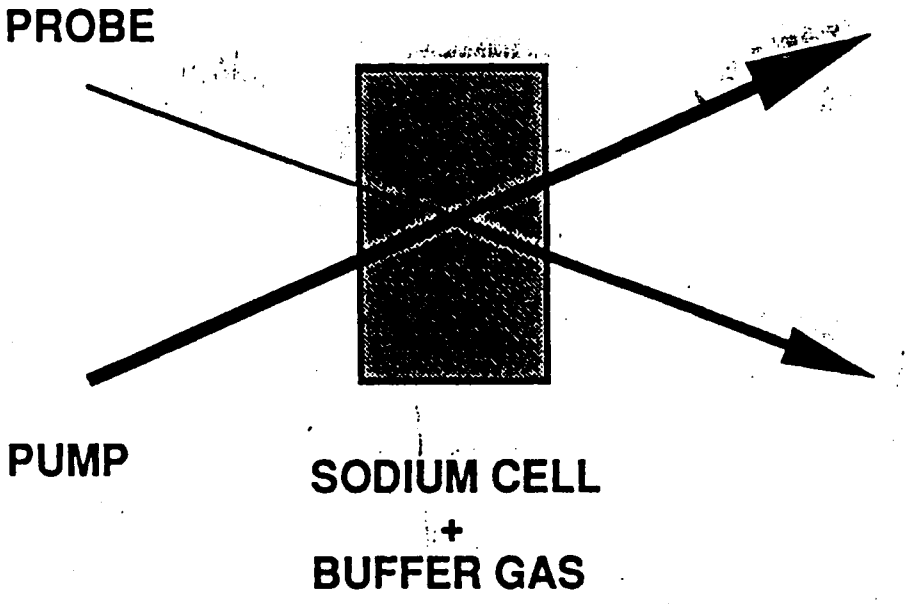

Figure H-1

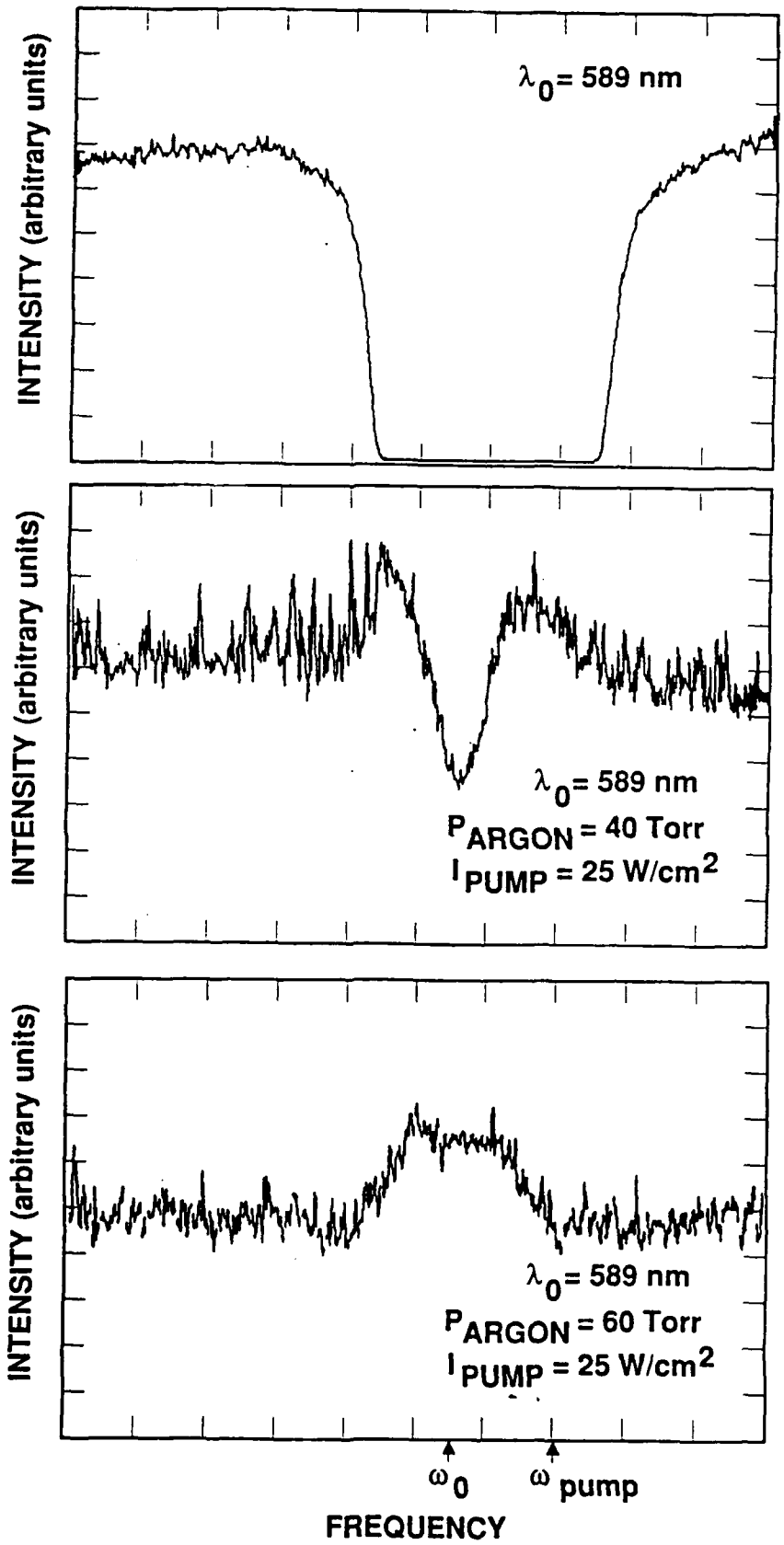
INTENSITY (arbitrary units)
λ_0= 589 nm
INTENSITY (arbitrary units)
λ_0= 589 nm
P_{ARGON} = 40 Torr
I_{PUMP} = 25 W/cm^2
INTENSITY (arbitrary units)
λ_0= 589 nm
P_{ARGON} = 60 Torr
I_{PUMP} = 25 W/cm^2
ω_0
ω_{pump}
FREQUENCY

Figure H-2

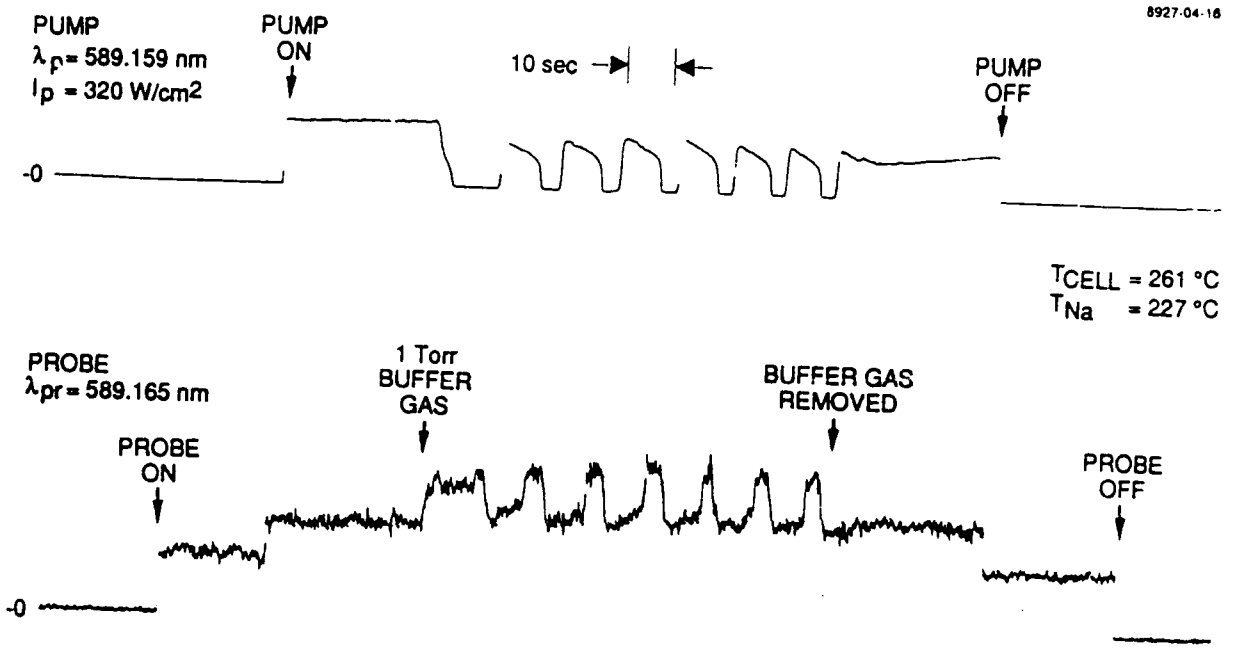
8927-04-18
PUMP
λ_p = 589.159 nm
I_p = 320 W/cm2
PUMP ON
10 sec
PUMP OFF
-0
T_{CELL} = 261 °C
T_{Na} = 227 °C
PROBE
λ_{pr} = 589.165 nm
1 Torr BUFFER GAS
BUFFER GAS REMOVED
PROBE ON
PROBE OFF
-0

Figure H-3

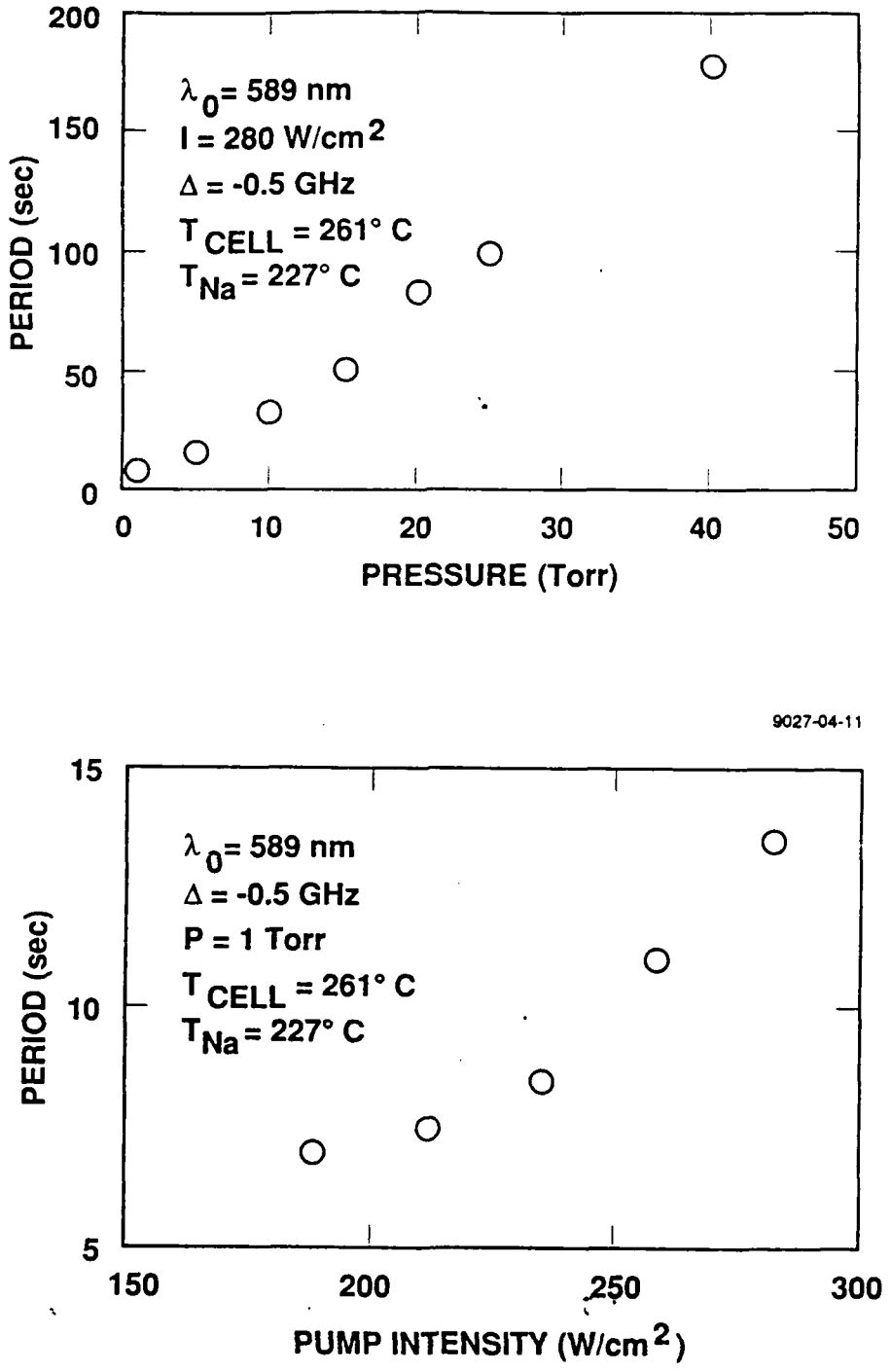
200
150
100
50
0
PERIOD (sec)
λ0= 589 nm
I = 280 W/cm2
Δ = -0.5 GHz
T CELL = 261° C
TNa = 227° C
0
10
20
30
40
50
PRESSURE (Torr)
9027-04-11
15
10
5
PERIOD (sec)
λ0= 589 nm
Δ = -0.5 GHz
P = 1 Torr
T CELL = 261° C
TNa = 227° C
150
200
250
300
PUMP INTENSITY (W/cm2)

Figure H-4

APPENDIX I

OPTICAL NONLINEARITIES IN CRYSTALLINE ORGANIC MULTIPLE QUANTUM WELLS

Juan F. Lam*, Stephen R. Forrest** and Gregory L. Tangonan*

*Hughes Research Laboratories

Malibu, California 90265

**University of Southern California

Center for Photonic Technology

Departments of Electrical Engineering and Materials Science

Los Angeles, California 90089-0241

ABSTRACT

A study of the linear and nonlinear optical behavior of recently demonstrated crystalline organic semiconductor quantum wells are reported. Using the Davydov Hamiltonian, we find analytical solutions for the optical response function, and we predict the existence of intrinsic optical bistability and two-wave mixing energy transfer in these materials.

Current research in the optical properties of organic materials has been directed toward the elucidation of the dominant mechanism that gives rise to their nonlinear optical behavior.[1] In spite of the many experiments performed over the past decade,[2] little depth of understanding has been achieved. The complications arise from the competing effects between the delocalization of the photogenerated charge carriers[3], and formation of the excitations or quasi-particles.[4] Recent nonlinear optical absorption experiments[5] performed on the quasi-1 D semiconductor polydiacetyline appeared to confirm the concept[6] that excitons are responsible for the nonlinear optical behavior of 1-D organic materials.

In this work, we have extended the studies of semiconductor multiple quantum wells (MQWs) to the case of crystalline organic MQWs[7] (CO-MQW) and have found that the response of quantum confined charge transfer (CT) excitons to external fields have novel nonlinear optical properties. CT excitons are known to exist in molecular crystals[8] and their electronic structure can be described by means of the Wannier picture[9] with an appropriate static dielectric constant. However, their interaction with the lattice is significantly different from the Wannier excitons found in inorganic semiconducting hosts. The CT exciton binding energy lies in the few eVs range, making them less susceptible to phonon-induced ionization as compared to Wannier excitons in inorganic semiconductors.

In previous work, the linear optical properties of CO-MQWs were measured in some detail[7]. It was found that the lowest energy CT exciton absorption line was blue shifted with decreasing well width. This observation is consistent with quantum confinement of the CT exciton by energy wells formed in one of the two MQW layers (consisting of 3,4,9,10 perylenetetracarboxylic dianhydride or PTCDA), sandwiched between layers of a second material (3,4,7,8 naphthalene tetracarboxylic dianhydride or NTCDA) forming energy barriers. A variational study of the dependence of exciton energy on well width indicates that the exciton radius is approximately 15 A. This number is significantly smaller than that found in III-V semiconducting compounds because of the smaller static dielectric constant of organic crystals. The strong Coulomb binding energy (as compared with

the kinetic energy of each charge carrier) in the CO-MQW materials implies that the quantization due to the well thickness, L, is determined by the center-of-mass motion of the exciton. Hence the exciton binding energy is given by $\hbar\omega_x = \hbar\omega_B + (\hbar\pi n)^2/2ML^2$ for an infinitely deep potential well, where ω_B is the bulk exciton binding energy, n is an integer, and M is the total mass of the exciton. This expression provides a qualitative explanation to the observed blue shift that was reported in the linear absorption measurements. Since the CT exciton represents a correlated electron-hole pair between nearly adjacent molecules in a stack, we can consider this radius to be the spatial dimension in an electric dipole moment. Such a large dipole moment should, in turn, lead to large optical nonlinearities in these materials. These optical nonlinearities are the focus of this study.

The starting point of our analysis of the optical properties of CT excitons in CO-MQWs is the Davydov Hamiltonian which describes the interaction of excitons with phonons and external radiation fields. Assuming the rotating wave approximation, existence of one phonon mode and keeping only the linear exciton-phonon interaction, the Hamiltonian is

$$H = \hbar(\omega_x - \omega)a^{\dagger}a + \hbar\omega_0 b^{\dagger}b - \hbar\lambda a^{\dagger}aQ - (\frac{1}{2})\mu a^{\dagger}E - (\frac{1}{2})\mu aE^{*} \qquad (1)$$

where $\hbar\omega_x$ and $\hbar\omega_0$ are the quantum confined exciton binding and phonon energies; respectively. Also, λ is the exciton-phonon coupling constant, μ is the electric dipole moment of the exciton. $a^{\dagger}a$ and $b^{\dagger}b$ are the exciton and phonon populations; respectively. Further, $Q = b + b^{\dagger}$ is the phonon amplitude and E is the slowly varying envelope of the external field, and a and b are the exciton coherence and phonon annihilation operators; respectively.

Careful interpretation of the constants λ and μ must be considered. Current measurements appear to be inconclusive concerning the effects of quantization on these constants. From a theoretical point of view, quantum confinement should play a role since the envelope wavefunctions are quantized and they enter in the computation of the matrix elements of the observables. That is, the quantum confinement modifies the bulk values by a factor

that reflects the overlap of the spatial wavefunctions for the electrons and holes.

The temporal evolution of the exciton coherence, a , and phonon amplitude, Q , are determined by the Heisenberg equation of motion, and are given by

$$\frac{da}{dt} + [i(\omega_x - \omega) + \gamma]a = i\lambda Qa + i\frac{\mu E}{2\hbar} \tag{2a}$$

$$\frac{d^2Q}{dt^2} + \Gamma\frac{dQ}{dt} + (\omega_o)^2 Q = 2\omega_o \lambda a^\dagger a \tag{2b}$$

where γ and Γ are phenomenological exciton dephasing and phonon decay rates, respectively. Eq. (2) provides an insight into the nonlinear optical behavior of exciton-phonon coupled systems. The term $i\lambda Qa$ in Eq.(2a) is a renormalization of the exciton frequency due to its coupling to the phonon structure of the material. Since it depends on the phonon amplitude Q, the renormalization factor can be seen to be proportional to the exciton density from the steady state solution of Eq.(2b). This implies that the effective exciton frequency is a function of the population of photogenerated excitons, which is proportional to the light intensity. Hence optical nonlinearities in these materials have their origin in an exciton-phonon induced frequency shift,[5] in a manner similar to the dynamic Stark shift in polaritons.[10]

The nonlinear evolution of coupled waves are determined by the Maxwell equations. In the slowly varying envelope approximation, they are given as

$$2ik_\alpha \frac{dE_\alpha}{dz} = -(\frac{\omega}{c})^2 P_\alpha \tag{3a}$$

where the nonlinear polarization density, P_α, is defined by

$$P_\alpha = N\mu\langle a\rangle \tag{3b}$$

Here, N is the number density of CT excitons and $\langle a\rangle$ is the expectation value of a. The subscript α denotes the radiation field oscillating at frequency ω_α.

Equations (1) through (3) have exact, closed form analytical solutions in the steady state regime. We shall consider three important cases. The first involves the linear response

of the medium to an optical radiation field . A comparison of the theoretical model to the available experimental data will provide an estimate of the coupling parameters. Second we will explore the nonlinear response of the medium by obtaining an exact solution to the CT exciton population $\langle a^{\dagger}a \rangle$. And finally we will use the results to understand the process of two-wave mixing in these materials. The latter involves the nonlinear coupling of strong and weak radiation fields.

For the case of a single input optical wave, the analytical solution of Eq.(2) is obtained under the condition of factorization of the respective variables, a and Q. First, in the low intensity regime, the population of photogenerated excitons is proportional to the intensity of the optical wave, and the polarization density is determined by the steady state small signal solution of Eqs.(2). That is,

$$P = \frac{N\mu^2}{2\hbar} E e^{-i\omega t} \langle \langle \frac{1}{\omega_x - \omega + i\gamma} \rangle \rangle \tag{4}$$

Figure 1 depicts the linear absorption (solid line) measurement and the theoretical fit (dashed line) which assumes the existence of two exciton lines. In order to obtain reasonably good qualitative agreement, the imaginary part of the polarization density was averaged over a Maxwellian distribution with two distinct widths. The use of the Maxwellian distribution is consistent with the fast phonon-induced relaxation processes that exist in these materials.

Second in the fully nonlinear regime, the solution for the population, $\langle a^{\dagger}a \rangle$ of the CT exciton is given by the cubic equation:

$$\langle a^{\dagger}a \rangle = \frac{\Omega^2}{\gamma^2 + \left[\Delta - (\frac{2\lambda^2}{\omega_o})^2 \langle a^{\dagger}a \rangle\right]^2} \tag{4}$$

where $\Delta = \omega_x - \omega$ is the detuning from the exciton resonance, and $\Omega = \mu E/2\hbar$ is the Rabi frequency. Figure 2 shows the solution of this cubic equation as a function of the Rabi frequency, for different values of the detuning parameter Δ. In this plot, all physical variables have been normalized to $2\lambda^2/\omega_o$. A transition to multivalue behavior is observed

for a sufficiently large value of the detuning parameter Δ. This behavior can be understood in the following manner. Multivalue behavior of Eq.(5) is achieved if the derivative of the Rabi frequency with respect to the exciton population changes sign. A simple calculation of this criterion asserts that bistability is present provided that

$$\Delta > \sqrt{3}\gamma \qquad (6)$$

This condition is valid even in the absence of an optical cavity. Hence, the coupled exciton-phonon system posseses the property of intrinsic bistable behavior which arises from the renormalization of the exciton frequency mediated by the exciton-phonon interaction.

Finally, we consider the interaction between a strong wave, E_o, oscillating at frequency ω, and a weak wave E_1 oscillating at frequency $\omega + \delta$. Their nonlinear coupling yields a coherent traveling wave excitation in the medium oscillating at frequency δ. The scattering of the strong wave from the coherent excitation changes the absorption coefficient and the index of refraction experienced by the weak wave. A calculation of the optical response function in the undepleted pump approximation gives the following expression for the spatial evolution of the weak wave:

$$\frac{1}{E_1}\frac{dE_1}{dz} = -(\frac{\omega+\delta}{2n_1}) \times \frac{N\mu^2\omega_o}{\epsilon_o\hbar 2\lambda^2}\{\alpha + i\beta\} \qquad (7a)$$

where the dimensionless (all physical parameters are normalized to $2\lambda^2/\omega_o$) nonlinear absorption coefficient α is

$$\alpha = \frac{(\omega_o^2 - \delta^2)C - \delta\Gamma D}{C^2 + D^2} \qquad (7b)$$

and the dimensionaless nonlinear index of refraction is given by

$$\beta = \frac{(\omega_o^2 - \delta^2)D + \delta\Gamma C}{C^2 + D^2} \qquad (7c)$$

with the following expressions for C and D:

$$C = \gamma(\omega_o^2 - \delta^2) + \delta\Gamma(\Delta - \delta) - \delta\Gamma\langle a^\dagger a\rangle$$

$$D = (\omega_o^2 - \delta^2)(\Delta - \delta) - \delta\Gamma\gamma - (2\omega_o^2 - \delta^2)\langle a^\dagger a\rangle$$

Figure 3 shows the behavior of the nonlinear absorption coefficient, $\alpha + i\beta$, of the weak wave as a function of the Rabi frequency induced by the strong wave for different values of the quantum well dimension. A transition to bistable behavior, accompanied by gain (negative values of the nonlinear absorption coefficient) of the weak wave at the expense of the strong wave, is observed for a critical value of the normalized Rabi frequency and a small enough value of the quantum well dimension . The dimension of the quantum well plays a key role in the detuning parameter Δ. For large enough detuning or small enough well size, the value of the detuning parameter satisfies the bistability condition (6). Hence, a coherent energy transfer from the strong to the weak wave takes place with a threshold behavior. This phenomenon can be thought of as a coherent bistable optical switch. That is, the energy transfer takes place from the strong to the weak optical beams when a certain threshold is achieved. The bistable behavior is a reflection of the nonlinear functional dependence of the exciton population on the pump intensity.

The phenomena discused in the previous paragraphs provide an insight into subtle effects that appear in the Davidov Hamiltonian. Estimates of the physical parameters such as λ and ω_o are crucial to the understanding of the materials growth conditions as well as the future applications of these novel materials for opto-electronics. The beauty and simplicity of our results is contained in one single physical parameter, the Franck-Condon shift (FC). This frequency shift is related to λ and ω_o by the following expression

$$FC = \frac{\lambda^2}{\omega_o}$$

and is a measure of the degree of reduction of the potential energy of the material due to the exciton-phonon coupling. From measured values in aromatic molecules [11], λ is approximately equal to ω_o. These numbers imply a FC of 700 cm^{-1} for the case of naphtalene compounds.

It is interesting to calculate the laser power required to observe the onset of optical bistability and two-beam energy transfer. Assuming a FC shift of approximately 1000 cm^{-1} expected for large molecules such as PTCDA [12]. and an oscillator strength of unity, a normalized linewidth of 3, one finds that the power density is of the order of $10^{10}\ W/m^2$. A more accurate value must wait for a detail measurement of the FC shift.

In summary, we presented new results on the optical behavior of these newly discovered materials. We predict the existence of intrinsic bistability as well a coherent energy transfer from a strong wave to a weak wave. The energy exchange occurs under bistable condition, leading to the possibility of novel optical devices using these materials.

This work was first presented at the International Quantum Electronics Conference in Anaheim, California on April 1990.

ACKNOWLEDGEMENT

This work is supported by the Air Force Office of Scientific Research (Dr. Howard Schlossberg and Maj. G. Pomrenke). One of us (JFL) would like to thank Dr. R.N. Schwartz for enlightening discussion on organic materials.

REFERENCES

1. See **NONLINEAR OPTICS OF ORGANICS AND SEMICONDUCTORS**, edited by T. Kobayashi, Springer-Verlag, Berlin (1989)
2. M. Sinclair, D. Moses, A.J. Heeger, K. Vilhelmsson, B. Valk, and M. Salour, Solid State Commun. **61**, 221 (1987)
3. See **NONLINEAR OPTICAL PROPERTIES OF ORGANIC MOLECULES AND CRYSTALS**, edited by D.S. Chemla and J. Zyss, Academic Press, New York (1987)
4. W.P. Su, J.R. Schrieffer, and A.J. Heeger, Phys. Rev. Lett. **42** , 1698 (1979); L. Rothberg, T.M. Jedju, S. Etemad and G.L. Baker, Phys. Rev. Lett. **57**, 3229 (1986)
5. B.I. Greene, J.F. Mueller, J. Orenstein, D.H. Rapkine, S. Schmitt-Rink, and M. Thakur, Phys. Rev. Lett. **61**, 325 (1988)
6. S.A. Brazovskii and N.N. Kirova, Sov. Phys. JETP Lett. **33**, 4 (1981)
7. F.F. So, S.R. Forrest, Y.Q. Shi, and W.H. Steier, Appl. Phys. Lett. 56, 674 (1990). The first crystalline organic superlattice structure was fabricated using the Langmuir-Blodgett technique. See B. Holcroft, M.C. Petty, G.G. Roberts and G.J. Russell, Thin Solid Films **134**, 83 (1985)
8. M. Pope and C.E. Swenberg, **ELECTRONIC PROCESSES IN ORGANIC CRYSTALS**, New York, Oxford University Press (1982)
9. P.J. Bounds and W. Siebrand, Chem. Phys. Lett. **75**, 414 (1980)
10. A.L. Ivanov and L.V. Keldysh, Sov. Phys. JETP **57**, 234 (1983)
11. V.L. Broude, E.I. Rashba and E.F. Sheka, in **SPECTROSCOPY OF MOLECULAR EXCITONS**, Springer-Verlag , Berlin, 1985
12. D. Haarer and N. Karl, Chem. Phys. Lett. **21**, 49 (1973)

FIGURE CAPTIONS

Figure 1. Linear absorption coefficient of PTCDA/NTCDA mqws. The experimentAl data (solid line) contains two additional sidebands on the left hand side sue to the presence of the NTCDA. The theoretical fit (dashed line) from the solution of the exciton-phonon equations is based on thermalization by phonons

Figure 2. Dependence of the exciton population on the normalized Rabi frequency to the second power. The linewidth and the detuning are also normalized to the $2\lambda^2/\omega_o$, which has the unit of freqquency. (a) The normalized detuning, $\Delta = 0$; (b) $\Delta = 5.19$, which corresponds to the transition region for bistability to begin taking place; (c) $\Delta = 8$.

Figure 3. Two-wave mixing gain (negative value) and absorption (positive value) coefficient for three different values of the quantum well size. Prediction of optical bistablity and energy transfer is given for L = 62 A. The normalized probe-pump detuning parameter $\acute{\delta}$ is set equal to -1

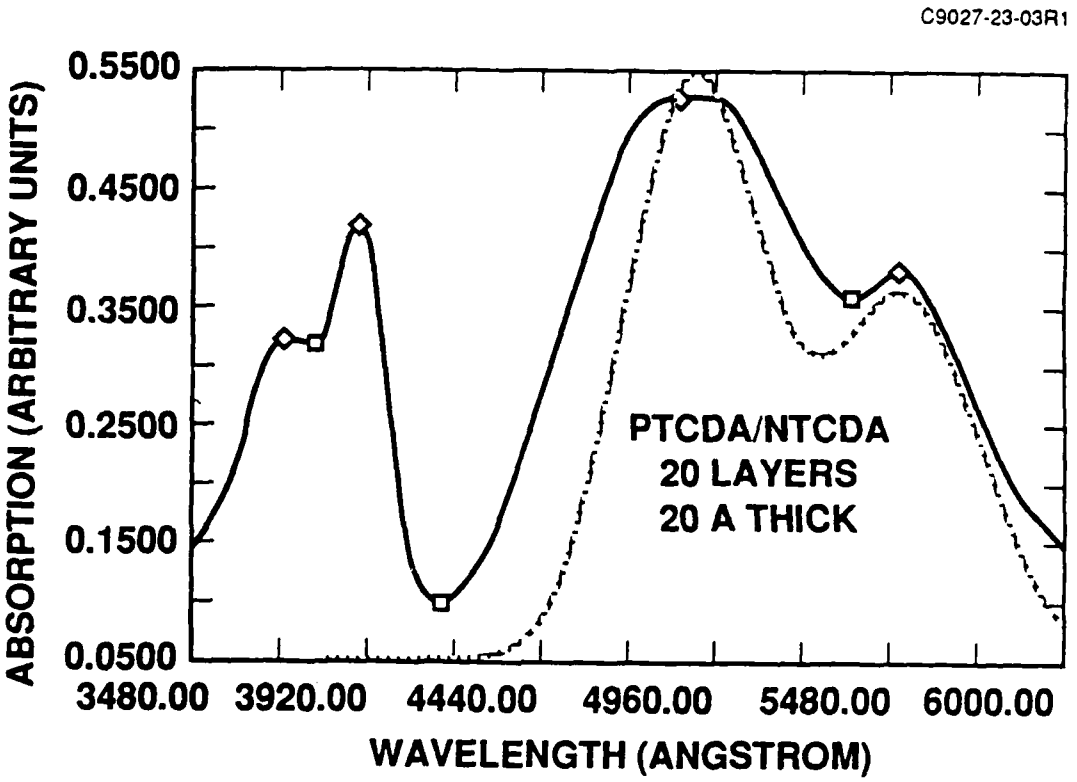
C9027-23-03R1
0.5500
0.4500
0.3500
0.2500
0.1500
0.0500
ABSORPTION (ARBITRARY UNITS)
PTCDA/NTCDA
20 LAYERS
20 A THICK
3480.00
3920.00
4440.00
4960.00
5480.00
6000.00
WAVELENGTH (ANGSTROM)

Figure I-1

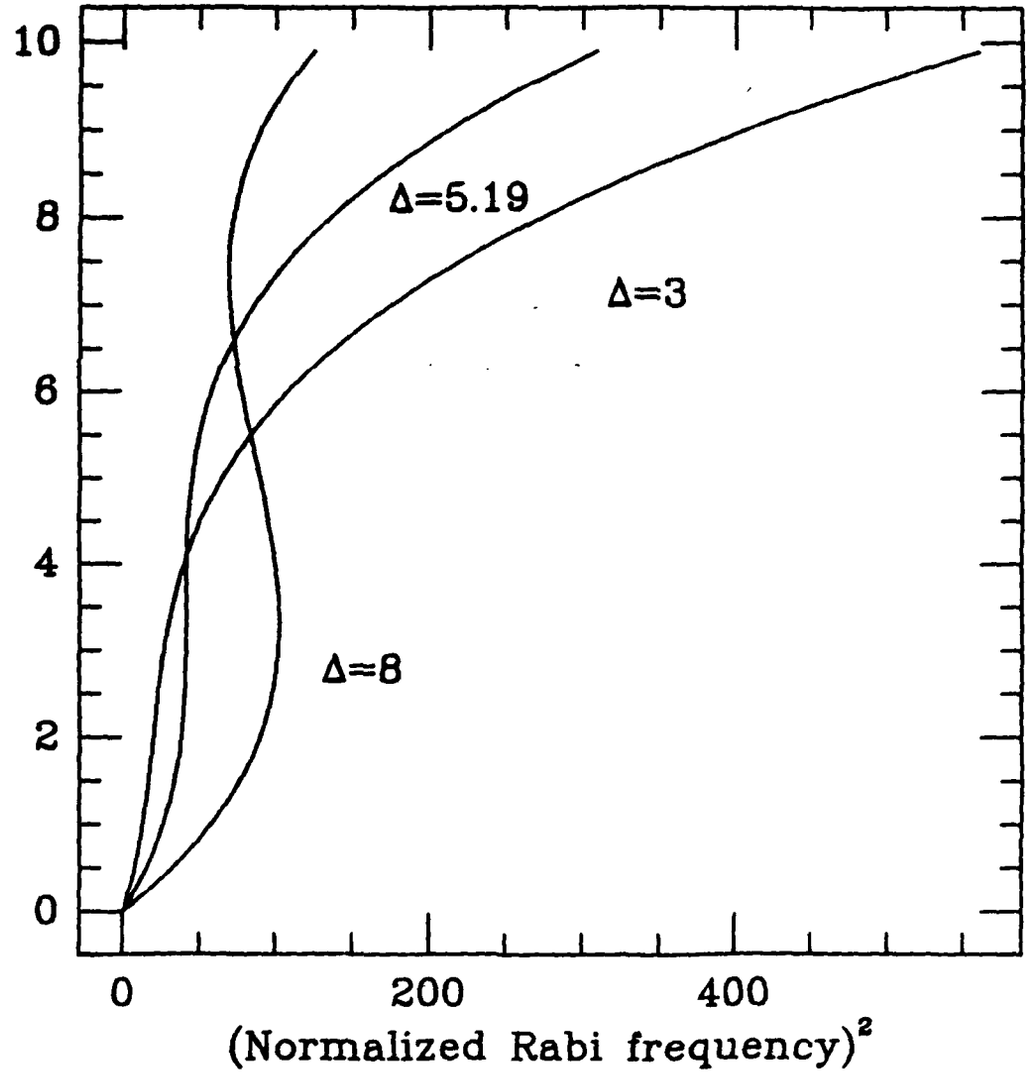
10
8
6
4
2
0
Exciton Population
Δ=5.19
Δ=3
Δ=8
0
200
400
(Normalized Rabi frequency)²

Figure 1-2

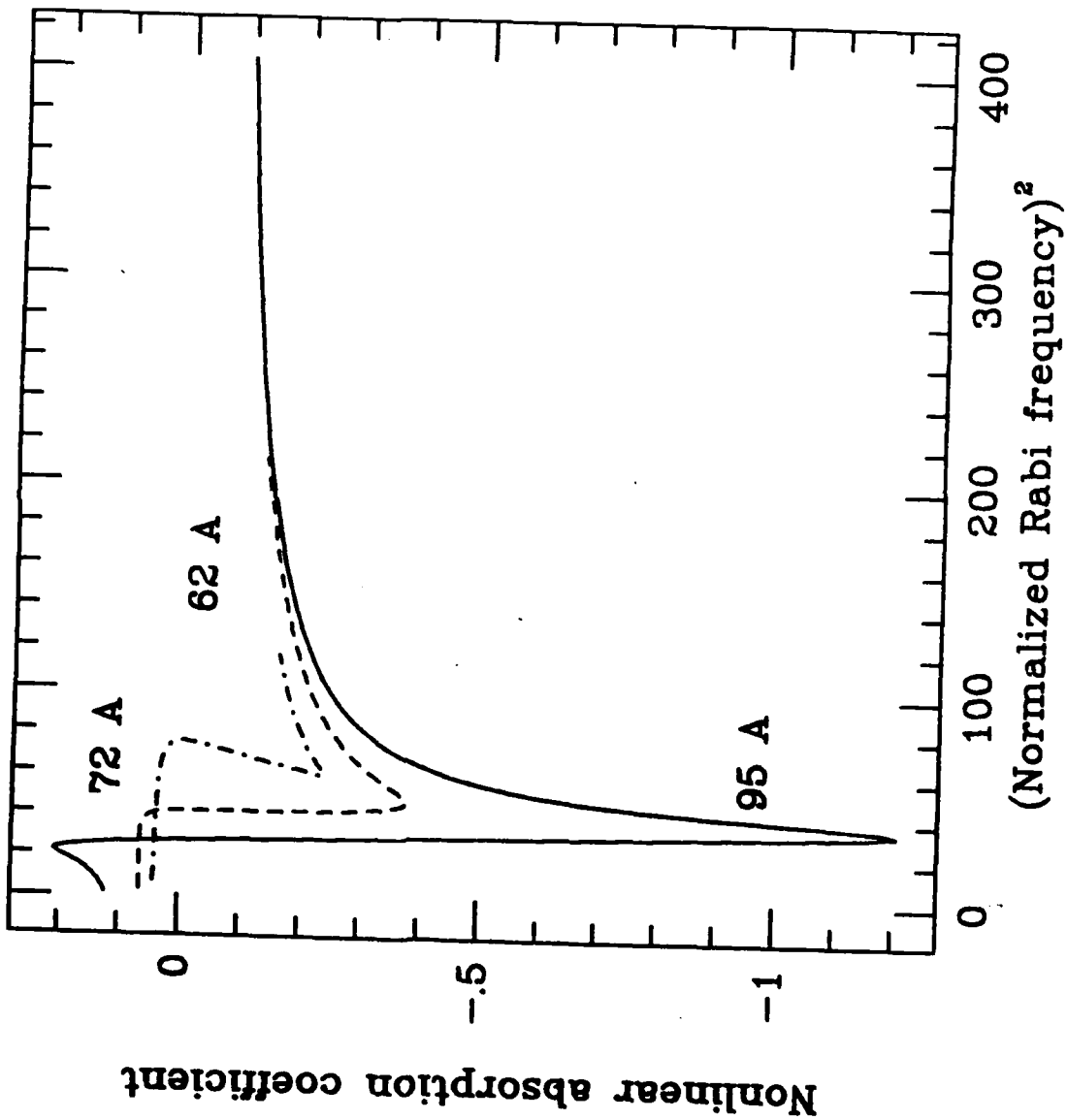
Nonlinear absorption coefficient
0
-.5
-1
0
100
200
300
400
(Normalized Rabi frequency)²
72 A
62 A
95 A

Figure I-3